Weathering, Landscape Equilibrium, and Carbon in Four Watersheds in Eastern Puerto Rico

By Robert F. Stallard

Chapter H of
Water Quality and Landscape Processes of Four Watersheds in Eastern Puerto Rico
Edited by Sheila F. Murphy and Robert F. Stallard

Professional Paper 1789–H

U.S. Department of the Interior
U.S. Geological Survey

Contents

Figures

Table

Abbreviations Used in This Report

*	calculated bedrock-derived constituent
<	less than
>	greater than
μm	micrometer
μmol L^{-1}	micromoles per liter
eq mol^{-1}	equivalents of charge per mole
h	hour
kmol	kilomole
kmol km^{-2} yr^{-1}	thousand moles per square kilometer per year
m	meter
mg L^{-1}	milligrams per liter
mm	millimeter
mm h^{-1}	millimeters per hour
mm $k.y.^{-1}$	millimeters per thousand years
mm yr^{-1}	millimeters per year
pg yr^{-1}	petagrams per year (1 petagram=1 $gram^{15}$)
ppm	parts per million
t km^{-2} yr^{-1}	metric tons per square kilometer per year
DBrx	dissolved bedrock
DIC	dissolved inorganic carbon
DOC	dissolved organic carbon
LOI	loss on ignition

PIC	particulate inorganic carbon
POC	particulate organic carbon
SBrx	suspended bedrock
SSol	suspended solids
WEBB	Water, Energy, and Biogeochemical Budgets
ZBrx	total bedrock-derived cation charge

Conversion Factors

Multiply	By	To obtain
	Length	
micrometer (μm)	0.00003937	inch (in.)
millimeter (mm)	0.03937	inch (in.)
meter (m)	3.281	foot (ft)
	Flow rate	
millimeters per hour (mm h^{-1})	0.03937	inches per hour (in. h^{-1})
millimeters per year (mm yr^{-1})	0.03937	inches per year (in. yr^{-1})
millimeters per 1,000 years (mm $k.y.^{-1}$)	0.03937	inches per 1,000 year (in. $k.y.^{-1}$)
	Mass	
milligrams per liter (mg L^{-1})	0.05841	grains per gallon (gr gal^{-1})
	Other	
petagrams per year	1.102	billions of short tons per year (t yr^{-1})[9]
metric tons per square kilometer per year (t km^{-2} yr^{-1})	2.855	short tons per square mile per year (tons mi^{-2} yr^{-1})

Weathering, Landscape Equilibrium, and Carbon in Four Watersheds in Eastern Puerto Rico

By Robert F. Stallard

Abstract

The U.S. Geological Survey's Water, Energy, and Biogeochemical Budgets (WEBB) program research in eastern Puerto Rico involves a double pair-wise comparison of four montane river basins, two on granitic bedrock and two on fine-grained volcaniclastic bedrock; for each rock type, one is forested and the other is developed. A confounding factor in this comparison is that the developed watersheds are substantially drier than the forested (runoff of 900–1,600 millimeters per year compared with 2,800–3,700 millimeters per year). To reduce the effects of contrasting runoff, the relation between annual runoff and annual constituent yield were used to estimate mean-annual yields at a common, intermediate mean-annual runoff of 1,860 millimeters per year. Upon projection to this intermediate runoff, the ranges of mean-annual yields among all watersheds became more compact or did not substantially change for dissolved bedrock, sodium, silica, chloride, dissolved organic carbon, and calcium. These constituents are the primary indicators of chemical weathering, biological activity on the landscape, and atmospheric inputs; the narrow ranges indicate little preferential influence by either geology or land cover. The projected yields of biologically active constituents (potassium, nitrate, ammonium ion, phosphate), and particulate constituents (suspended bedrock and particulate organic carbon) were considerably greater for developed landscapes compared with forested watersheds, consistent with the known effects of land clearing and human waste inputs. Equilibrium rates of combined chemical and physical weathering were estimated by using a method based on concentrations of silicon and sodium in bedrock, river-borne solids, and river-borne solutes. The observed rates of landscape denudation greatly exceed rates expected for a dynamic equilibrium, except possibly for the forested watershed on volcaniclastic rock. Deforestation and agriculture can explain the accelerated physical erosion in the two developed watersheds. Because there has been no appreciable deforestation, something else, possibly climate or forest-quality change, must explain the accelerated erosion in the forested watersheds on granitic rocks. Particulate organic carbon yields are closely linked to sediment yields. This relation implies that much of the particulate organic carbon transport in the four rivers is being caused by this enhanced erosion aided by landslides and fast carbon recovery. The increase in particulate organic carbon yields over equilibrium is estimated to range from 300 kilomoles per square kilometer per year (6 metric tons carbon per square kilometer per year) to 1,700 kilomoles per square kilometer per year (22 metric tons carbon per square kilometer per year) and is consistent with human-accelerated particulate-organic-carbon erosion and burial observed globally. There is no strong evidence of human perturbation of silicate weathering in the four study watersheds, and differences in dissolved inorganic carbon are consistent with watershed geology. Although dissolved organic carbon is slightly elevated in the developed watersheds, that elevation is not enough to unambiguously demonstrate human causes; more work is needed. Accordingly, the dissolved organic carbon and dissolved inorganic carbon yields of tropical rivers, although large, are of secondary importance in the study of the anthropgenically perturbed carbon cycle.

Introduction

The humid tropics presently occupy about 25 percent of the Earth's land surface, and the warm temperatures, moist conditions, and luxuriant vegetation promote especially rapid biological and chemical processes—photosynthesis, respiration, decay, and chemical weathering—making the region particularly important at a global scale from the perspective of weathering, erosion, and carbon cycling. Tropical forests alone cover only 12 to 13 percent of the Earth's land surface, but they contain 45 to 52 percent of terrestrial biomass carbon and 11 to 17 percent of soil carbon, and they account for 23 to 35 percent of net primary productivity (Prentice and others, 2001). This productivity equates to between 780 and 1,250 metric tons per square kilometer per year of carbon ($t\ km^{-2}\ yr^{-1}$ C). Other widespread humid-tropical land cover includes grasslands, wetlands, and various types of agricultural lands. According to Meybeck (1979), rivers in the humid tropics supply about 65 percent of the dissolved silica and 38 percent of the ionic load delivered by rivers to the ocean. Data compiled by Milliman and Meade (1983) and Milliman and Syvitski (1992) indicate that the humid tropics contribute about 50 percent of the total solid load delivered by rivers to the ocean. These and related studies demonstrate that about 30 percent of the solid load comes from steep, undammed,

coastal rivers that drain active orogenic belts and island arcs in the tropics (Lyons and others, 2002). These rivers are an especially strong source of particulate organic carbon (POC) in the ocean (Ver and others, 1999; Lyons and others, 2002; Syvitski and others, 2005; Galy and others; 2007; Hilton and others, 2008a,b).

When examined at both human and geologic time scales, today's world is in a state of exceptionally rapid change caused by human activities (Science Magazine, 2011). For the last several thousand years, we humans have been modifying the Earth's landscape with fire and tools for food and agriculture, and for the past few hundred years, we humans have remodeled the Earth's surface and altered biogeochemical cycles with a technology fueled by geologic and biospheric energy sources, a time period commonly referred to as the Anthropocene. Associated with this remodeling is a vast mobilization and redistribution of soils, sediments, and rock at a scale comparable to that of natural erosion (Hooke, 1994, 2000). Rivers and materials transported by rivers have been profoundly affected by human activities related to hydraulic engineering, water consumption, waste introduction, and land-cover modification (Meybeck, 2003).

Human impacts motivate one of the great developing themes of contemporary biogeochemistry, that of describing the anthropogenically modified carbon cycle and understanding how it relates to changes in atmospheric and seawater composition, land use, and land cover. The ongoing accumulation of carbon dioxide in the atmosphere, derived from fossil-fuel burning, deforestation, and land clearing, is now a major concern, because of potentially severe consequences on climate (Schneider, 2009). Examination of natural and technological mechanisms that limit CO_2 accumulation in the atmosphere through sequestration has become a global research focus. This theme is now a major thrust of the current U.S. Geological Survey Strategic Plan (U.S. Geological Survey, 2007). For reference, current characterizations of the global carbon budget (Denman and others, 2007) estimate that the combined emissions from fossil fuels and cement release 7.2±0.3 petagrams of carbon per year (pg C yr^{-1}). Of this total, 4.1±0.1 pg C yr^{-1} accumulate in the atmosphere; 2.2±0.5 pg C yr^{-1} enter the ocean, and 0.9±0.6 pg C yr^{-1} are stored on land. The large error in the terrestrial carbon sink reflects the relative difficulty in accounting for all carbon on land.

Studies of terrestrial CO_2 sequestration normally take place at a landscape scale, because the size of the technological perturbation of the carbon cycle is so large that any substantial sequestration must be either quite strong or quite widely distributed. For a suite of processes to be prominent in the technologically perturbed carbon cycle, it must affect about 1 pg C yr^{-1} globally. Distributed over the Earth's land surface ($149 \cdot 10^6$ km^2), this amount corresponds with about 6.7 t km^{-2} yr^{-1} C. Forest regrowth and densification of woody vegetation are clearly important at this scale (Pacala and others, 2001; summaries in Denman and others, 2007). The land area of humid tropical mountains is not large, about $4 \cdot 10^6$ km^2 (United Nations Environment Programme World Conservation Monitoring Centre, 2002). If a process capable of sequestering 1 pg C yr^{-1} were to be confined to just humid tropical mountains, it would need to sequester 250 t km^{-2} yr^{-1} C; this mass is about one third to one fifth of tropical forest net primary productivity.

Weathering and erosion have a smaller effect on the carbon cycle than do plant growth and decay. The combined fluvial transport to the ocean of dissolved inorganic carbon (DIC), dissolved organic carbon (DOC), and POC is less than 1 pg C yr^{-1} (Sarmiento and Sundquist, 1992). It is difficult to envision changes caused by human activities that could alter current dissolved-carbon fluxes on the order of 1 pg C yr^{-1}. Particulate carbon fluxes to the ocean have increased somewhat because of human activities despite the interception of considerable masses of sediment behind artificial reservoirs (Syvitski and other, 2005), and vast quantities of POC are stored on land as soils, colluvium, alluvium, and lacustrine deposits. Stallard (1998) estimated that globally averaged upland physical erosion caused by human activities has increased twofold to sixfold as compared with preagricultural rates and has increased erosion by 10 to 50 pg yr^{-1} sediment; most of this eroded sediment is stored in terrestrial sediments rather than being transported to the ocean. This deposition results in long-term storage of carbon in terrestrial sediments on the order of 0.6 to 1.5 pg C yr^{-1}. Stallard (1998) asserted that much of this carbon is being replaced through the creation of new POC at the sites of erosion, and that carbon stores in depositional sites may also be augmented with additional POC from autochthonous production in surface waters and wetlands. Considerable work has gone into estimating the POC fluxes in the landscape and testing whether the deposited carbon is stable and whether the deposited carbon is being replaced by newly produced POC (Berhe and others, 2007; Van Oost and others, 2007, 2008; Harden and others, 2008; Lal and Pimentel, 2008; Quinton and others, 2010). The most recent estimate of the amount of carbon being removed from the atmosphere by erosion, deposition, and replacement is about 0.5 pg C yr^{-1}; increased erosion produces about 35 pg yr^{-1} sediment (Quinton and others, 2010). This estimate does not include the contribution of carbon to fluvial and lacustrine sediments by autochthonous production.

The U.S. Geological Survey's Water Energy and Biogeochemical Budgets (WEBB) program research in eastern Puerto Rico, described herein, provided a unique opportunity to examine major biogeochemical processes in headwater river systems in humid tropical mountains, to examine their role in the carbon cycle, and to judge whether climate change or human activities have pushed these systems out of equilibrium. Up to now, research into the biogeochemical functioning of headwater river systems in such settings has been limited despite their obvious importance in erosion and biogeochemical processes. The fieldwork is quite challenging. To assess the importance of interannual variations, years of monitoring are required, and huge storms, which are extremely difficult and can be dangerous to sample, have a dominant role in transport processes.

Research Setting

The U.S. Geological Survey initiated the WEBB program in 1991. The WEBB site in eastern Puerto Rico (Larsen and others, 1993), one of five sites, was chosen because it is in a montane humid-tropical environment having a bedrock geology that is representative of many parts of the world. Puerto Rico is part of the volcanically inactive Greater Antilles island arc (fig. 1) that has been moderately to deeply eroded in a humid tropical climate. The qualities of geology, climate, land cover, and land use make Puerto Rico similar to vast swaths of the humid tropics, including the remainder of the Greater Antillean island arc, much of Central America, many island arcs extending from the southwest Pacific to the eastern Indian Ocean such as the Indonesian Archipelago, and considerable portions of the Southeast Asian mainland. These landscapes are agriculturally productive and support large human populations (Bot and others, 2000; Webb, 2006; Foley and others, 2011).

Puerto Rico has undergone a rapid transformation in the past several centuries from pre-European conditions of relatively undisturbed forest, to intensive agriculture in the 19th and early 20th century, to a post-1950 industrial economy. In the past 60 years land cover has shifted from almost entirely deforested to forest covering about half of the island (Brandeis, 2007; Kennaway and Helmer, 2007). For further background, see Murphy and others (2012).

The Puerto Rico WEBB work involves a double pair-wise comparison of montane streams on granitic bedrock compared with fine-grained volcaniclastic bedrock and of forested compared with agricultural landscapes (Murphy and others, 2012, their table 1). Unlike some island-arc regions, Puerto Rico has not had active volcanoes for tens of millions of years. Its soils lack abundant allophane, which is commonly derived from tephras in younger volcanic landscapes. Allophane stabilizes soil organic matter and is associated with especially productive agricultural soils (Parfit, 2009). The selection of the two types of geology was predicated on the idea that the abundance of coarse-grained quartz in the granitic rocks would result in soils with sufficiently different properties from soils on the quartz-poor volcanic rocks that the differences would be manifested in the erosional styles, water flow paths, and solute-load chemical composition. The soils of the volcanic watersheds are, for instance, richer in secondary clay minerals and in base cations. For each bedrock type, one watershed is covered with mature rainforest (drained by Río Icacos and Río Mameyes), and the other watershed is affected by land use typical of eastern Puerto Rico (drained by Río Cayaguás and Río Canóvanas). Two watersheds are located on coarse-grained granitic rocks (Icacos and Cayaguás), and two are located on fine-grained volcanic rocks and volcaniclastic sedimentary rocks derived from closely allied magmas (Mameyes and Canóvanas). Data from the Quebrada Guabá, a tributary of the Icacos which was monitored for 10 years (1993–2002), is included in many calculations and tables as a surrogate for the Icacos (the Guabá streamgaging station failed in April 2003 during a large storm (appendix 1 of this report; Murphy and Stallard, 2012)).

The double pair-wise comparison of physical and chemical weathering processes has been a major objective of the Puerto Rico WEBB program since its inception (Larsen and others, 1993). To this end, the program depended upon the collection of time-series of meteorologic, hydrologic, soil-water, and groundwater samples and data. Long-term monitoring of biogeochemical budgets of the four major watersheds included water, major dissolved constituents, nutrients, carbon, and sediment. Weathering and mass-wasting processes were to be examined in each rock type and land cover by comparing budgets calculated for each. Sampling major hydrologic events was especially important. A benefit of working in Puerto Rico is that at a given altitude and rainfall, similar natural vegetation exists on all types of bedrock (see Murphy and others, 2012), presumably because as an island, Puerto Rico lacks high floral diversity (Ashton and others, 2004). A confounding factor in this comparison, however, is that both agricultural watersheds are substantially drier than the forested watersheds (runoff of 900–1,600 millimeters per year (mm yr^{-1}) as compared with 2,800–3,700 mm yr^{-1}).

An initial snapshot of a four-way comparison, covering 1991 to 1995, was published by Larsen and Stallard (2000). Four-way sediment budgets have been examined by Larsen (1997, 2012). Detailed descriptions of the regional geography (Murphy and others, 2012), atmospheric inputs (Stallard, 2012), the study watersheds and intercomparisons of their hydrology (Murphy and Stallard, 2012), physical erosion (Larsen, 2012), and water quality (Stallard and Murphy, 2012) are found elsewhere in this volume.

Purpose and Scope

The present chapter focuses on a four-way comparison of the rates of chemical and physical erosion as related to carbon transport and in turn to rates of runoff. Simple models are used to project annual constituent-yield data for each river basin to a single intermediate runoff, thereby circumventing the confounding factor of having different mean-annual runoff between forested and developed pairs. The same models are also used to consider the consequences of climate change on chemical and physical weathering and on fluvial carbon transport. Six questions are asked:

1. What are the measured rates of chemical and physical denudation and how do these relate to runoff in each watershed?

2. How do watersheds compare in weathering, erosion, carbon export, and nutrient export with regard to geology and land cover? Do geology and land cover matter?

3. Is the forested landscape in a steady state? In essence, are the Luquillo Mountains a model of a quiescent, stable, natural landscape, or are they changing?

4. What does the present dynamic state of the landscape imply regarding past and future response to climate change?

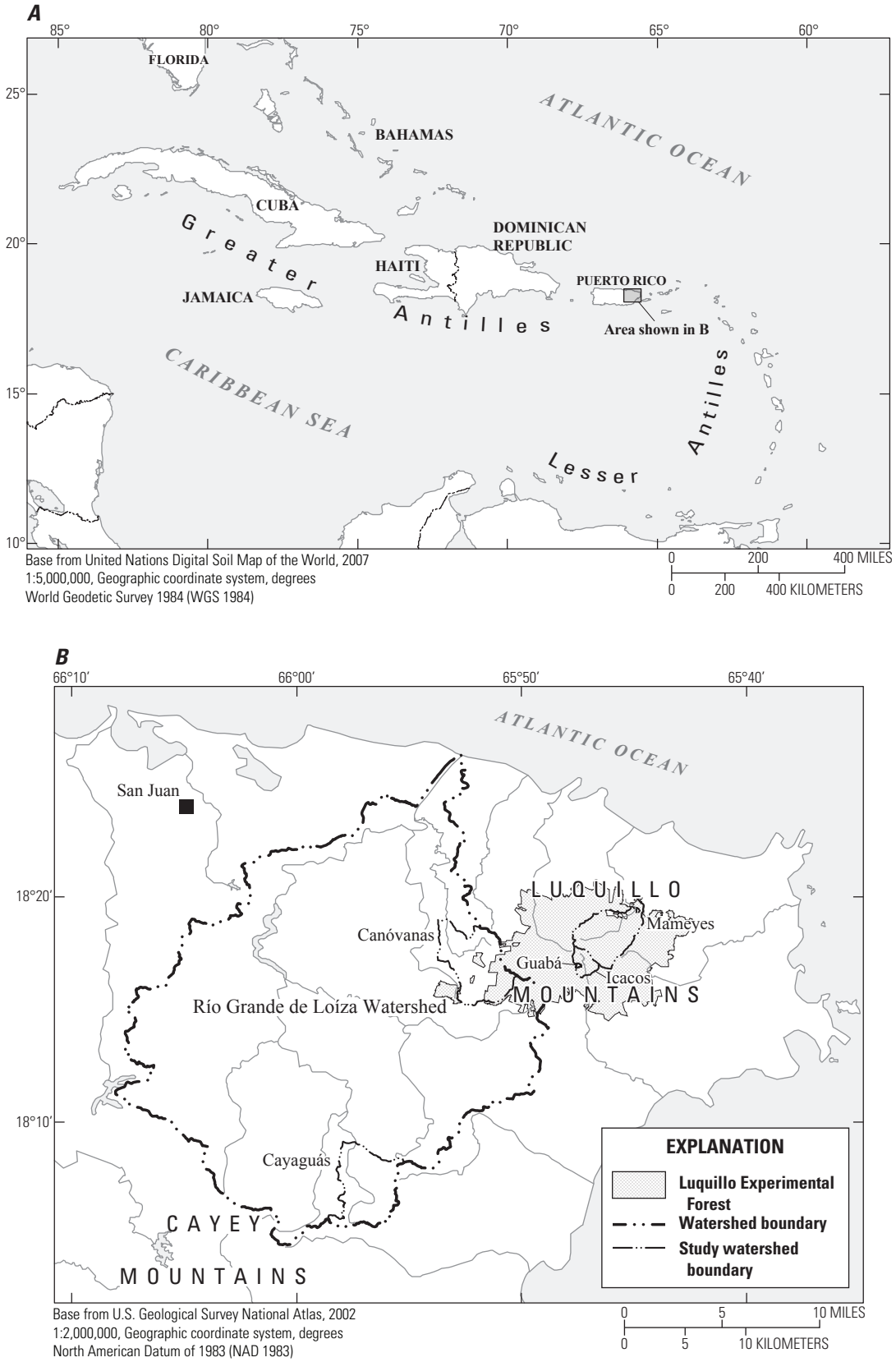

Figure 1. Location of Puerto Rico and study watersheds.

5. What are the rates of export of carbon in its various forms; how do these rates relate to runoff, and is this exported carbon being replaced by new photosynthetically fixed carbon?

6. Are rates of carbon processing through the landscape notable on the time scales of human-induced climate change?

The models used in this paper with minor modifications, as noted, were developed in parallel with the WEBB data-collection program. Stallard (1995a,b) introduced the concept of dissolved and solid bedrock and how major-element compositional information can be rigorously used to characterize steady-state erosion. Brown and others (1995, 1998) expanded on the concept of steady state and perturbed landscapes as determined by measurements of cosmogenic ^{10}Be in bedrock, soils, and sediments. Stallard (1998) developed tools that link physical erosion that has been greatly accelerated by human activities to the anthropologically modified carbon cycle. Carbon dioxide is removed from the atmosphere through accelerated soil loss and subsequent deposition and burial of the eroded soil and associated particulate organic carbon. The buried soil carbon is replaced by new soil carbon at the site of erosion, thereby creating a net carbon-dioxide sink. Stallard (1999) and Stallard and Kinner (2005) formulated models to include landslide-producing events in characterizations of annual sediment yields.

Weathering, Erosion, and the Carbon Cycle

Soils, river-borne solutes, and sediments are all derived from weathering processes that produce both dissolved and solid products. Most parent material must weather before becoming soil or being transported by flowing water. During chemical weathering, some minerals react congruently to produce only dissolved weathering products. Common minerals that always weather congruently are halite, anhydrite, gypsum, aragonite, calcite, dolomite, and quartz. Halite, anhydrite, and gypsum are so unstable that they almost never occur in the solid load of rivers. Calcite and dolomite sometimes occur in alkaline rivers that are supersaturated with respect to these minerals; for example, rivers within the Yukon River system in Alaska (Striegl and others, 2007). Quartz (crystalline SiO_2) is the most persistent of all common primary minerals and is typically abundant in river sediments. Most silicate and sulfide minerals weather incongruently to produce both dissolved cations (Na^+, K^+, Mg^{2+}, Ca^{2+}), silica ($Si(OH)_4$), sulfate (SO_4^{2-}) and sometimes minor constituents along with solid products that are depleted in cations and usually in silica. Minerals that contain aluminum and iron typically weather incongruently to produce clays and aluminum/iron sesquioxides (oxides and hydroxides of Al^{3+} and Fe^{3+}). Magnesium, potassium and, to a lesser extent, calcium and sodium are retained in cation-rich clays such as the smectites, vermiculites, illites, and chlorites (Stallard, 1985, 1988; Stallard and Edmond, 1983, 1987; Stallard and others, 1991; Stallard, 1995a).

To this point, most studies of weathering associated with the WEBB program in eastern Puerto Rico have focused on the Río Icacos watershed, because of its homogenous granitic bedrock. As White and Blum (1995) state, "the pristine Icacos watershed in the Luquillo Mountains in eastern Puerto Rico has the fastest documented weathering rate of silicate rocks on the Earth's surface." The earliest biogeochemical work in the Icacos watershed was associated with the Luquillo Long-Term Ecological Research program (McDowell and others, 1992; McDowell and Asbury, 1994; McDowell, 1998; Bhatt and McDowell, 2007). Brown and others (1995) examined denudation rates using cosmogenic ^{10}Be in exposed bedrock, soils, and fluvial quartz and concluded that denudation rates calculated from ^{10}Be match those determined from solid and solute loads. Various aspects of chemical weathering have been examined by White and Blum (1995), Dong and others (1998), Murphy and others (1998), White and others (1998, 1999a,b), Schulz and White (1999), White (2002), Turner and others (2003), Buss and others (2004, 2005, 2008), Derry and others (2006); Fletcher and others (2006), Pett-Ridge and others (2008, 2009), Pett-Ridge (2009), and Buss and White (2012). Water quality of the measured river-borne constituents is discussed in chapter E of this report (Stallard and Murphy, 2012). McDowell and Asbury (1994) compared mass balances of the Icacos with two other rivers in the Luquillo Mountains that drain volcaniclastic rocks, the Sonadora and Toronja. Peters and others (2006) compared mass balances for 1991 to 1996 for the Icacos with rivers from each of the other four WEBB sites in the conterminous United States. Shanley and others (2011) examined 25 years of data from the Icacos starting in 1983.

Solute Loads and Chemical Erosion in Eastern Puerto Rico

Virtually all dissolved constituents in surface waters either arrive in rainfall or are acquired as water falls through vegetation and moves through soil and bedrock. Soils on the quartz-rich granitic rocks tend to be considerably thicker than soils on the volcanic and volcaniclastic rocks (see Murphy and others, 2012). Infiltration in all soils tends to be slow, and water infiltration to depths below 0.5 meters (m) takes many hours to several days, although rates are about three times as fast in soils on the granitic rocks as in soils on volcaniclastic rocks (Simon and others, 1990). At the lowest rainfall rates, water in all soils flows vertically into deeper soils, through deeper riparian zones, and then as hyporheic discharge. Water moving through these deep-soil environments typically flows past some unweathered primary minerals and relatively little organic matter. Studies of weathering in the granitic Icacos watershed demonstrate the importance of deep-flowing water in the weathering process (Turner and others, 2003; Buss and others, 2004, 2005, 2008; Fletcher and others, 2006; Buss and White, 2012). Silicon and strontium isotopes confirm

that deep-flowing water, emerging as base flow, interacts with primary minerals (Ziegler and others, 2005; Derry and others, 2006; Pett-Ridge and others, 2009). Shallow flow paths increase in relative importance with increasing rates of runoff (Derry and others, 2006; Stallard and Murphy, 2012). Similar patterns are recorded in volcaniclastic rocks (Larsen and others, 1999; Schellekens and others, 2004). At intermediate runoff rates, water also moves through shallow-soil pathways, and riparian zones are typically saturated. Shallow flow paths commonly have abundant organic matter and plant roots, but little unweathered primary minerals except for quartz. Finally, at the highest runoff rates, overland flow can become increasingly important, reducing the overall interactions of water with plant roots and deeper soil while also entraining higher particulate loads (Larsen and others, 1999; Schellekens and others, 2004; Larsen, 2012; Stallard and Murphy, 2012).

The relation between runoff and concentration of the various measured constituents is discussed in Stallard and Murphy (2012). Briefly, constituents that are not particularly bioactive and are derived from bedrock weathering or precipitation decrease in concentration with increasing runoff, reflecting the decreasing relative importance of flow paths that pass deep into the soil. Water that enters deeper soil generally passes through shallow-soil roots and is subject to more transpiration. Such constituents include sodium (Na^+), magnesium (Mg^{2+}), calcium (Ca^{2+}), silica ($Si(OH)_4$), alkalinity, and (Cl^-). Strongly bioactive constituents commonly display steady or increasing concentration with increasing runoff rates. These constituents include dissolved organic carbon (DOC), potassium (K^+), nitrate (NO_3^-), ammonium ion (NH_4^+), and phosphate (PO_4^{3-}). The concentrations of many of the bioactive constituents eventually decrease at runoff rates greater than 3 to 10 millimeters per hour (mm h^{-1}), presumably reflecting an increased dilution by rain and less-concentrated overland flow; DOC consistently increases and then decreases with increasing runoff rates. Note, however, that water interactions with vegetation (throughfall and stemflow) affect stream composition even in intense storms (Heartsill-Scalley and others, 2007). Sulfate (SO_4^{2-}) behaves like a bedrock-derived constituent in the Canóvanas, Cayaguás, and Mameyes rivers but like a bioactive constituent in the Icacos and Guabá (Stallard and Murphy, 2012).

Solid Loads and Physical Erosion in Eastern Puerto Rico

The most stable primary minerals are usually physically eroded before they have a chance to chemically decompose. Minerals that decompose contribute to the dissolved load in rivers, and their solid chemical-weathering products contribute to the secondary minerals in the solid load. The secondary minerals and the more stable primary minerals are the most important constituents of clastic sedimentary rocks. If physical erosion processes are weak, most of the erosion products are dissolved, and stable primary minerals and secondary minerals accumulate on top of bedrock to form soil (Stallard, 1985, 1988).

Landslides are a dominant component of physical erosion in steeper landscapes of eastern Puerto Rico (see Larsen, 2012), and the volume moved by landslides exceeds the volume moved by surficial erosion through mechanisms such as direct impaction by raindrops on soil, sheet wash, rill formation, and gullying. On the basis of 60 years of aerial photography, shallow landslides appear to affect approximately 1 percent of the forested eastern Puerto Rican landscape per century (Guariguata, 1990; Larsen and Torres-Sánchez, 1998). This rate is equivalent to a recurrence interval of about 10,000 years for landslides at a given site. Landslides erode remarkable quantities of solids in an exceedingly short time, typically in association with extreme rainfall events. Landslides in the Luquillo Mountains occupy a continuum from simple slumps to slides and debris flows, and most are entirely composed of soil produced by chemical weathering of bedrock.

Human activities greatly exacerbate landsliding. Aerial photographs demonstrate that landslides are much more common on deforested lands in eastern Puerto Rico (Larsen and Torres-Sánchez, 1998; Larsen and Santiago-Román, 2001). Of particular note is the agriculturally developed basin of the Río Cayaguás, on granodiorite. Here the thick soils that had developed under forest conditions were consumed by massive, regional, shallow-soil landsliding related to land clearing that lowered the landscape on average about 660 millimeters (mm) since 1820 (Larsen and Santiago-Román, 2001). This study of aerial photographs suggests that optimal factors promoting landslides are moderate to steep (>12°) slopes, sufficient rainfall, typically greater than some threshold, and nonnatural land cover, notably construction sites and roads. Road building alone increases rates of landslides sixfold to eightfold in an 85-m swath bordering the roads (Larsen and Parks, 1997).

Typical prerequisites for landslides are steep slopes and bedrock that is structurally unstable (relatively noncohesive, sheared, or fractured) or, in the case of stable bedrock, the formation of unstable soils through chemical or physical weathering. Landslides typically come in clusters that are triggered by events such as large amounts of precipitation, typically exceeding some regional slide-inducing threshold (Starkel, 1972; Caine, 1980; Scatena and Larsen, 1991; Larsen and Simon, 1993; Montgomery and Dietrich, 1994; Crosta, 1998; Reid, 1998; Molnia and Hallam, 1999; Montgomery and others, 2000; Larsen and others, 2001) or earthquakes (Simonett, 1967; Garwood and others, 1979; Keefer, 1984).

Work in the Puerto Rico WEBB program (Larsen, 2012) has focused on the landslide process and emphasizes the importance of shallow-soil landslides in physical erosion. Tropical disturbances and northern-hemisphere, wintertime cold fronts trigger most of the landslides in the Puerto Rico WEBB watersheds (Scatena and Larsen, 1991; Larsen and Simon, 1993; Larsen and Torres-Sánchez, 1998). Larsen and Simon (1993) derived an empirical landslide threshold relation, relating rainfall, P (in millimeters), to storm duration and to T (in hours) that must be exceeded for landslides to happen:

$$P\,1 \geq 91.46 \cdot T^{0.18}. \quad (1)$$

The essence of this relation is that if more than the requisite rain falls in specified time, and if the terrain is sufficiently steep (>12° slope), then there may be landslides. This relation was field tested in Puerto Rico after Hurricane Hugo in 1989 and found to be valid (Larsen and Torres-Sánchez, 1992). For storms with a duration of 24, 48, and 72 hours, the threshold rainfall is 162, 184, and 197 mm respectively, or roughly 200 mm. Stallard (1999) and Stallard and Kinner (2005) note that in the Panama Canal watershed (where runoff variation among rivers was similar to that of the Puerto Rico WEBB rivers), the transition to landslide-driven erosion is in the range of 800 mm to 1,000 mm mean-annual runoff, but that this transition might be lower in basins subjected to intense storms such as hurricanes. Accordingly, attempts to predict solid yields for wetter and drier conditions need to explicitly account for the presence or absence of landslide-producing storms at higher runoff regimes.

Without chemical weathering, there would be few landslides. Shallow-soil landslides typically occur near the interface between hard and soft saprolite, commonly on zones of weakness formed on former exfoliation surfaces that had become conduits for soil water (Simon and others, 1990). The thickness of the soil that slides is about 1 to 4 m (Simon and others, 1990; Larsen and Torres-Sánchez, 1992; Larsen and Simon, 1993; Larsen, 1997, 2012; Larsen and Santiago-Román, 2001). Landslide erosion can enrich the solute load in cations that are largely leached out of hard saprolite (Na^+ and Ca^{2+}) compared with those that partially leach (K^+ and Mg^{2+}) (Stallard, 1985, 1988). In the Icacos watershed, which is underlain by granitic rocks, an analysis of in-place-produced cosmogenic ^{10}Be in quartz as a function of grain size shows that the fine material in the river is largely derived from surficial erosion, whereas the coarse material is derived from deep erosion, presumably landslides (Brown and others, 1995). Sediment-discharge calculations indicate that about half of the river-borne quartz is derived from deep erosion.

Vegetation regrowth and succession following a landslide are quite rapid—perhaps 100 to 200 years (Guariguata, 1990; Walker and others, 1996), starting with the bare slip face. Soon after, a characteristic sequence of vegetation grows on the slide (lichens and moss, then ferns and grass, then second-growth trees, and finally mature forest), anchoring the soil. Similarly, soil development and restoration of soils to preslide nutrient conditions is on the same time scale (Zarin, 1993; Zarin and Johnson, 1995a,b). Conditions in Puerto Rico appear to be especially favorable to the rapid regrowth of vegetation; in the nearby Blue Mountains of Jamaica, plant succession appears to be much slower (Dalling and Tanner, 1995).

In addition to delivering sediment directly to rivers during storms, landslides are strong secondary sources of sediments. First, landslides normally deliver far more debris to a valley than rivers can remove in a single flood. This debris is then eroded by subsequent storms. Second, the bare slip face itself becomes a source of sediment (Larsen, 1997, 2012). Initially, sediment yield from the slip face was more than tenfold as great as yield from the adjacent forest, but after 4 to 5 years, sediment yields dropped to less than those of the forest.

Steady-State Erosion

Erosion under steady-state conditions, or dynamic equilibrium, is a useful frame of reference for studying a river system (Stallard, 1995a,b, 1998), especially in a landscape with such varied and intense physical erosion as eastern Puerto Rico. The core idea is that the geomorphic properties of the landscape are not changing substantially through time. Steady-state erosion also implies a chemical mass balance, such that the sum of the fluxes of all solid and dissolved weathering products leaving a landscape should equal the mass of bedrock being degraded by weathering. When rates of physical erosion are less than rates of the production of loose material by weathering, soils thicken. When the opposite holds true, there is net soil erosion. Human activities, mostly land clearing and agriculture, have substantially accelerated upland erosion as compared with presumed steady-state rates, causing greatly increased carbon burial in sediments (Stallard, 1998). When chemical weathering reactions control the rate of production of erodible solid materials, rates of chemical weathering and the composition of weathering products can be used to calculate yields of dissolved constituents and thus predict equilibrium yields of solids (Stallard, 1995a,b).

For the Icacos watershed, Brown and others (1995) compared rates of erosion estimated by using cosmogenic ^{10}Be to rates estimated by using chemical and sediment data for 1983–1986 from McDowell and Asbury (1994) and from the earliest years of the Puerto Rico WEBB program. The data indicated that the Icacos landscape is near a dynamic equilibrium. Chemical mass balance calculations by White and others (1998) supported this assertion. In contrast, studies of ^{10}Be in the sediments transported by the Río Cayaguás indicate that erosion rates today are considerably greater than they were in the past (Brown and others, 1998).

Carbon, Weathering, and Erosion

The largest export of carbon from watersheds is not fluvial; it is the conversion of carbon fixed into organic matter by net primary productivity back into atmospheric carbon dioxide by respiration and decay. Fluvial transport typically exports the next largest amount of carbon from a watershed (excluding agricultural and timber harvest), and this transport is tightly linked to weathering and erosion. Rivers export carbon from watersheds in four broad classes of material (Meybeck, 1993): dissolved inorganic carbon (DIC), dissolved organic carbon (DOC), and particulate organic carbon (POC) are important in the streams of Puerto Rico, whereas particulate inorganic carbon (PIC), which consists of calcium-magnesium carbonates, is not typically present in

tropical rivers because tropical waters are typically strongly undersaturated with respect to these minerals (Stallard and Edmond, 1987; Stallard and others, 1991; Stallard, 1995a). The fluvial export of carbon may be related to either inventory changes or new transfers from the atmosphere.

Carbon transport by rivers is tightly coupled with chemical and physical erosion processes. Dissolved inorganic carbon is derived from dissolved carbon dioxide that is converted to bicarbonate and carbonate ions through the chemical weathering of most silicate rocks and all carbonate rocks. In these weathering reactions, hydrogen ions are consumed and soluble cations (Na^+, K^+, Mg^{2+}, Ca^{2+}) are released (Garrels and Mackenzie, 1971). The weathering of sulfide minerals, which generates mostly insoluble sesquioxides and sulfuric acid, has the reverse effect, converting bicarbonate and carbonate ions into dissolved carbon dioxide (Garrels and Lerman, 1984).

The weathering of carbonate rocks is a source of non-atmospheric DIC (Garrels and Mackenzie, 1971; Garrels and Lerman, 1984; Meybeck, 1993). Minor carbonates are present in the granitic and volcaniclastic rocks in the study watersheds (see Murphy and others, 2012). Trace carbonate weathering in the granitic rocks in the Luquillo Mountains appears to be limited by the general advance of weathering fronts into the rocks (White and others, 1999b). My own observations suggest that no geomorphic evidence indicates preferential weathering of extensive carbonate rocks in the Luquillo Mountains, such as one sees in karst limestone landscapes of north-central Puerto Rico.

Igneous rocks do not contain fossil carbon, a conspicuous research advantage in constructing carbon budgets in the Puerto Rico WEBB watersheds. Many rivers in island arcs and orogenic belts erode organic-rich shales, and in determining POC loads, it is important to distinguish between eroded fossil carbon (kerogen) and young (soil) carbon, because the reburial of fossil carbon does not affect atmospheric carbon budget (Leithold and Blair, 2001; Blair and others, 2003; Galy and others, 2007; Hilton and others, 2008a). Carbon budget calculations for such rivers are further complicated by the oxidation of fossil carbon and pyrite during weathering, which effectively releases carbon dioxide to the atmosphere (Petsch and others 2000, 2001). In the study WEBB watersheds, we can assume that all eroded carbon is geologically young.

The export of DIC from a watershed is operationally defined and is best compared with the export of alkalinity, which is commonly equated with the bicarbonate ion in streamwater. Alkalinity is strictly the amount of anion charge per unit volume that can be titrated with a strong acid to reach the first equilibrium endpoint for the carbon dioxide system (Stumm and Morgan, 1981). Another name for alkalinity is acid-neutralization capacity. Alkalinity is a conservative property and is also equal to the total charge of nontitratable cations (which include ammonium ion at pH<9.3) minus the total charge of nontitratable anions (including NO_3^-). Alkalinity is also independent of the pH and the carbon-dioxide vapor pressure (P_{CO_2}) of the sample. If a strong base is required to titrate to the endpoint, then the alkalinity is negative and is sometimes is referred to as acidity. In this report DIC is treated as equal to alkalinity.

Dissolved organic carbon (DOC) is derived from carbon dioxide that has been "fixed" into soluble organic compounds though photosynthesis by plants and has been released as plant, fungal, or algal exudates or by the decay of biomass (Meybeck, 1993; Hedges and others, 2000; Aufdenkampe and others, 2001, 2007; Striegl and others, 2007).

Particulate organic carbon (POC) comes mostly from fragments of plant material in various stages of decay and from DOC that has become bound to surfaces of mineral grains (Hedges and others, 2000; Aufdenkampe and others, 2001, 2007). Grain-surface POC and fine-grained POC form a large component of total POC. Clay-size (<0.2 micrometer (μm)) mineral grains, including aggregated grains, have an especially large surface-area–to–volume ratio; they are most important in stabilizing organic carbon as POC. In headwater streams, such as those described here, organic carbon is largely allochthonous (soil and plant debris). In eastern Puerto Rico, surface soils in the agricultural watershed are 1 to 3 percent carbon, whereas soil carbon in the forested landscape is somewhat greater (Beinroth and others, 1992). The estimated POC yields for many mountainous rivers having high runoff and smaller drainage areas greatly exceed the global-average POC yield of 2–3 t km^{-2} yr^{-1} C (Stallard, 1998). Organic-carbon molecules range considerably in size, so the transition between DOC and POC is operational, based on the effective pore size of the filters that were used to process the sample. Most Puerto Rico WEBB samples were filtered through 0.2-μm membrane filters that rapidly clogged (appendix 2).

Landslides, Erosion, and Carbon

Landslides, including those induced by tropical disturbances, probably have a major role in the erosional export of young organic carbon to the ocean (Hilton and others, 2008a,b). Landslide erosion has many parallels with accelerated agricultural erosion, which is a substantial component of the technologically modified carbon cycle, provided that carbon eroded from agricultural lands is buried and then replaced at the site of erosion with new photosynthetic carbon (Stallard, 1998). Landslides are even more effective than agricultural erosion at removing the entire soil profile along with all of its organic carbon (Simon and others, 1990; Zarin, 1993; Zarin and Johnson, 1995a,b; Walker and others, 1996). Zarin (1993) and Zarin and Johnson (1995a,b) have documented the regeneration of soils in chronosequences of slide scars in and around the Icacos watershed. A zero-order accumulation, first-order-loss model of soil carbon for soils (Stallard, 1998, equation 5) can be applied to the soil organic carbon data of Zarin (1993) (fig. 2). It is assumed that little physical erosion occurs on the slide scar once it is stabilized by pioneer plants. It is

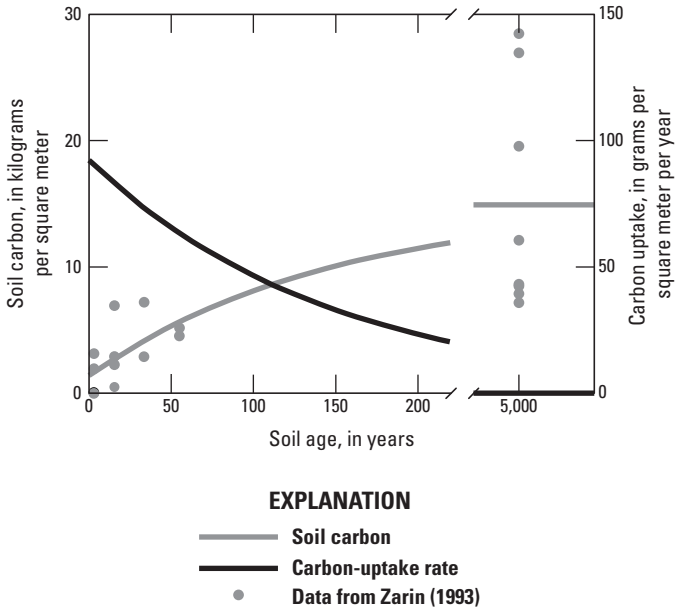

Figure 2. A zero-order accumulation, first-order-loss model of soil carbon accumulation on a chronosequence of landslides from the Luquillo Mountains based on data from Zarin (1993). This version of the model includes initial carbon on the slide face.

also assumed that the age of old soils in this dataset is a large fraction of 10,000 years, the approximate landslide recurrence interval calculated for the Luquillo Mountains. The variability of the old-soil carbon values reflects the several types of forest that eventually develop following landslides (Guariguata, 1990). The initial model soil-carbon accumulation rate for landslide scars is about 80 t km^{-2} yr^{-1} C or 6,700 kilomoles moles per square kilometer per year (kmol km^{-2} yr^{-1}) C, if one assumes minor initial carbon on the fresh scars. If the fresh slide faces are assumed to be carbon-free, initial rates are 150 t km^{-2} yr^{-1} C or 12,000 kmol km^{-2} yr^{-1} C. These fluxes represent upper limits on rates of POC generation for the eastern Puerto Rico landscape. This rate is 10 to 20 percent of net primary productivity for tropical forests, in general. The rapid regeneration of soil carbon, about half in 80 years, indicates that all POC removed from the watersheds by landslides and subsequent fluvial transport is rapidly being replaced by new carbon.

Methods Used to Assess the Effects of Weathering and Erosion in the Carbon Cycle

An analysis of weathering and erosion of bedrock and its relation to fluvial-carbon transport requires the introduction of several properties derived from the concentrations of measured constituents. For simplicity, these are referred to as "derived constituents." Two important derived constituents are dissolved bedrock and suspended bedrock, concepts that were introduced by Stallard (1995b). Dissolved bedrock (DBrx) is derived using the concentrations of various solutes to determine the quantity of original bedrock that this represents, which is then expressed as a concentration. Similarly, suspended bedrock (SBrx) is the concentration of original bedrock represented by solids in suspension. To determine DBrx and SBrx, one models atmospheric contributions to the dissolved and solid load using mass balances and reconstructions of weathering reactions. These and other derived constituents can then be used to formulate erosion models and yield-estimation procedures that can be compared among the four watersheds.

Chemical Analyses of Dissolved and Solid Phases

During 1991 to 2005 in the five rivers of the Puerto Rico WEBB program, automated samplers collected data on 507 hydrologic events from 263 storms, including all major hurricanes (Stallard and Murphy, 2012; appendix 1 of this report). A total of 4,894 samples were sufficiently analyzed to determine dissolved and solid denudation rates, and 860 of these were analyzed for a comprehensive suite of chemical constituents. Of samples analyzed for comprehensive chemistry and sediment, 543 were collected at runoff rates greater than 1 mm h^{-1}, 256 at rates exceeding 10 mm h^{-1}, and three that exceed 90 mm h^{-1}. Globally, few samples have been collected and analyzed for chemistry and suspended solids at runoff rates exceeding 1 mm h^{-1} (appendix 1). In terms of process studies, these data represents a new realm of water-quality data.

The analysis of dissolved constituents and sediment is discussed by Stallard and Murphy (2012) and in appendix 2 of this report.

Samples of soil, sediment, and bedrock, selected on the basis of freshness of exposure, were analyzed for chemical composition. Solid samples were ground using a chrome steel grinder such that they could pass through a 250 mesh (65 micrometer) stainless steel sieve. Samples were analyzed as a lithium-metaborate fused disk by X-ray fluorescence and reported as oxides (table 1). Analyses included SiO_2, Al_2O_3, CaO, MgO, Na_2O, K_2O, Fe_2O_3, MnO, TiO_2, and P_2O_5, and loss on ignition (LOI) with a detection limit of 0.01 percent, and Ba, Nb, Rb, Sr, Y, and Zr with a detection limit of 10 parts per million (ppm). Cr_2O_3 was analyzed to check for grinder contamination, which proved negligible. Ba and Nb were generally below detection and are not included in table 1. In addition, some samples were analyzed for ferrous iron (FeO in table 1), CO_2, H_2O^+, and H_2O^- by wet chemistry and for sulfur and chloride by pressed-pellet X-ray fluorescence. Analyses were performed at XRAL Activations Services, Ann Arbor, Michigan.

Table 1. X-ray fluorescence and wet-chemical analysis of geologic materials and water from the Luquillo Mountains, eastern Puerto Rico.

[Units are percent unless otherwise noted; LOI, loss on ignition; --, not analyzed]

Description	SiO_2	Al_2O_3	CaO	MgO	Na_2O	K_2O	Fe_2O_3	MnO	TiO_2	P_2O_5	S	Cl[1]	LOI	H_2O^+	H_2O^-	CO_2	FeO	Rb[1]	Sr[1]	Zr[1]
Solids																				
Quartz diorite, Icacos Route 191, lower road	61.1	17.6	7.18	2.50	3.36	1.23	6.85	0.14	0.56	0.09	--	--	0.69	--	--	--	--	37	223	62
Quartz diorite, landslide 43 [2]	64.2	16.6	6.17	2.13	3.56	1.39	5.96	0.13	0.44	0.09	--	--	0.60	--	--	--	--	37	220	76
Quartz diorite, landslide 43	63.4	16.9	6.04	2.10	3.53	1.25	6.53	0.14	0.471	0.12	0.06	0.05	0.34	0.8	0.2	0.01	4.0	38	232	78
Quartz diorite, landslide 43	62.4	16.8	6.05	2.27	3.42	1.22	6.60	0.14	0.47	0.12	0.1	0.05	0.46	0.7	0.2	0.0	4.1	39	226	79
Xenolith in quartz diorite, landslide 43	55.2	12.0	6.19	6.00	2.11	1.97	14.70	0.36	1.156	0.24	0.06	0.09	0.72	1.4	0.2	0.02	9.4	64	84	164
Xenolith in quartz diorite, landslide 43	56.6	15.3	7.21	5.30	3.30	1.20	9.17	0.27	0.78	0.21	0.2	0.06	0.82	1.2	0.2	0.0	6.6	34	173	145
Aplite vein in quartz diorite, landslide 43	64.4	20.1	3.01	0.14	5.72	4.56	1.19	0.02	0.097	0.02	0.22	0.02	0.39	0.3	0.2	0.01	0.7	49	230	187
Volcanic rock, landslide 8 [3]	49.1	17.4	8.93	6.64	3.84	0.52	9.78	0.14	0.83	0.11	--	--	3.47	--	--	--	--	0	615	60
Volcanic rock, landslide 8	50.9	14.4	9.82	7.82	2.00	0.43	8.11	0.12	0.78	0.14	0.1	0.01	4.27	4.1	0.4	0.6	6.1	0	402	65
Volcanic rock, landslide 8	51.4	14.1	9.19	7.78	2.10	0.45	8.02	0.12	0.822	0.16	0.09	0.01	4.00	3.9	0.3	0.50	6.0	19	416	61
Volcanic rock, landslide 8	50.4	14.1	10.10	7.80	1.99	0.47	8.27	0.12	0.76	0.15	0.1	0.01	4.46	3.8	0.3	1.1	6.3	19	406	70
Granitic rock, surface soil, on divide, landslide 43	70.3	11.7	0.03	0.12	0.08	0.25	0.91	0.03	0.48	0.03	--	--	14.35	--	--	--	--	31	0	226
Granitic rock, surface soil, mid-slope, landslide 43	63.2	14.4	0.25	0.20	0.00	0.23	4.65	0.03	0.52	0.04	0.0	0.02	15.34	10.0	1.8	0.0	0.9	9	0	256
Icacos gage, sand sample	79.3	6.9	0.98	1.00	0.33	0.41	7.55	0.10	0.54	0.03	--	--	2.99	--	--	--	--	24	9	557
Icacos gage, overbank sediment	36.6	28.1	0.58	0.76	0.22	0.46	12.90	0.17	0.890	0.13	--	--	20.40	--	--	--	--	16	39	140
Volcaniclastic rock, surface soil, landslide 8	46.8	19.6	0.34	0.44	0.04	0.27	10.25	0.02	1.527	0.09	0.03	0.02	20.64	13.2	3.1	0.00	1.7	19	43	161
Dissolved bedrock oxide concentrations, calculated as described in the text																				
Canóvanas, dissolved bedrock	43.6	--	30.5	13.2	9.45	2.49	--	--	--	0.06	0.69	--	--	--	--	--	--	--	--	--
Cayaguás, dissolved bedrock	54.3	--	18.0	5.67	15.1	5.20	--	--	--	0.09	1.67	--	--	--	--	--	--	--	--	--
Mameyes, dissolved bedrock	54.0	--	28.8	6.39	7.25	2.35	--	--	--	0.04	1.17	--	--	--	--	--	--	--	--	--
Icacos, dissolved bedrock	64.9	--	17.5	5.13	9.65	2.84	--	--	--	0.02	0.00	--	--	--	--	--	--	--	--	--
Guabá, dissolved bedrock	71.0	--	12.9	3.30	9.92	2.88	--	--	--	0.02	0.0	--	--	--	--	--	--	--	--	--

[1]Parts per million.

[2]Landslide 43 of Guariguata and Larsen (1990) is located in the Icacos watershed, at the first large stream crossing on Route 191, west side.

[3]Landslide 8 of Guariguata and Larsen (1990) is located on Route 988, about 1 kilometer west of the Mameyes gage site.

Estimation of Constituent Yields

The loads and yields (loads divided by watershed area) of most constituents, including derived constituents, were calculated using LOADEST (load estimator; Runkel and others, 2004) as described in Stallard and Murphy (2012) and in appendix 1. The process involved merging thousands of chemical measurements with nearly continuous discharge measurements calculated from stage recordings. LOADEST was used to estimate constituent yields for hourly and yearly intervals and for the entire study period (15 years in the Canóvanas, Cayaguás, Mameyes, and Icacos rivers and 10 years in the Guabá; tables 2, 3; figs 3–6).

Alkalinity can have negative values because of addition of organic acids from soil process and sulfuric and nitric acids from rain. LOADEST, because it works with

Table 2. Discharge-weighted average concentrations of each percentile class estimated by using LOADEST and hourly discharge from study watersheds, eastern Puerto Rico.

[DIC, dissolved inorganic carbon; DOC, dissolved organic carbon; POC, particulate organic carbon; LOI, loss on ignition; mm h^{-1}, millimeters per hour; mg L^{-1}, milligrams per liter; µmol L^{-1}, micromoles per liter]

Sample percentile class	Runoff rate (mm hr^{-1})	SiO_2 (mg L^{-1})	Bedrock Na_2O (mg L^{-1})	Dissolved bedrock (mg L^{-1})	Suspended bedrock (mg L^{-1})	DIC (µmol L^{-1})	DOC (µmol L^{-1})	POC (µmol L^{-1})	LOI (percent of suspended solids)	POC (percent of suspended solids)
					Canóvanas					
0–10 percent	0.021	34.8	9.9	90	8	2,044	164	19	23	2.3
>10–25 percent	0.061	29.3	6.8	70	24	1,450	232	51	20	2.1
>25–50 percent	0.158	24.7	4.9	55	72	1,035	299	139	18	1.9
>50–75 percent	0.765	17.5	3.2	37	380	586	414	647	15	1.7
>75–90 percent	4.49	12.4	2.5	26	1,050	349	420	1,786	15	1.7
>90–95 percent	15.3	9.6	2.3	20	1,489	282	374	2,669	17	1.8
>95–99 percent	32.0	8.3	2.3	18	1,669	265	323	3,141	18	1.8
>99–100 percent	59.2	7.1	2.3	16	1,723	254	266	3,457	20	1.9
					Cayaguás					
0–10 percent	0.041	40.9	18.2	83	12	1,395	123	14	11	1.3
>10–25 percent	0.095	35.6	11.7	67	37	997	168	37	10	1.1
>25–50 percent	0.195	29.6	7.6	53	128	669	221	116	8	1.0
>50–75 percent	0.860	18.9	3.4	31	995	250	312	806	6	0.9
>75–90 percent	4.35	11.2	1.8	19	3,237	80	324	2,580	6	0.9
>90–95 percent	12.1	7.6	1.4	13	5,366	48	278	4,287	6	0.9
>95–99 percent	26.2	5.5	1.2	10	6,727	38	231	5,391	6	0.9
>99–100 percent	41.0	4.7	1.1	9	6,484	33	212	5,015	7	0.9
					Mameyes					
0–10 percent	0.068	34.3	5.1	61	1	914	80	5	35	3.5
>10–25 percent	0.179	22.3	3.2	41	3	615	133	13	32	3.2
>25–50 percent	0.324	17.8	2.3	32	9	469	178	30	28	2.8
>50–75 percent	0.887	12.3	1.4	22	43	297	245	111	23	2.4
>75–90 percent	2.81	8.3	0.9	15	176	173	308	362	19	2.0
>90–95 percent	7.26	5.9	0.8	11	479	106	358	835	15	1.8
>95–99 percent	21.2	4.2	0.8	8	1,101	61	347	1,692	14	1.6
>99–100 percent	45.6	3.2	0.7	6	1,778	42	320	2,540	13	1.5
					Icacos					
0–10 percent	0.115	28.6	3.7	41	3	426	75	9	30	2.8
>10–25 percent	0.252	19.9	2.7	30	8	332	125	24	27	2.7
>25–50 percent	0.429	15.4	2.2	24	21	265	186	58	24	2.5
>50–75 percent	1.197	9.3	1.6	15	139	165	299	269	18	1.9
>75–90 percent	3.96	5.2	1.1	9	728	79	368	983	12	1.4
>90–95 percent	9.04	3.6	0.8	6	1,901	41	349	1,998	10	1.1
>95–99 percent	20.8	2.4	0.7	4	5,291	17	285	3,830	6	0.8
>99–100 percent	51.6	1.5	0.5	3	21,372	–2	149	7,811	3	0.4
					Guabá					
0–10 percent	0.104	26.6	3.2	36.1	4	321	79	14	29	2.9
>10–25 percent	0.250	18.8	2.4	26.1	12	235	120	38	27	2.7
>25–50 percent	0.383	15.8	2.0	22.1	28	194	142	76	25	2.5
>50–75 percent	0.950	10.28	1.5	15.0	161	130	205	326	19	2.0
>75–90 percent	4.48	5.00	1.0	8.0	1,275	59	265	1,801	13	1.5
>90–95 percent	14.48	3.03	0.8	5.3	2,956	30	264	3,621	11	1.3
>95–99 percent	33.1	2.03	0.8	3.9	4,484	16	259	4,998	9	1.2
>99–100 percent	68.6	1.50	0.9	3.1	6,299	8	223	6,667	8	1.2

Table 3. Average annual net, atmospheric, and bedrock inputs in 1991 to 2005 to study watersheds, eastern Puerto Rico.

[DOC, dissolved organic carbon; POC, particulate organic carbon; DBrx, dissolved bedrock; SBrx, suspended bedrock; mm yr^{-1}, millimeters per year; kmol km^{-2} yr^{-1}, kilomoles per square kilometer per year; kEq km^{-2} yr^{-1}, kiloequivalents per square kilometer per year; t km^{-2} yr^{-1}, metric tons per square kilometer per year; -- not analyzed]

Watershed	Runoff (mm yr^{-1})	Na^+	K^+	Mg^{2+}	Ca^{2+}	$Si(OH)_4$	Cl^-	SO_4^{2-}	NO_3^-	NH_4^+	$-PO_4^{3-}$	Alkalinity (kEq km^{-2} yr^{-1})	DOC (kmol km^{-2} yr^{-1})	POC (kmol km^{-2} yr^{-1})	DBrx (t km^{-2} yr^{-1})	SBrx (t km^{-2} yr^{-1})
		(kmol km^{-2} yr^{-1})														
Annual net yields																
Canóvanas	970	417	31.8	193	280	357	324	43.8	43.5	3.6	0.39	918	313	627	47.0	355
Cayaguás	1,620	672	88.1	136	249	662	411	78.1	81.5	4.4	0.94	865	389	1,594	72.6	1,979
Mameyes	2,750	634	50.7	174	439	739	541	84.5	26.1	2.1	0.41	1,137	573	503	87.3	270
Icacos	3,760	733	58.1	150	264	853	585	54.4	44.5	3.7	0.18	800	837	1,787	78.0	1,983
Guabá	3,630	657	54.0	109	173	779	623	42.7	38.9	2.6	0.18	502	576	2,282	67.0	1,717
Annual atmospheric inputs																
Canóvanas	970	276	5.8	31	13	0	324	32.8	18.8	7.2	--	–32	313	627	0.0	21
Cayaguás	1,620	350	7.4	40	14	0	411	41.7	23.9	9.1	--	–44	389	1,594	0.0	21
Mameyes	2,750	461	9.7	52	17	0	541	54.9	31.5	12.0	--	–61	573	503	0.0	21
Icacos	3,760	498	10.5	57	17	0	585	59.3	34.0	13.0	--	–67	837	1,787	0.0	21
Guabá	3,630	531	11.2	60	18	0	623	63.2	36.3	13.8	--	–73	576	2,282	0.0	21
Annual bedrock-derived/non-rain-derived yields[1]																
Canóvanas	970	141	26.0	162	267	357	0	11.0	24.7	–3.6	--	950	0	0	47.0	334
Cayaguás	1,620	322	80.8	96	235	662	0	36.4	57.6	–4.7	--	908	0	0	72.6	1,958
Mameyes	2,750	173	41.0	122	422	739	0	29.6	–5.4	–9.9	--	1,199	0	0	87.3	249
Icacos	3,760	235	47.7	93	246	853	0	–4.9	10.5	–9.3	--	867	0	0	78.0	1,962
Guabá	3,630	126	42.9	49	154	779	0	–20.6	2.6	–11.2	--	574	0	0	67.0	1,696

Watershed	Runoff (mm yr^{-1})	Na^+	K^+	Mg^{2+}	Ca^{2+}	$Si(OH)_4$	Cl^-	SO_4^{2-}	NO_3^-	NH_4^+	$-PO_4^{3-}$	Alkalinity	DOC	POC	DBrx	SBrx
		(percent)														
Atmospheric inputs as percentage of net yield																
Canóvanas	970	66	18	16	4	0	100	75	43	201	--	–3	100	100	0	6
Cayaguás	1,620	52	8	29	6	0	100	53	29	207	--	–5	100	100	0	1
Mameyes	2,750	73	19	30	4	0	100	65	121	582	--	–5	100	100	0	8
Icacos	3,760	68	18	38	7	0	100	109	76	353	--	–8	100	100	0	1
Guabá	3,630	81	21	55	11	0	100	148	93	534	--	–14	100	100	0	1

[1]Negative values indicate that atmospheric input exceeds river export.

logarithmic transforms of the data, cannot handle situations with legitimate negative values. Instead, alkalinity loads and average concentrations were calculated using the loads and concentrations of other constituents as estimated by LOADEST (concentrations in mole units):

$$\text{alkalinity} = Na^+ + K^+ + NH_4^+ + 2\bullet(Mg^{2+} + Ca^{2+} + Sr^{2+}) - (Cl^- + NO_3^- + 2\bullet SO_4^{2-} + Z_{DOC}\bullet DOC) \quad (2)$$

where Z_{DOC} is the negative charge per carbon atom in DOC. For each river, Z_{DOC} was calculated by adjusting predicted alkalinity to measured alkalinity such that the ratio of averages was 1:1. The range of estimated values was 0.5 equivalents of charge per mole (eq mol^{-1}) to 0.8 eq mol^{-1} (appendix 1). For reference, Tardy and others (2005) found an optimal Z_{DOC} of 0.64 eq mol^{-1} for Amazonian lowland rivers.

Data Manipulation and Processing of Dissolved Constituents

One of the main motivations for introducing derived constituents is the need to subtract atmospherically derived contributions to the dissolved load, much of it seasalt, from bedrock-derived contributions. This subtraction is also termed a cyclic-salt correction (Stallard and Edmond, 1981, 1983). Once such a subtraction is accomplished, it is possible to calculate DBrx, which when combined with SBrx, can be used to accurately estimate erosion and determine whether erosion is in disequilibrium.

Correction for Atmospherically Derived Contributions to the Dissolved and Solid Load

A substantial portion of the dissolved load in rivers is derived from the atmosphere. Historically, estimates of denudation have not corrected for this component. One atmospheric source is precipitation; another is direct transfer from the atmosphere to plant and ground surfaces by impaction and dry deposition. Another pathway is "fixation" from the gas phase into a solid or soluble form by biological processes, mostly photosynthesis and nitrogen fixation. Finally, chemical weathering involves fixation of water and carbon dioxide from the atmosphere into dissolved ionic forms and into soil minerals as structural or bound water. In the eastern Puerto Rico watersheds, which are underlain almost entirely by igneous rocks, virtually all the inorganic and organic carbon is atmospherically derived. The same is true for all forms of nitrogen. Almost all river-borne Cl^- has a seasalt origin, and almost all ions that are abundant in surface seawater make considerable atmospheric contributions to the dissolved load. Biogenic gases and pollution contribute SO_4^{2-}, NO_3^-, and NH_4^+. Desert dust contributes notable amounts of soluble calcium (see Stallard, 2012).

Atmospheric sources also contribute to the solid load. All of the organic carbon and much of the water bound into clays in river-borne sediment has an atmospheric origin (table 1, LOI, H_2O^+, H_2O^-). For reference, kaolinite and halloysite ($Al_2Si_2O_5(OH)_4$) are 14.0 percent by weight water. Clays and other minerals in desert dust also make a minor contribution to the solid load (Pett-Ridge, 2009; Stallard, 2012).

In order to estimate bedrock contributions to the dissolved load, the major cations (Na^+, K^+, Mg^{2+}, Ca^{2+}), and SO_4^{2-} require corrections for atmospheric inputs. For Na^+, K^+, and Mg^{2+}, the correction involves subtracting a seasalt contribution on the basis of the ratio of that ion to Cl^- either in rain or in seasalt. If we use Na^+ as an example, the Na^+:Cl^- mole ratio for seasalt is 0.8525:

$$Na^* = Na^{2+} - (Na^+{:}Cl^-)\bullet Cl^-. \quad (3)$$

The "*" designates a calculated bedrock-derived constituent. The Mg^{2+}:Cl^- ratio in rain is 0.09689, less than the seasalt ratio of 0.10145 (Stallard, 2012). The seasalt SO_4^{2-}:Cl^- ratio is 0.052, and in some storms, especially high-chloride events, the rain and runoff are near this ratio (Stallard and Murphy, 2012, their fig. 10). However, additional sulfur comes from pollution and emissions of organic sulfur compounds (dimethyl sulfide and methyl sulfide) from the marine environment. To further complicate matters, the forest environment may also emit organic sulfur compounds back to the atmosphere (Stallard and Edmond, 1981; Stallard and Murphy, 2012). The overall SO_4^{2-}:Cl^- ratio is 0.10614 in rain, and this ratio was used in calculations. The K^+:Cl^- ratio in rain is 0.02306, whereas the seasalt ratio is 0.0179. Because throughfall is so rich in K^+ (Heartsill-Scalley and others, 2007), the greater rain ratio is seen as reflecting local, minor plant contamination, so the seasalt ratio was used. The Ca^{2+}:Cl^- ratio is 0.01876, and seasalt is a minor contributor to the calcium budget.

In individual samples, the atmospheric-correction calculation occasionally yields a negative value. This result may be due to real processes, such as cation exchange in soil that can alter cation proportions, or it may be due to true variations in the ratios to Cl^- for individual storms, as happens with SO_4^{2-}. In constructing annual and long-term budgets, the atmospheric corrections incorporate calculated yields using the Cl^- yield as the basis for the correction. The calculation was checked against LOADEST calculations of Na* and Ca*.

Constituent yields estimated using LOADEST were compared with atmospheric inputs (Stallard, 2012) (table 3). Several constituents (Na^+, Cl^-, SO_4^{2-}, and NO_3^- plus NH_4^+, DOC, and POC) are largely atmospheric in origin. Potassium and Mg^{2+} receive a contribution of about 10 to 50 percent from the atmosphere. Calcium, silica, dissolved bedrock, and suspended bedrock receive minor atmospheric contributions, 0 to about 10 percent. Alkalinity has a small negative atmospheric contribution; in essence, acidity in rain is titrating the landscape. The atmospheric contribution for phosphate, which is quite large (Pett-Ridge, 2009), was not included in table 3; phosphate is biologically and chemically quite reactive, and without more information it would be hard to apportion atmospheric inputs to the dissolved or solid load.

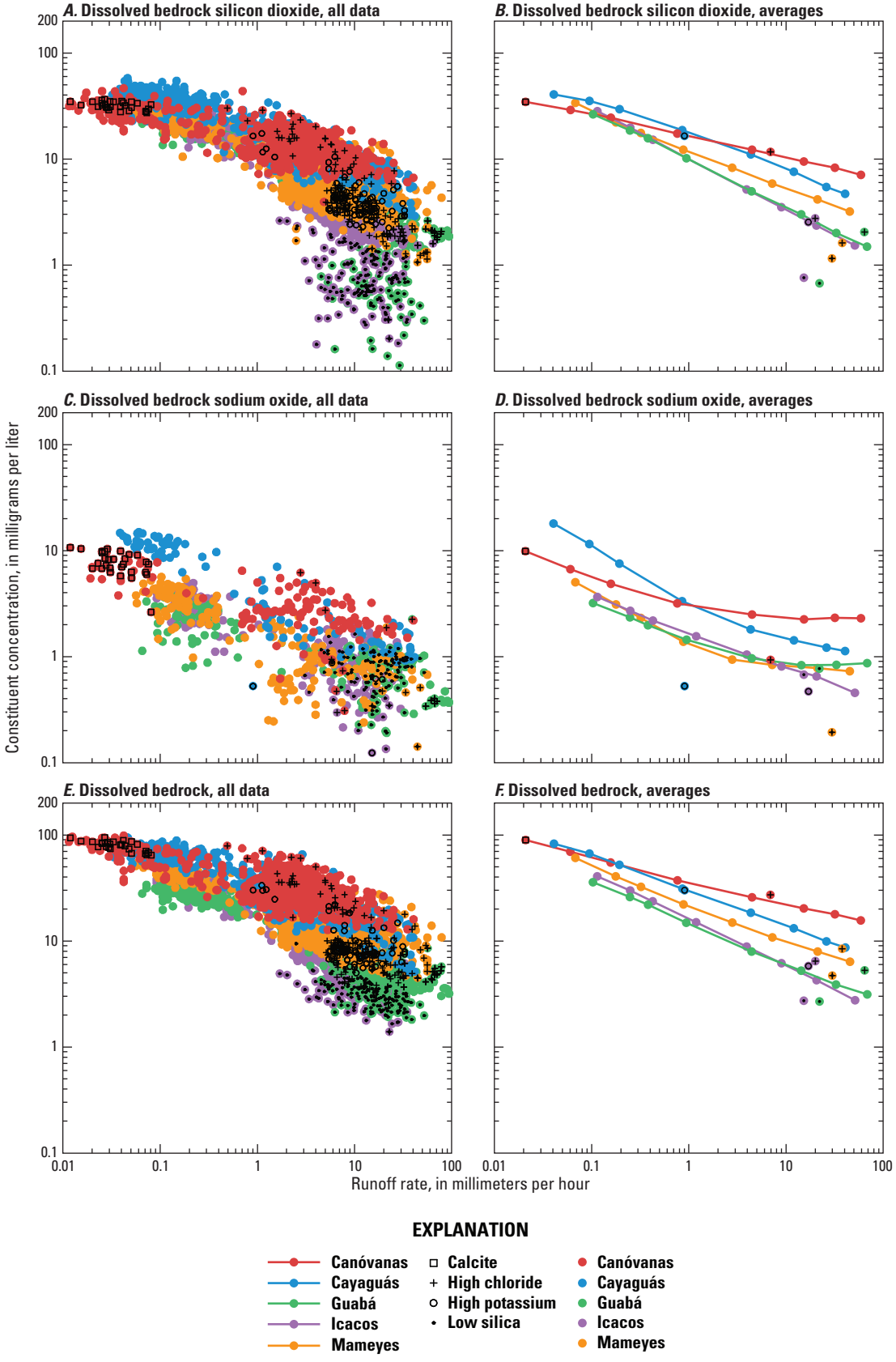
A. Dissolved bedrock silicon dioxide, all data
B. Dissolved bedrock silicon dioxide, averages
C. Dissolved bedrock sodium oxide, all data
D. Dissolved bedrock sodium oxide, averages
E. Dissolved bedrock, all data
F. Dissolved bedrock, averages
Constituent concentration, in milligrams per liter
Runoff rate, in millimeters per hour
200
100
10
1
0.1
0.01
0.1
1
10
100
EXPLANATION
Canóvanas
Cayaguás
Guabá
Icacos
Mameyes
Calcite
High chloride
High potassium
Low silica
Canóvanas
Cayaguás
Guabá
Icacos
Mameyes

Figure 3. (facing page) The concentration of dissolved silicate bedrock (DBrx) and two dissolved constituents, bedrock Na_2O and silicon dioxide, Na_2O, used in calculating DBrx and in estimating equilibrium physical denudation rates in eastern Puerto Rico. Bedrock Na_2O is dissolved sodium ion, Na^+, corrected for seasalt sodium, and then expressed as an oxide. SiO_2 is dissolved silica, $Si(OH)_4$, expressed as an oxide. DBrx is the sum of all bedrock-derived cations, expressed as oxides or sulfide, after correction for atmospheric inputs. The left panels represent the WEBB dataset. The right panels represent averages calculated from hourly estimates determined using LOADEST. For a number of samples, additional sample characteristics are indicated with black symbols. These categories are discussed in detail in Stallard and Murphy (2012): calcite, samples supersaturated with respect to calcite; high chloride, samples with exceptionally high chloride concentrations collected during huge storms; high potassium, samples with high potassium but not high chloride; low silica, Icacos and Guabá samples with unusually low silica concentrations for the runoff rate. The points separated from the sample-average curves represent the averages of the classes of sample indicated by the superimposed character. These samples are not included in LOADEST models.

Sahara dust brings in additional Ca^{2+} and insoluble clays (Stallard, 2012). Because this Ca^{2+} is also a minor part of the overall Ca^{2+} budget, and because the dust fallout comes from variable long-range transport, a uniform dust correction (6.4 kmol km^{-2} Ca) was subtracted from the final Ca^{2+} budget for each watershed. All silicon, aluminum, and iron in Sahara dust were assumed to reside in nonreactive clays and sesquioxides and therefore to be insoluble (Stallard, 2012; Stallard and Murphy, 2012). Sahara dust deposition rates of 21 t km^{-2} yr^{-1} estimated by Pett-Ridge and others (2009) were subtracted equally from the solid bedrock yields for all study watersheds.

Total Dissolved Bedrock

Solute denudation rates were calculated using the approach of Stallard (1995a,b) that expresses the concentrations of most bedrock-derived constituents as dissolved oxides for mass-balance calculations. Silica and each cation, after correction for atmospheric inputs, were converted into a mass concentration of the corresponding bedrock oxide. For example, the calculation of dissolved sodium concentration expressed as an oxide ($Na_2O[d]$) (table 2) from bedrock-derived sodium, Na*, was performed as follows:

$$Na_2O[d]\ (\text{mg L}^{-1}) = 0.03098 \bullet Na^*\ (\mu\text{mol L}^{-1}), \quad (4)$$

where mg L^{-1} is milligrams per liter, and µmol L^{-1} is micromoles per liter.

Dissolved SO_4^{2-} was converted into sulfide. The concentrations of the dissolved oxides and sulfide were summed to get total dissolved bedrock (DBrx) (fig. 3; tables 2, 3). If the bedrock of a watershed were to contain abundant carbonate rocks, for which the charge of Ca^{2+} and Mg^{2+} is balanced by carbonate ions (CO_3^{2-}) rather than oxygen (O^{2-}), the amount of dissolved bedrock would be markedly underestimated.

In addition to calculating DBrx of samples with complete chemistry (about 870 samples), DBrx was also estimated in all samples for which conductivity, Cl^-, and $Si(OH)_4$ were measured (about 3,780 samples). This calculation involved three steps. First, the bedrock contribution to conductivity was estimated by subtracting an atmospheric contribution, which was calculated by using a factor determined by estimating the conductivity of water having ions in the atmospheric-correction ratios to Cl^- just indicated, and by using the specific conductivities of each ion (appendix 1):

$$\text{conductivity}^* = \text{conductivity} - 0.13028 \bullet Cl^-. \quad (5)$$

The relation between conductivity* and total bedrock-derived cation charge, ZBrx, is estimated through a regression that used the 1,040 completely analyzed samples. A single set of regression coefficients worked for all Puerto Rico WEBB rivers:

$$ZBrx = a \bullet (\text{conductivity}^*)^b, \quad (6)$$

where a (1.08612) and b (0.83239) were regression coefficients (coefficient of determination (r^2) = 0.96). Using ZBrx, an estimated total dissolved bedrock, DBrx′, was determined by

$$DBrx' = c \bullet (ZBrx)^d + SiO_2[d], \quad (7)$$

where c and d are regression coefficients determined for each river (table 3 in appendix 1), and $SiO_2[d]$ is the dissolved silica concentration expressed as an oxide (table 2, fig. 3):

$$SiO_2[d]\ (\text{mg L}^{-1}) = 0.06008 \bullet Si(OH)_4\ (\mu\text{mol L}^{-1}). \quad (8)$$

The correlation between DBrx′ and DBrx for all 1,040 samples is $r^2 = 0.990$; between log(DBrx′) and log(DBrx), $r^2 = 0.986$. About 4,650 samples were used in load calculations for both DBrx and DBrx′, providing a rigorous estimate of dissolved bedrock erosion (table 2).

Equilibrium Model: Calculating Steady-State Erosion from Dissolved Bedrock

When chemical weathering reactions control the rate of production of solid materials, the yields of dissolved constituents can be used to predict equilibrium yields of solids (Stallard, 1995a,b). The sodium-to-silica ratio of the dissolved and solid load compared with the ratio in bedrock (after correction for atmospheric inputs) is especially useful.

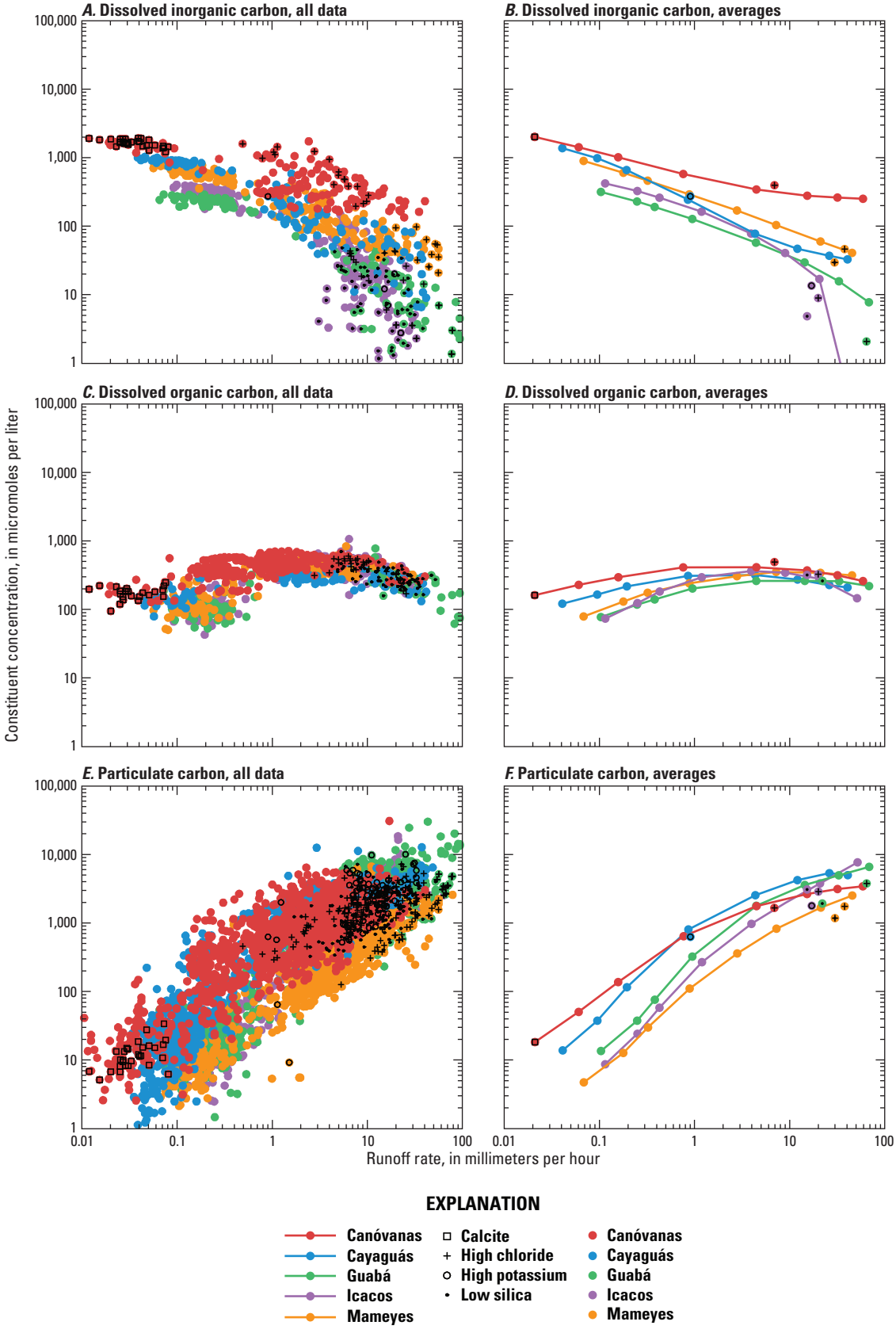
A. Dissolved inorganic carbon, all data
B. Dissolved inorganic carbon, averages
C. Dissolved organic carbon, all data
D. Dissolved organic carbon, averages
E. Particulate carbon, all data
F. Particulate carbon, averages
Constituent concentration, in micromoles per liter
Runoff rate, in millimeters per hour
100,000
10,000
1,000
100
10
1
0.01
0.1
1
10
100
EXPLANATION
Canóvanas
Cayaguás
Guabá
Icacos
Mameyes
Calcite
High chloride
High potassium
Low silica

Figure 4. (facing page) The concentration of the three major components of carbon transport in tropical rivers in eastern Puerto Rico: dissolved inorganic carbon (DIC = alkalinity), dissolved organic carbon (DOC), and particulate organic carbon (POC). The left panels represent the WEBB dataset. The right panels represent averages calculated from hourly estimates determined using LOADEST. For a number of samples, additional sample characteristics are indicated with black symbols: calcite, samples supersaturated with respect to calcite; high chloride, samples with exceptionally high chloride concentrations collected during huge storms; high potassium, samples with high potassium but not high chloride; low silica, Icacos and Guabá samples with unusually low silica concentrations for the runoff rate. The points separated from the sample-average curves represent the averages of the classes of sample indicated by the superimposed character. These samples are not included in LOADEST models.

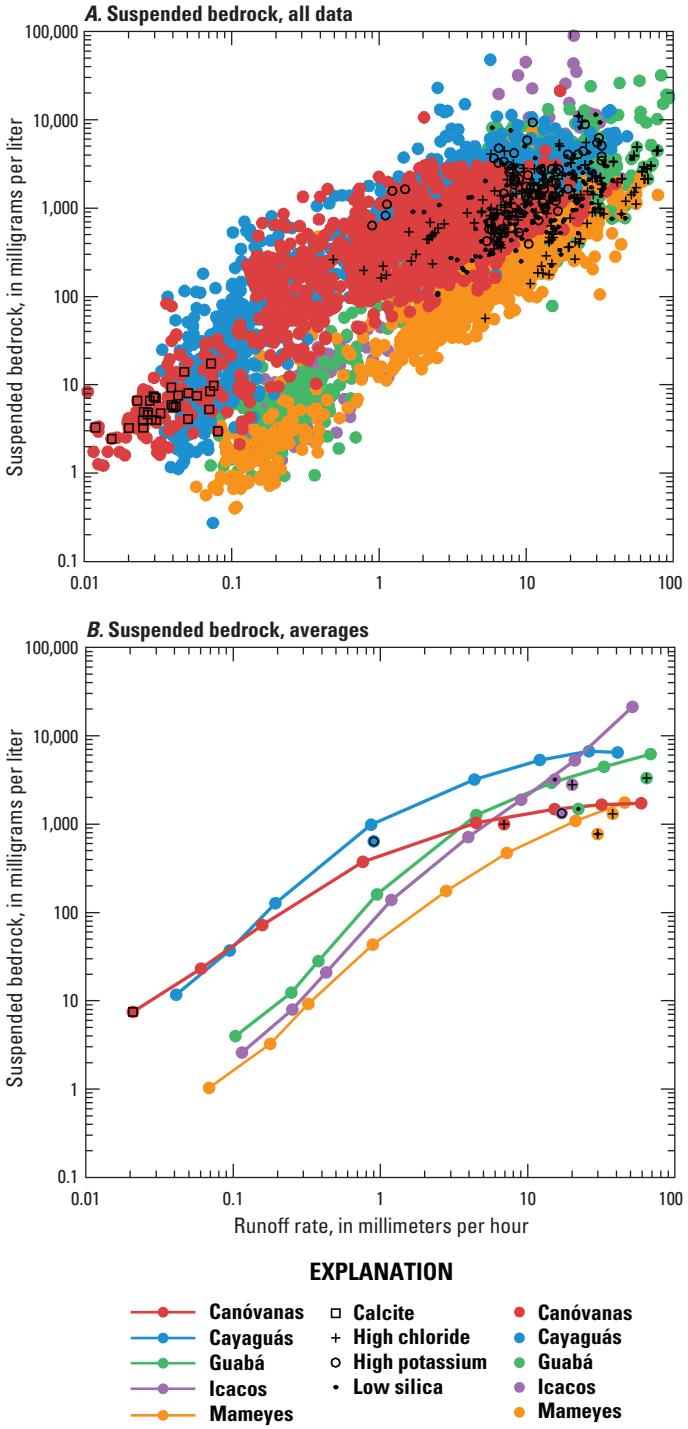

Figure 5. The concentration of an operationally derived constituent, suspended bedrock (SBrx) used in calculating physical denudation rates in eastern Puerto Rico. SBrx is the mass of the sample after heating to 550°C. For a number of samples, additional sample characteristics are indicated with black symbols: calcite, samples supersaturated with respect to calcite; high chloride, samples with exceptionally high chloride concentrations collected during huge storms; high potassium, samples with high potassium but not high chloride; low silica, Icacos and Guabá samples with unusually low silica concentrations for the runoff rate. The points separated from the sample-average curves represent the averages of the classes of sample indicated by the superimposed character. These samples are not included in LOADEST models.

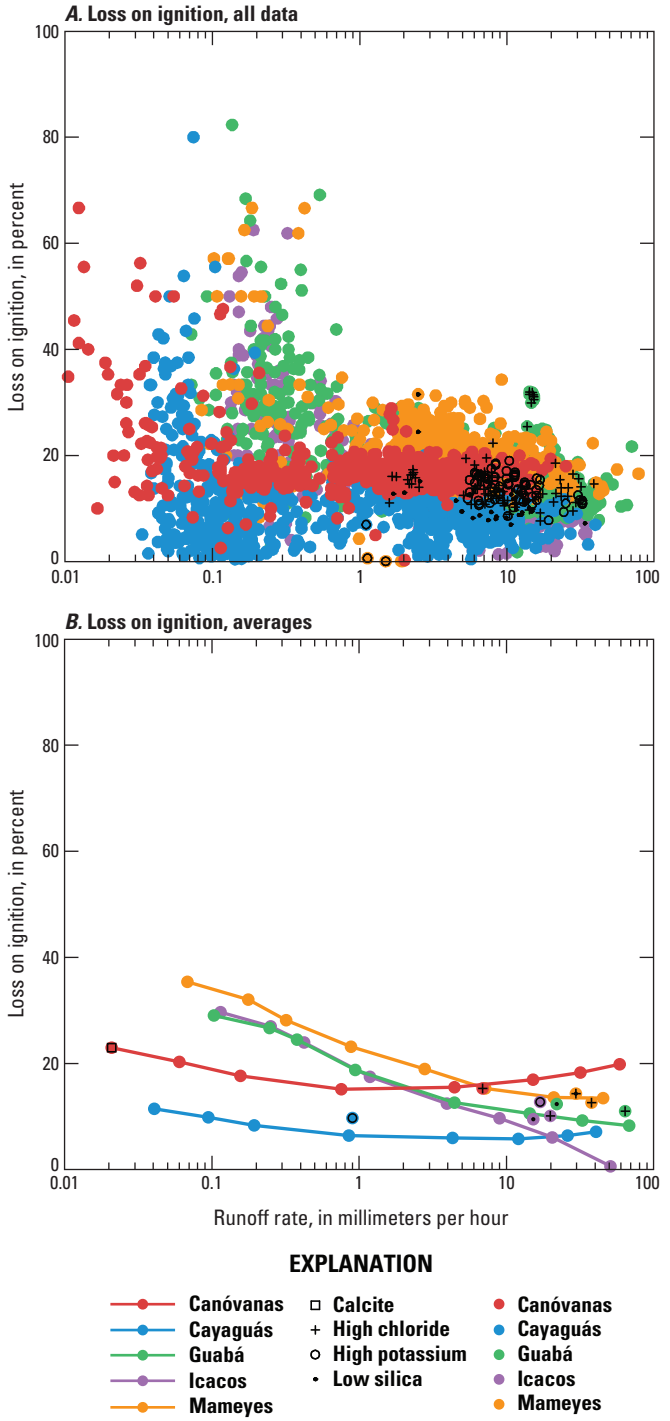

Figure 6. Percent loss on ignition (LOI). For a number of samples, additional sample characteristics are indicated with black symbols: calcite, samples supersaturated with respect to calcite; high chloride, samples with exceptionally high chloride concentrations collected during huge storms; high potassium, samples with high potassium but not high chloride; low silica, Icacos and Guabá samples with unusually low silica concentrations for the runoff rate. The points separated from the sample-average curves represent the averages of the classes of sample indicated by the superimposed character. These samples are not included in LOADEST models.

In headwater streams, such as those studied in eastern Puerto Rico, neither sodium nor silica are particularly bioactive; igneous and metamorphic rocks have a narrow range of sodium-to-silica ratios, and sodium weathers out of bedrock sufficiently early in the weathering process, such that the sodium-to-silica ratios of solid weathering products are quite low (table 1) throughout the soil profile and as river-borne sediments. Calcium shares most of these characteristics, except that the calcium-to-silica ratio ranges more widely in igneous and metamorphic rocks and is influenced by carbonate rocks (Stallard, 1995a).

To calculate the proportions of dissolved and solid weathering products that are being produced, one needs to express the compositions of bedrock, river-borne solids, and bedrock-derived solutes as weight-percent oxides. This goal is simple for the solid phases, because bulk analyses are normally reported this way (table 1). For solutes, the concentration of dissolved bedrock oxides, calculated as described earlier (for example, equation 4), must be normalized to total 100 percent (table 4):

$$Na_2O[d'] = 100 \bullet Na_2O[d] / DBrx \, . \qquad (9)$$

Following Stallard (1995a, equations 3 and 5 of that report), the leaching efficiency of bedrock, W, is the ratio of the yield of bedrock weathered into solution, Y_{DBrx}, to the yield of total bedrock weathered, $Y_{DBrx} + Y_{SBrx}$:

$$W = Y_{DBrx} / (Y_{DBrx} + Y_{SBrx}) \, . \qquad (10)$$

The hypothetical yield of solid weathering products, Y'_{SBrx}, expressed in terms of the observed yield of dissolved weathering products, Y_{DBrx}, is given by

$$Y'_{SBrx} = Y_{DBrx} \bullet (1-W)/ W \, . \qquad (11)$$

Similarly, the efficiency of leaching of silica, W_{Si}, is given by

$$W_{Si} = W \bullet SiO_2[d'] / SiO_2[b] \, , \qquad (12)$$

where $[d']$ refers to the weight percent oxide in the dissolved load and $[b]$ to the weight percent oxide in bedrock. When one has a constituent pair, such as sodium paired with silica, W_{Si} can also be expressed in terms of concentrations of both constituents ($[s]$ refers to weathered solids):

$$W_{Si}(Si,Na) = ((Na_2O[b] / SiO_2[b]) - (Na_2O[s] / SiO_2[s])) / ((Na_2O[d'] / SiO_2[d']) - (Na_2O[s] / SiO_2[s])) \, . \qquad (13)$$

With this equation, Y'_{SBrx} is expressed in terms of measureable or easily estimated parameters, all of which are concentration ratios. The use of ratios limits the effect of many shared errors, such as errors in discharge measurements. Finally, from equations 11 and 13,

Table 4. Parameters and coefficients used in modeling equilibrium erosion in study watersheds, eastern Puerto Rico, by using sodium-silicon and calcium-silicon pairs.

[*A* and *B* are dimensionless coefficients defined in equations 16–18]

Description	Bedrock			Sediment			Dissolved			Sodium model		Calcium model	
	SiO_2	Na_2O	CaO	SiO_2	Na_2O	CaO	SiO_2	Na_2O	CaO	*A*	*B*	*A*	*B*
	(percent)			(percent)			(percent)						
Canóvanas, dissolved bedrock	53.8	3.31	8.12	50.3	0.03	1.31	43.6	9.45	30.5	30.5	0.018	14.9	0.388
Cayaguás, dissolved bedrock	62.9	3.84	6.07	58.0	0.27	0.78	54.3	15.09	18.0	28.3	0.134	19.1	0.258
Mameyes, dissolved bedrock	53.8	3.31	8.12	50.3	0.03	1.31	54.0	7.25	28.8	30.5	0.018	14.9	0.388
Icacos, dissolved bedrock	61.4	3.45	6.90	58.0	0.27	0.78	64.9	9.65	17.5	31.6	0.150	16.5	0.222
Guabá, dissolved bedrock	61.4	3.45	6.90	58.0	0.27	0.78	71.0	9.92	12.9	31.6	0.150	16.5	0.222

$$Y'_{SBrx} = Y_{DBrx} \bullet (SiO_2[d'] / SiO_2[b]) \bullet (1 - W_{Si}(Si,Na)) / W_{Si}(Si,Na) . \quad (14)$$

When the observed weathered bedrock yield equals the steady-state weathering yield, $Y_{SBrx} = Y'_{SBrx}$, the denudation of the landscape is in equilibrium. If $Y_{SBrx} > Y'_{SBrx}$, solid weathering products are accumulating on the landscape as soils, alluvium, and colluvium, and if $Y_{SBrx} < Y'_{SBrx}$, physical erosion exceeds the generation of solids, and there must be net loss of soil or stored sediment.

Equations 13 and 14 have a number of terms that, in a given watershed, are constant for all calculations, such as the bedrock and solid-load compositions. These constants allow the equations to be simplified into a form that involves either measured or easily estimated parameters. For example, the concentrations of dissolved bedrock oxides (equation 9), expressed as percent, can also be calculated from solute yields. Using sodium as an example:

$$Na_2O[d'] = 100 \bullet Y_{Na_2O[d]} / Y_{DBrx} . \quad (15)$$

Accordingly,

$$Y'_{SBrx} = (A \bullet Y_{Na_2O[d]} - B \bullet Y_{SiO_2[d]}) - Y_{DBrx} , \quad (16)$$

where

$$A = 100 \bullet SiO_2[s] / (Na_2O[b] \bullet SiO_2[s] - Na_2O[s] \bullet SiO_2[b]) , \quad (17)$$

and

$$B = 100 \bullet Na_2O[s] / (Na_2O[b] \bullet SiO_2[s] - Na_2O[s] \bullet SiO_2[b]) . \quad (18)$$

Note that the denominators (the terms in parentheses) in equations 17 and 18 are the same; accordingly, *A* is more sensitive to errors in estimating $SiO_2[s]$, and *B*, which is quite a small term, is more sensitive to errors in $Na_2O[s]$. In fact, so long as $Na_2O[s]$ is small, even with considerable error, this equation is quite robust. Moreover, in the equations for *A* and *B*, the numerator represents a concentration of river-borne solids and the difference terms in the denominator are multiplied by concentrations of river-borne solids. This combination of terms eliminates any need to correct for LOI, despite the assumption that LOI is atmospherically derived water and organic matter.

By using equation 16, LOADEST-based yield estimates were used to calculate equilibrium denudation rates and test whether erosion is in equilibrium and how equilibria may respond to changes in average long-term runoff; this method is referred to as the equilibrium model. Denudation rates were calculated using calcium, as a check, but because of the caveats regarding variability of bedrock $CaO[s]:SiO_2[s]$ ratios and the influence of possible calcite inputs, the sodium calculations are much preferred.

Table 4 presents the concentrations of solids and solutes needed to calculate equilibrium yields, using either sodium or calcium, along with respective coefficients *A* and *B*. In addition to analyses of samples collected for this study (table 1), table 4 is based on averaged data that includes published analyses of volcanic rocks from other sources. For the bedrock of the Mameyes and Canóvanas watersheds, analyses of volcanic rocks from Jolly and others (1998; samples DG–12, DG–14, DG–16; FG–17, FG–7, FG–9; INF–7, J–77, LOM–12) were averaged with the volcanic samples in table 1. For the Icacos and Guabá, data from the Río Blanco stock from Smith and others (1998, Río Blanco samples 6513, PRP–4, PRP–5, PRP–6, PRP–12, PRP–14, PRP–16, PRP–17) were averaged with quartz-diorite samples from table 1, excluding xenoliths and aplite. For the Cayaguás, data from Smith and others (1998; San Lorenzo samples PP–1, PRP–1, PRP–2, PRP–10, PRP–11; PRP–100, PRP–103, PRP–104, PRP–105; SL–1) were averaged.

Suspended Bedrock, Loss on Ignition, and Particulate Organic Carbon

River-borne solids are composed of material from three sources: primary and secondary mineral matter derived from the weathering of bedrock, water that has been incorporated into secondary minerals during weathering, and organic matter. For about two-thirds of the measurements of suspended sediment (see Stallard and Murphy, 2012, and appendices 1, 2), we also measured loss on ignition (LOI), which involves measuring the mass loss upon heating to 550°C samples that have been dried at temperatures of 105°C. Studies summarized in Mackenzie (1957) and Mackenzie and Caillère (1979) show that in heating to 550°C, all of the clays and sesquioxides lose nonstructural water (most below 200°C). In addition, all sesquioxides, most kaolins, and substantial illites and vermiculites lose lattice water below 550°C; however, smectites, talcs, and chlorites do not. Nonmineral organic carbon and most mineral carbon (coal and graphite) are also oxidized in this range. Carbonate rocks are generally stable.

In this work, the mass of the sample after heating to 550°C was equated with SBrx (fig. 5). The sample dried to 105°C is referred to as suspended solids or suspended sediment (SSol). For samples in which suspended bedrock was not measured, regressions for each river related SBrx to SSol and LOI:

$$\mathrm{SBrx} = \mathrm{SSol} \bullet (a + b \bullet \log(\mathrm{SSol})) , \quad (19)$$

and

$$\mathrm{LOI} = \mathrm{SSol} - \mathrm{SBrx} , \quad (20)$$

where *a* and *b* are regression coefficients. Values for *a* and *b* for each river are given in appendix 1. At lowest runoff rates, LOI is elevated in the forested rivers (Mameyes, Icacos, and Guabá; fig. 6). Given that LOI for kaolinite and halloysite is 14.0 percent, values greater than 14.0 percent likely reflect organic matter. At low runoff rates, the overall contribution of sediments to the net sediment load is very small (Stallard and Murphy, 2012). At highest runoff rates, LOI values of sediment in rivers that drain granitic rocks are low because of the large contribution of quartz sand to these samples.

POC was not measured on most of the sediment samples; instead, LOI (fig. 6) is used as a surrogate measurement. LOI is commonly equated with organic matter; however, the study samples are rich in kaolinite, halloysite, or iron and aluminum sesquioxides. Instead, it is assumed here that POC is a fixed fraction of LOI for all study samples. This fraction was determined such that the 15-year yield of SSol for the Río Icacos consisted of 1 percent carbon, a value that is typical of world rivers (Stallard, 1998). The result is that LOI for the study rivers consists of 11 percent carbon. For reference, pure organic matter is about 50 percent carbon by mass (Stallard, 1998). The water contribution to average LOI never exceeds the value of 14.0 percent of pure kaolinite (table 5). The average POC of forested rivers, at low runoff rates of less than 1 mm h^{-1}, is 2 to 3.5 percent SSol (table 2), similar to values reported elsewhere (McDowell and Asbury, 1994). For estimates of LOI, POC, and organic matter, see table 5.

Table 5. Analysis of loss on ignition for a discharge-weighted average sample of solid load from study rivers, eastern Puerto Rico.

[LOI, loss on ignition; POC, particulate organic carbon]

River	LOI	Weight percent of suspended solids		
		Water	Organic matter[1]	POC
Canóvanas	16.3	12.8	3.5	1.8
Cayaguás	6.1	4.3	1.8	0.9
Mameyes	16.9	13.2	3.7	1.9
Icacos	7.5	5.5	2.0	1.0
Guabá	11.7	8.9	2.8	1.4

[1]Organic matter is assumed to be twice POC.

Projection to a Common Intermediate Yield

The principal confounding issue in the comparison of constituent yields of the various Puerto Rico WEBB watersheds is that among them, the long-term, mean-annual runoff differs markedly. The forested watersheds are considerably wetter (Mameyes—2,750 mm yr^{-1}, Icacos—3,760 mm yr^{-1}, Guabá—3,630 mm yr^{-1}) than the developed watersheds (Canóvanas—970 mm yr^{-1}, Cayaguás—1,620 mm yr^{-1}). To compare sites, regressions between annual runoff and constituent yields were used to project annual yields to an annual intermediate runoff, 1,860 mm yr^{-1}, about halfway between the runoff for the Canóvanas and the Mameyes. This value is within the observed range of annual runoffs for the Mameyes and Cayaguás and represents an extrapolation for the Canóvanas, Icacos, and Guabá. These relations were also used to establish whether these landscapes are in a state of dynamic equilibrium such that the yield of solid bedrock is the same as the rates at which solid weathering products are being generated (equation 16).

Annual constituent yields, including derived constituents, were calculated using LOADEST (appendix 1). Annual runoff varied considerably from year to year (fig. 7). The highs and lows were mirrored by constituent yields (figs. 7–9).

The relation between annual runoff and annual dissolved-constituent yields was a simple linear relation for all dissolved constituents (figs. 10–12). Many rivers produce linear relations such as these (6 rivers, White and Blum, 1995; 57 rivers, Godsey and others, 2009). The buffering or "chemostatic" behavior can be explained by many mechanisms, such as ion exchange, buffering with amorphous phases, large soil reservoirs of solutes, or weathering reactions that respond proportionally to the water flux passing through the soil. Godsey and others (2009) presented a "permeability-porosity-aperture model" that predicts that in a given watershed, the relation between log(concentration) and log(runoff) should be linear and with the same slope for all bedrock-derived constituents. The authors allow that differences for slopes among various constituents could be attributable to differences in the depth distribution of reactive minerals throughout soil profiles.

Suspended Bedrock and Runoff

Unlike solute erosion, for which a linear relation between annual runoff and annual solute yield agrees well with the data, physical erosion is decidedly nonlinear, and concentrations of solid constituents typically increase markedly with discharge. Two issues must be addressed with respect to solid loads. First is selecting the relation between runoff and solid yield for individual years. Landslides add complexity, because landslide-producing storms do not occur every year. The second is the problem of averaging the effects of variation in interannual runoff. Long-term averages reflect a mix of drier and wetter years. For linear processes the average solute yield of many years is the same as the solute yield of the average runoff for all the same years. For solid yields, years that have high runoff and abundant high-runoff storms heavily influence long-term averages, and computational procedures need to capture this increased weighting of wet-year contributions.

Solid Loads for Individual Years

Surficial erosion, the combined effects of direct impaction by raindrops on soil, sheet wash, rill formation, and gullying, is driven by flowing water and tends to increase exponentially with increasing discharge. Physical erosion is most simply described using power-law formulations relating annual suspended solids yield, Y_{SSol}, to annual runoff, R:

$$Y_{SSol}(\text{year}) = a \cdot R(\text{year})^{b}, \qquad (21)$$

where a and b are regression coefficients. For the eastern Puerto Rico rivers, the coefficients were estimated iteratively by means of nonlinear regressions as opposed to regressions on log-transformed data (table 6). Landslides, which typically are caused by only the largest storms, distort this relation.

Table 6. Coefficients of power-law model relating annual suspended-bedrock yield to runoff (Yield=$a \cdot \text{Runoff}^{b}$) in study watersheds, eastern Puerto Rico.

River	Coefficient		Percent variance explained	Years
	a	*b*		
Canóvanas	0.002	1.72	43	15
Cayaguás	$9.2 \cdot 10^{-5}$	2.21	79	15
Mameyes	$5.6 \cdot 10^{-11}$	3.64	54	15
Icacos	$4.4 \cdot 10^{-8}$	2.93	40	15
Guabá	$1.9 \cdot 10^{-6}$	2.52	48	10

Stallard (1999) and Stallard and Kinner (2005) developed an approach for quantifying annual sediment yields in landslide-dominated watersheds; this approach empirically distinguishes surficial and landslide erosion by using datasets for rivers in the Panama Canal watershed that had a decade or more of daily sediment data. The Puerto Rico WEBB dataset does not have such daily measurements, but because of the emphasis on storm sampling, the yield estimations done using LOADEST are a reasonable substitute. A key assumption of this approach is that annual sediment discharge from each watershed is considerably greater than interannual storage. The volcaniclastic watersheds do not store fine-grained sediments in their riverbeds, so the assumption is valid in these watersheds. For the granitic watersheds, flood plain storage can be extensive (Brown and others, 1995, 1998; Larsen and Santiago-Román, 2001; Larsen, 2012). My repeated visits to many sites along the channels of the Río Icacos and the Quebrada Guabá during this project revealed little change, suggesting little net storage or loss, and that Quebrada Guabá has no floodplain. The Río Cayaguás channel, however, changed considerably in appearance, but it would be difficult to assess storage or loss.

As discussed earlier, rainfall must exceed some threshold before landslides occur (equation 1). Rather than use rainfall, which requires interpolation and is especially ambiguous in the Canóvanas watershed (see Murphy and Stallard, 2012), this analysis follows Stallard (1999) and Stallard and Kinner (2005) and uses daily runoff, R, calculated from the daily discharge (D).

A day is defined as a landslide day if

$$R\ (24, 48, \text{or } 72\text{ h}) > F \cdot 91.46 \cdot D^{0.18}$$
$$(D = 24, 48, \text{or } 72\text{ h}), \qquad (22)$$

where h is hour, F is an empirical coefficient between 0 and 1 that adjusts the threshold for three factors that reduce runoff relative to local rainfall, in essence stating $R = F \cdot$ precipitation for big storms. These three factors are evapotranspiration, infiltration, and rainfall patchiness, where in parts of a watershed rainfall will exceed the threshold but in other parts not do so. Stallard (1999) and Stallard and Kinner (2005) determined that F=0.85 for the Panama Canal watershed by using 10 to 16 years of daily sediment data on six rivers.

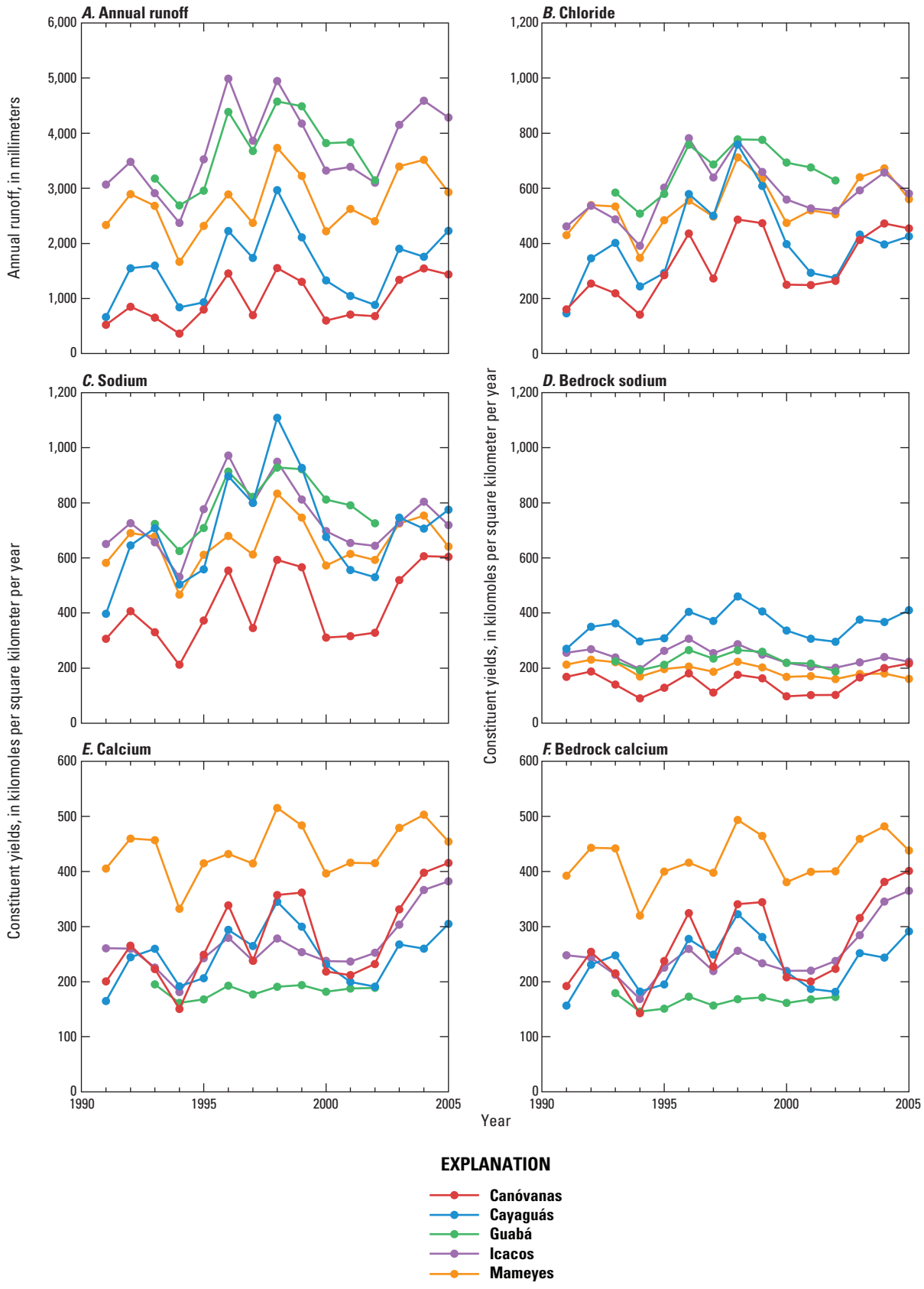

Figure 7. Time series of annual runoff (upper left) and the annual yields of chloride, sodium, calcium, and bedrock-derived sodium and calcium, eastern Puerto Rico.

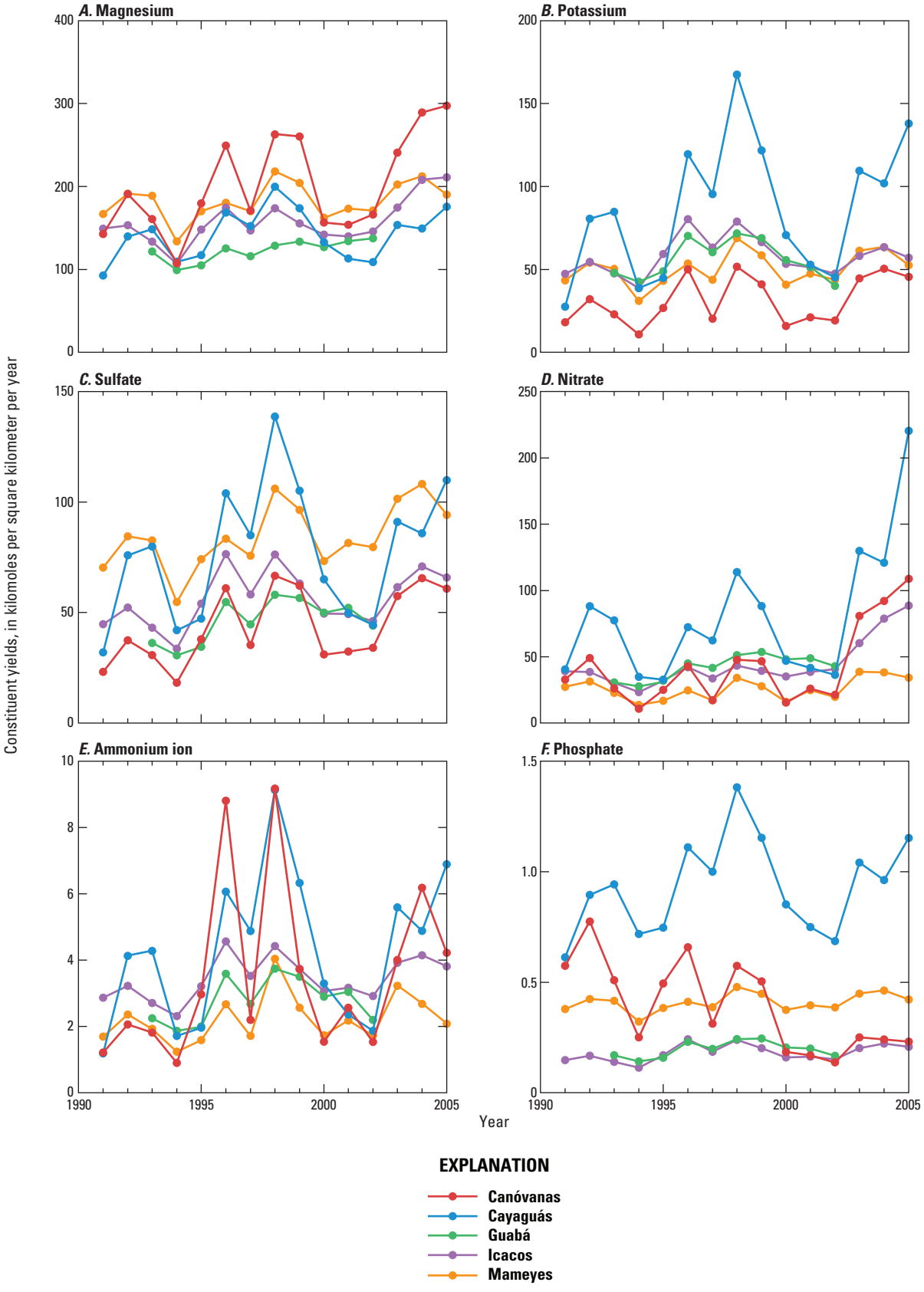

Figure 8. Time series of the annual yields of magnesium, potassium, sulfate, nitrate, ammonium ion, and phosphate, eastern Puerto Rico. Magnesium is mostly influenced by weathering and atmospheric inputs. The remaining constituents in this graph are strongly influenced by biological activities and in some cases by human activities such as fertilizer applications and domestic waste.

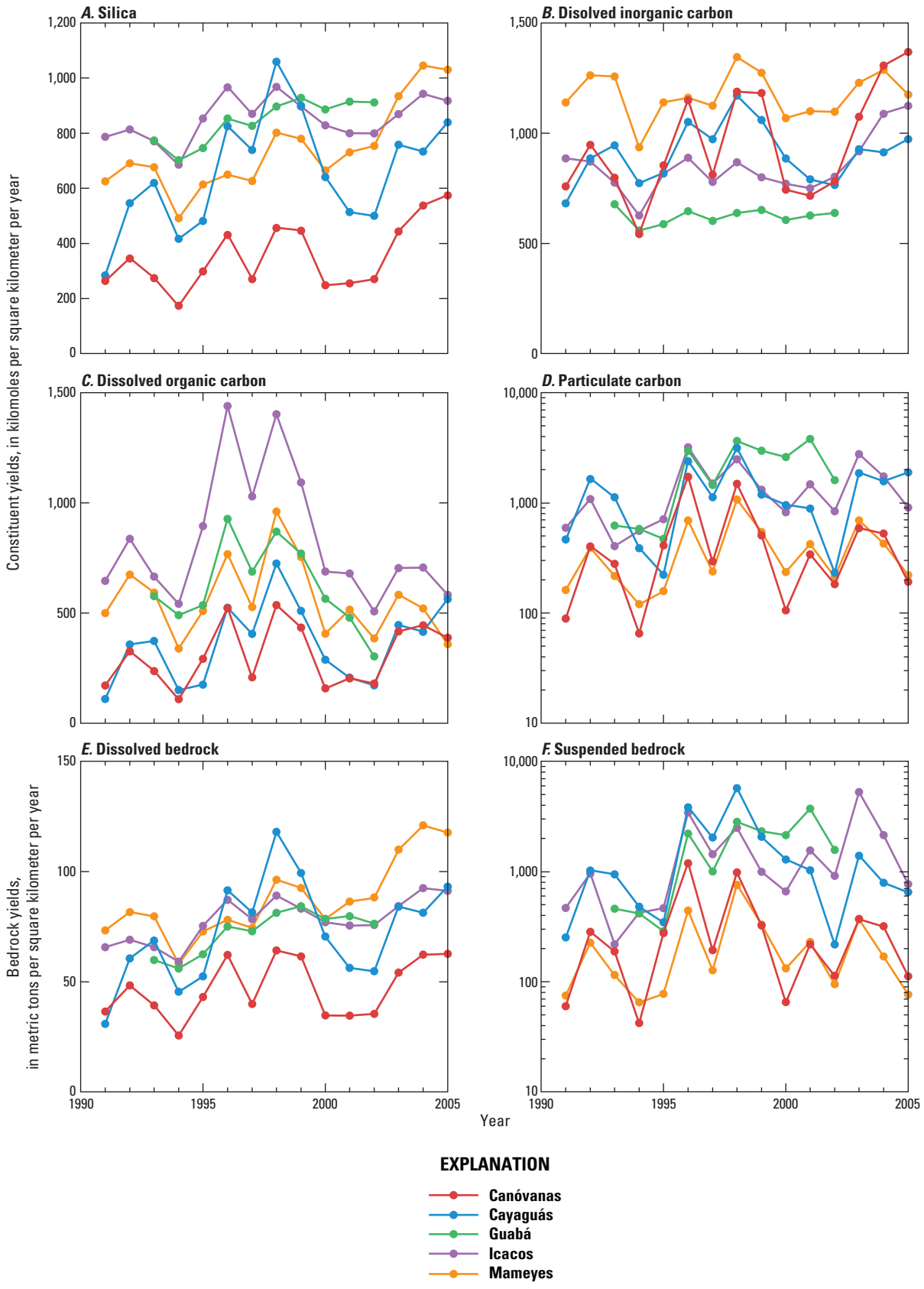

Figure 9. Time series of the annual yields of important constituents in characterizing erosion and the carbon cycle in eastern Puerto Rico: silica, dissolved inorganic carbon, dissolved organic carbon, particulate organic carbon, dissolved bedrock, and suspended bedrock.

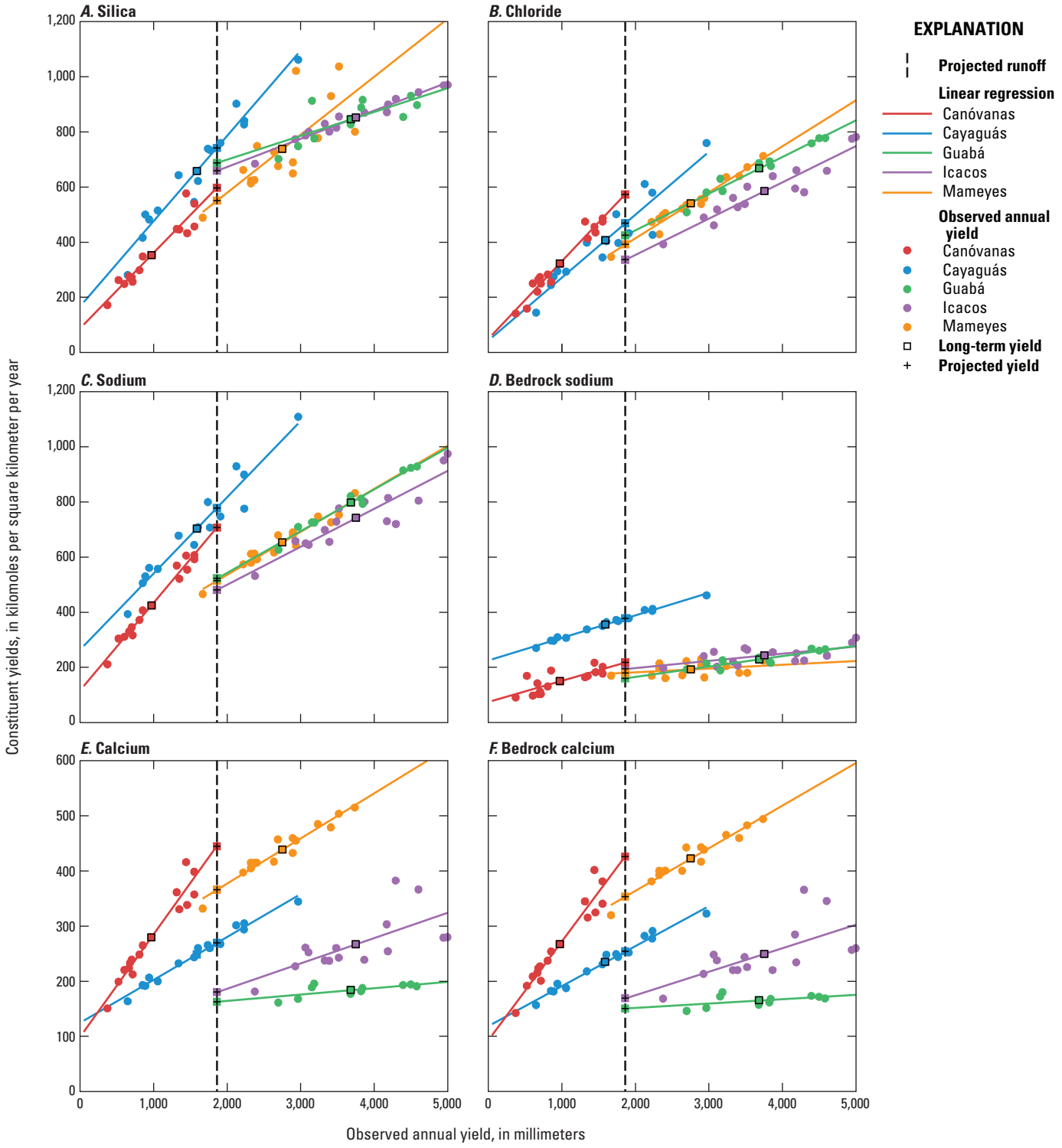

Figure 10. Annual runoff compared with the annual yields of silica, chloride, sodium, calcium, and bedrock-derived sodium and calcium for the five rivers studied, eastern Puerto Rico. The vertical gray line corresponds with 1,860 millimeters per year, and the solid squares with black plus symbols correspond with the projected annual yields. The points are observed annual yields; lines are linear regressions based on the assumption that annual yield responds linearly with changing runoff.

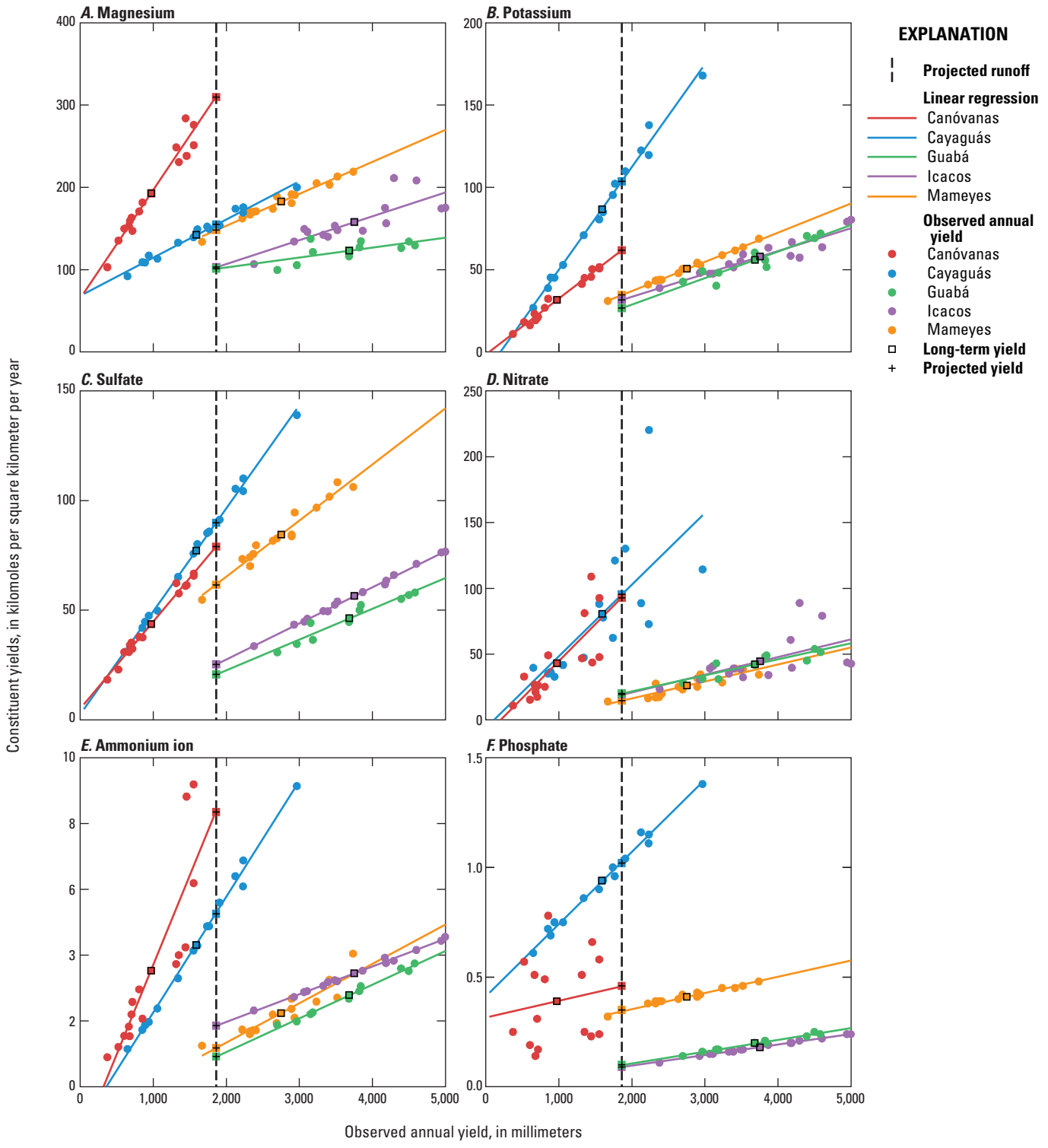

Figure 11. Annual runoff compared with the annual yields of magnesium, potassium, sulfate, nitrate, ammonium ion, and phosphate for the five rivers studied, eastern Puerto Rico. The vertical gray line corresponds with 1,860 millimeters per year, and the solid squares with black plus symbols correspond with the projected annual yields. The points are observed annual yields; lines are linear regressions based on the assumption that annual yield responds linearly with changing runoff. Except for magnesium, the constituents in this graph are strongly influenced by biological activities and in some cases by human activities such as fertilizer applications and domestic waste. Potassium, sulfate, and phosphate have bedrock sources. Yields of potassium, nitrate, ammonium ion, and phosphate are especially elevated in the developed watersheds indicating additional agricultural or domestic sources.

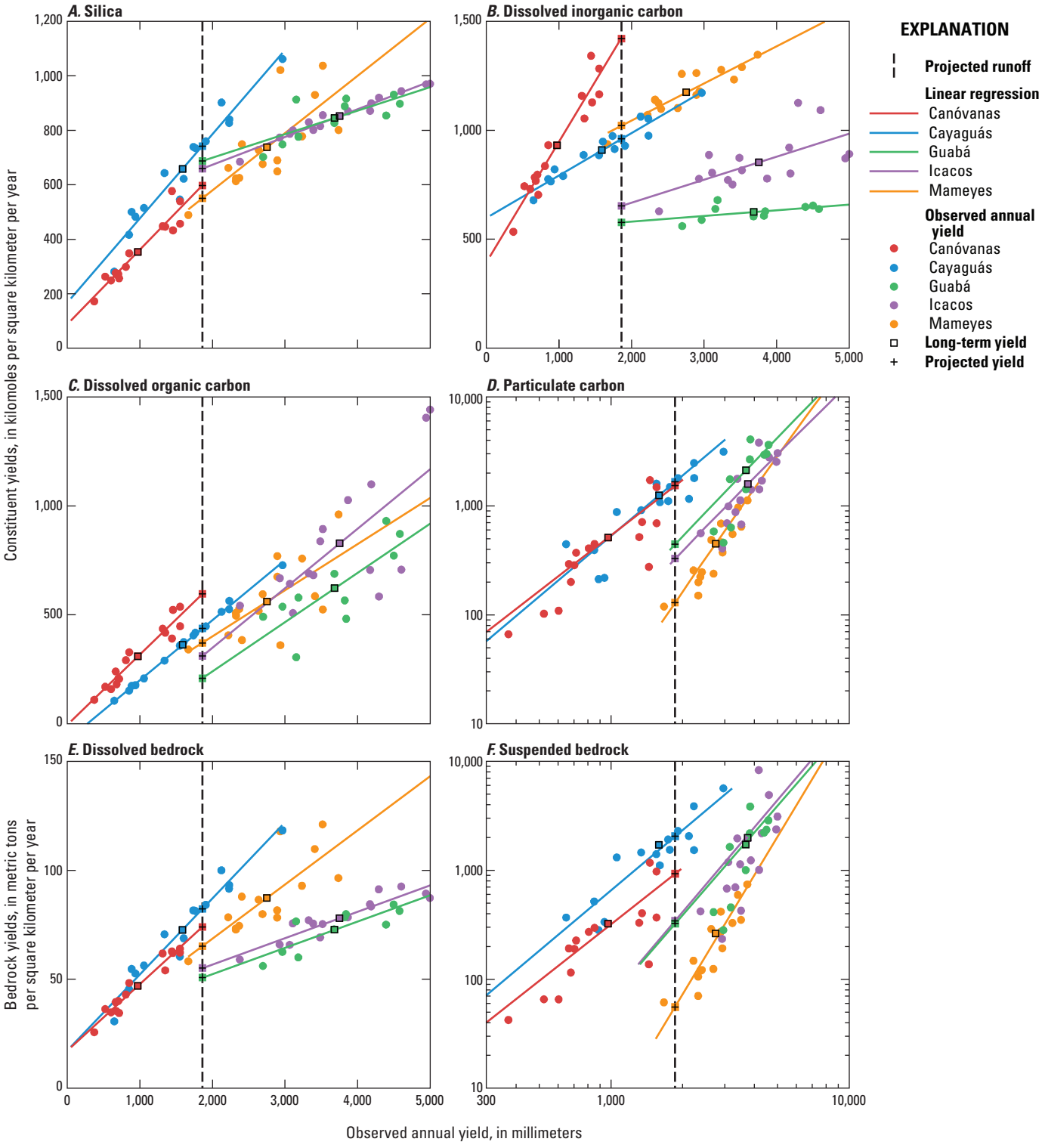

Figure 12. Annual runoff compared with annual yields of important constituents in characterizing erosion and the carbon cycle in eastern Puerto Rico: silica, dissolved inorganic carbon, dissolved organic carbon, particulate organic carbon, dissolved bedrock and suspended bedrock. The vertical gray line corresponds with 1,860 millimeters per year, and the solid squares with black plus symbols correspond with the projected annual yields. The points are the observed annual yields. The lines in parts *A*–*C* and *E* are linear regressions based on the assumption that annual yield responds linearly with changing runoff. The lines in parts *D* and *F* were produced by power-law models, on the basis of equation 21, which plot as lines on graphs with log-log scales. Because these power-law curves are being used to predict trends for a changing climate, and because of the variability of climate, a convolution, equation 26, was used to smooth the power-law curves. Such convolutions have no effect on linear models.

For each river and each year of the dataset, the number of landslide days, as defined by equation 22, were totaled as landslide days per year, *Ns*(year); successive landslide days were assigned to a single day. The resulting combined surface erosion–landslide erosion model is

$$Y_{SSol}(\text{year}) = a \bullet R(\text{year})^b + c \bullet Ns(\text{year}) , \quad (23)$$

where *a*, *b*, and *c* are regression coefficients. This first term on the right is a traditional sediment transport model (equation 21). The second term is a statement that each landslide day dumps a certain quantity of sediment into the river.

Ns(year) does not distinguish between small and large landslide-producing events, so in the present paper, the net runoff for landslide days is totaled to determine the landslide-day runoff per year, *Rs*(year).

$$Y_{SSol}(\text{year}) = a \bullet R(\text{year})^b + c \bullet Rs(\text{year}) \quad (24)$$

where *a*, *b*, and *c* are regression coefficients. The second term on the right side of equation 24 assumes that the amount of slide material dumped into rivers on landslide days is directly proportional to the runoff on those days.

There are four adjustable parameters in this surface-erosion–landslide-erosion model (equation 23). The landslide threshold adjustment parameter, *F*, is assumed to be the same for all of the watersheds. Because daily sediment data are not available for eastern Puerto Rico, a value of 0.85, as determined by Stallard (1999) and Stallard and Kinner (2005), was used. The remaining coefficients were estimated iteratively by means of nonlinear regressions. The first terms, *a* and *b*, were estimated for each river using data for years lacking landslide days; then the second term, *c*, was estimated using only those years with landslide days (table 7). When compared with the power-law model (equation 21) and on the basis of an F-test of model variance (Bevington and Robinson, 2003), the models that used landslide runoff, *Rs*(year), generally were statistically more significant (tables 6, 7), except for the Mameyes watershed, where the landslide model and the power-law model were indistinguishable. From 1991 through 2005, we observed landslides in the Mameyes watershed associated with large storms. The similarity of the two models may imply that, currently, landslides make a relatively small contribution to the sediment load of the Mameyes.

To adapt the landslide model to a continuum of runoff it is necessary to predict landslide-producing runoff, R_s(annual runoff), as a function of annual runoff, R_{annual}. The form used here was the simplest possible, a linear relation. Only years having landslide days are considered. The relation is:

$$R_s(R_{annual}) = a \bullet (R_{annual} - R_{s0}),\ R_{annual} > R_{s0} , \quad (25)$$

where *a* and $a \bullet R_{s0}$ are regression coefficients (table 8). This equation defines an annual runoff threshold, $R_{s0} = 0$, below which landslides should not occur. This threshold is R_{s0} = 1,272 mm yr^{-1} for the Canóvanas, R_{s0} = 1,656 mm yr^{-1} for the Cayaguás, R_{s0} = 2,440 mm yr^{-1} for the Mameyes, R_{s0} = 2,857 mm yr^{-1} for the Icacos, and R_{s0} = 3,098 mm yr^{-1} for the Guabá. The increasing threshold with increasing runoff among the five watersheds appears reasonable, because differences in interannual runoff appear to be primarily driven by orographic precipitation and numerous small storms, which do not produce landslides, and not by the number or size of the biggest storms (see Murphy and Stallard, 2012).

Table 8. Coefficients used to predict landslide-day runoff given annual runoff in study watersheds, eastern Puerto Rico.

[Landslide-day runoff=*a* • (annual runoff minus runoff threshold), provided annual runoff is greater than the runoff threshold]

River	Runoff threshold	Coefficient *a*	Percent variance explained	Years
Canóvanas	1,272	1.18	73	15
Cayaguás	1,656	0.58	85	15
Mameyes	2,440	0.32	68	15
Icacos	2,857	0.31	80	15
Guabá	3,098	0.45	77	10

Table 7. Coefficients of model relating annual suspended-bedrock yield to runoff and landslide day runoff in study watersheds, eastern Puerto Rico.

[Yield=*a* • Annual runoff^b + c • Slide-day runoff]

River	Coefficient			Percent variance explained	Years	F-test compared to power-law model[1]
	a	*b*	*c*			
Canóvanas	1.6	0.67	1.77	91	15	98
Cayaguás	$8.2 \bullet 10^{-4}$	1.87	2.84	94	15	86
Mameyes	$1.2 \bullet 10^{-10}$	3.53	0.13	74	15	52
Icacos	$8.7 \bullet 10^{-8}$	2.63	4.13	86	15	93
Guabá	0.059	1.17	3.20	84	10	78

[1]F-test gives the probability that this model is better than the power-law model (table 6); 50 percent implies that the models are indistinguishable.

Calculating the Long-Term Average for Nonlinear Sediment-Yield Models

Because river-borne-solid yields are strongly nonlinear with respect to runoff, the effects of interannual variation must be assessed and adjusted in order to estimate average yields.

Only one river in eastern Puerto Rico, the Río Fajardo, has a sufficiently long record, 45 years, to characterize the range and nature of interannual variation (see Murphy and Stallard, 2012). The annual discharge distribution is log normal with a standard deviation of 0.142 log units. For the purposes of data smoothing, this same log-normal distribution was assumed to apply to all the rivers, and to speed calculation, the effects of interannual variations were handled computationally as a convolution (see appendix 1). The Fajardo runoff data were ranked by increasing annual runoff and separated into seven roughly equivalent bins of 7, 6, 6, 7, 6, 6, and 7 years, successively. The average of log(runoff) for all the years of data was subtracted from each log(runoff), and the resultant values of log(runoff) minus average(log(runoff) were, in turn, averaged for each bin (table 9). A 7-point, B-spline convolution (Jupp, 1976, that report's table 6, m=4, k=2) was used such that the values of the model function were averaged using the B-spline coefficients for the runoff under consideration and three equally spaced log(runoff) values before and after (table 9). SBrx(r) is suspended bedrock as predicted by either the power-law model (equation 21) or the landslide model (equations 21, 24, 25). The convolved SBrx(r) at a given runoff, r, SBrxc(r), is given by

$$\begin{aligned}\mathrm{SBrxc}(r) = {} & w_1 \bullet \mathrm{SBrx}(c_1 \bullet r) + w_2 \bullet \mathrm{SBrx}(c_2 \bullet r) + w_3 \bullet \\ & \mathrm{SBrx}(c_3 \bullet r) + w_4 \bullet \mathrm{SBrx}(c_4 \bullet r) \\ & + w_5 \bullet \mathrm{SBrx}(c_5 \bullet r) + w_6 \bullet \mathrm{SBrx}(c_6 \bullet r) + w_7 \bullet \mathrm{SBrx}(c_7 \bullet r), \end{aligned} \quad (26)$$

where $c_1 \ldots c_7$ are logarithmic convolution factors and $w_1 \ldots w_7$ are weighting factors (table 9). The log(runoff) interval, 0.069, was adjusted so that the seven convolution points best matched the Río Fajardo bin averages (table 9). Presumably, SBrxc(r) captures the effect of interannual variation.

Table 9. Convolution information used to represent interannual variability.

[7-point convolution around a reference runoff such that $\mathrm{SBrx}c(r) = w_1 \bullet \mathrm{SBrx}(c_1 \bullet r) + w_2 \bullet \mathrm{SBrx}(c_2 \bullet r) + w_3 \bullet \mathrm{SBRX}(c_3 \bullet r) + w_4 \bullet \mathrm{SBrx}(c_4 \bullet r) + w_5 \bullet \mathrm{SBrx}(c_5 \bullet r) + w_6 \bullet \mathrm{SBrx}(c6 \bullet r) + w_7 \bullet \mathrm{SBrx}(c_7 \bullet r)$, where r is runoff; w is runoff weighting factor; and c is convolution weighting factor]

Convolution point	Relative position	Normalized runoff bin for Río Fajardo	*w*	*c*
1	–3	0.60	0.62	0.010
2	–2	0.77	0.73	0.083
3	–1	0.88	0.85	0.240
4	0	0.99	1	0.333
5	1	1.16	1.17	0.240
6	2	1.31	1.37	0.083
7	3	1.68	1.61	0.010

The relation between annual runoff and particulate constituents is best portrayed using log-log graphs (fig. 12, POC and SBrx). Power-law (equation 21) and landslide (equations 21, 24, 25) models, after convolution (equation 26), are represented separately (fig. 13). Note that the landslide models display a distinct hump in the Canóvanas and Icacos. These are the rivers for which the landslide model best represents the annual sediment-yield data when compared to power-law representations (tables 6, 7).

Interpretation of Projections to a Common Yield

It is assumed that constituents with yields that become more alike when projected to a common intermediate runoff are not strongly controlled by either geology or land cover. Atmospheric inputs, such as chloride, fall into this category because the source is external to the watersheds. Accordingly, to characterize the significance of projecting mean-annual yields to a common intermediate runoff (table 10), tests were designed to characterize the compactness of the projection and the degree of overlap in the two pair-wise comparisons: forested compared with developed landscape and granitic compared with volcanic bedrock. For each constituent, the compactness of the range of yields was compared though a simple test involving the minimum and maximum yields for constituent X, $Y_{X:min}$, and $Y_{X:max}$, respectively:

$$\text{Range ratio as a percent} = 200 \bullet (Y_{X:max} - Y_{X:min}) / (Y_{X:max} + Y_{X:min}). \quad (27)$$

The more compact the data range, the smaller this ratio. This range ratio for the averaged observed annual-mean yields was compared with the ratio of the projected yields for a common intermediate mean-annual runoff. Range reduction or no change was assumed to indicate that differences in geology or land cover did not strongly influence yields. Five rivers were too few to develop strong statistical comparisons; however, range is a reasonable surrogate for standard deviation and confidence intervals (Dean and Dixon, 1951). Accordingly, extreme examples of range reduction or extension are probably meaningful.

Overlap was characterized by using a simple ranking in which the maximum yields for a class of geology or land cover are compared to the minimum yields of the alternative class: forest compared to developed and granitic compared to volcanic (table 11). Increasing degrees of overlap were interpreted as reinforcing the effects of range reduction, and loss of overlap or major overlap reversals was interpreted as reinforcing the effects of range extension.

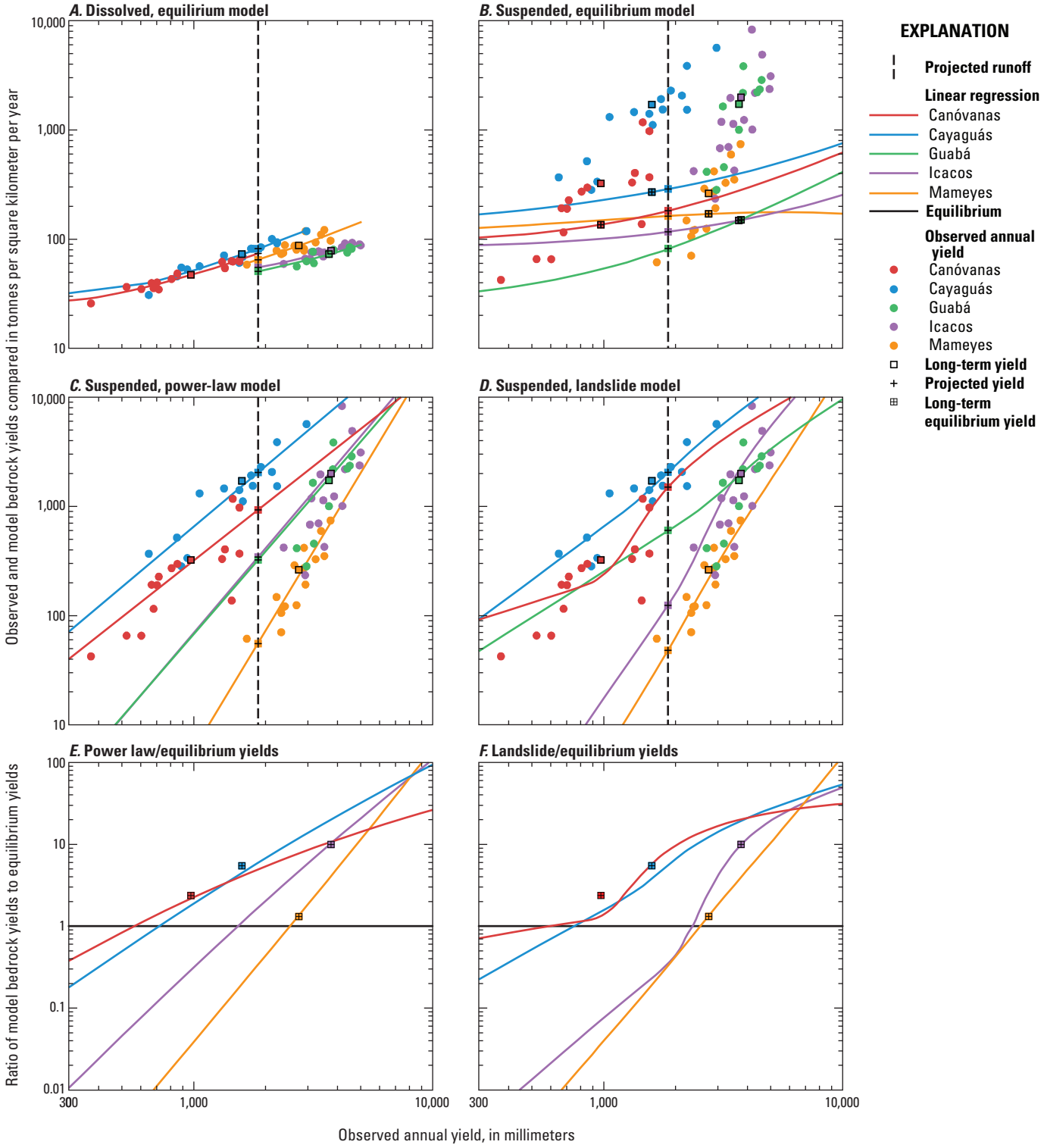
A. Dissolved, equilirium model
B. Suspended, equilibrium model
C. Suspended, power-law model
D. Suspended, landslide model
E. Power law/equilibrium yields
F. Landslide/equilibrium yields
Observed and model bedrock yields compared in tonnes per square kilometer per year
Ratio of model bedrock yields to equilibrium yields
Observed annual yield, in millimeters
10,000
1,000
100
10
1
0.1
0.01
300
EXPLANATION
Projected runoff
Linear regression
Canóvanas
Cayaguás
Guabá
Icacos
Mameyes
Equilibrium
Observed annual yield
Canóvanas
Cayaguás
Guabá
Icacos
Mameyes
Long-term yield
Projected yield
Long-term equilibrium yield

Figure 13. A model-based comparison of annual runoff compared with the annual yields of dissolved bedrock (part *A*) and suspended bedrock (parts *B*, *C*, *D*), eastern Puerto Rico. The vertical gray line in parts *A*–*D* corresponds with 1,860 millimeters per year, solid squares with black plus symbols correspond to the projected annual yields, and points are the observed annual yields. The curves in part *A* are linear regressions based on the assumption that the annual yield of dissolved bedrock responds linearly with changing runoff. The curves in part *B* relate dissolved bedrock to suspended bedrock through an equilibrium model discussed in the section Calculating Steady-State Erosion from Dissolved Bedrock. This relation is derived from the curves in figures 13*A*, 10*A*, and 10*D* using equation 16. The relation is almost linear and there has been no convolution smoothing. The lines in part *C* are power-law models, based on equation 21, which plot as lines on graphs with log–log scales. The curves in part *D* are derived from the landslide model, equations 24 and 25. Curves in parts *C* and *D* were smoothed by using equation 26 to account for climate variability. The ratio of the power-law model of suspended bedrock to equilibrium model and landslide model to the equilibrium model are presented in parts *E* and *F*, respectively. Note that observed suspended-bedrock yields are typically far greater than yields calculated by equilibrium models (part *B*). Compared with expected equilibrium yield, yield in the Mameyes watershed is slightly elevated and in the Canóvanas more so; the Cayaguás, Icacos, and Guabá are physically eroding at rates that greatly exceed expected equilibrium (parts *E* and *F*).

Results, Comparison of Constituent Yields, and Assessment of Landscape Equilibrium

Constituent-Yield Comparisons

Projection of annual yields to a common runoff, 1,860 mm yr^{-1}, brings several features to the fore (figs. 10–13, table 11). A characteristic of the linear relations for dissolved constituents (figs. 10–12) is that all have positive slopes and most have positive intercepts. In contrast to $Si(OH)_4$ in the study rivers, the linear relations between $Si(OH)_4$ and runoff presented by White and Blum (1995) all had negative intercepts. Annual solute yields must go to zero if annual runoff goes to zero (which would mean a profound desert), so these linear relations with nonzero intercepts must eventually reorganize as annual runoff approaches zero. For developed rivers, for which mean-annual runoff was below the projected runoff, all yields increased for all constituents following projection; the reverse was true for the forested rivers. For some constituents such as $Si(OH)_4$, however, the projected yields formed a more compact group than did the averaged observed mean-annual yields; for other constituents, such as POC, the projected yields became more widely dispersed.

The ranges for Na^+, $Si(OH)_4$, Cl^-, and dissolved bedrock became more compact upon projection to a common intermediate runoff (figs. 10, 12; table 11). This observation also applied to Na* (fig. 10), which is not included in the table. The wider ranges for DOC and calcium were slight and not significant (Dean and Dixon, 1951). The elevated DOC yield on the Canóvanas might be an anthropogenic effect; more research is needed. The constituents associated with compact ranges are also the principal constituents used to describe and assess inputs from chemical weathering, atmospheric sources, and biological processes. This compactness indicates that these three classes of inputs operated in a similar way in all four study watersheds. In particular, overall rates of chemical weathering cannot be strongly distinguished when they are compared in terms of land cover or bedrock type. Some slight differences may relate to bedrock geology. Yields of Na* and $Si(OH)_4$ from the Cayaguás watershed are distinctly greater than in the other three rivers, and Ca* yields from the Canóvanas and Mameyes watersheds were elevated. These latter watersheds are both on volcaniclastic rocks, which contain more calcium-bearing silicate minerals than do the granitic rocks, and the watersheds might also leach some calcium from minor sedimentary carbonate bedrock.

The ranges for the remaining constituents (Mg^{2+}, DIC, bioactive constituents, and particulate constituents) increased, most by large amounts (table 11; figs. 11, 12). In this group of constituents, developed watersheds tended to demonstrate a large increase in mean-annual yield relative to the forested watersheds once data were projected to a common mean-annual runoff. The only exception was DIC, for which developed and nondeveloped projected yields were intermingled. With the exception of SO_4^{2-}, Mg^{2+}, and DIC, the behavior of this group of constituents was consistent with our understanding of developed landscapes. Fertilizers and domestic wastes can contribute additional nutrients to developed watersheds, and increased erosion of deforested and agricultural landscapes can contribute to the particulate load.

Differences among watersheds for yields of sulfate, Mg^{2+}, and DIC (alkalinity) may have geologic causes. DIC is elevated in the Canóvanas watershed (figs. 4, 12). Note the similarity in diagrams of Mg^{2+} (fig. 11) and DIC (fig. 12). Carbonate rocks, which weather more rapidly than most silicate rocks, are a potential source of elevated alkalinity. A small amount of carbonate rock is found in the volcaniclastic rocks within the Canóvanas watershed (Murphy and others, 2012), and Ca* yields (fig. 10) are not especially elevated; however, Mg^{2+} yields (fig. 11) are exceptionally high. Perhaps bedrock contains abundant, easily weathered mafic minerals, such as serpentine. Serpentinites are found in Puerto Rico, but none have been described within the

Table 10. Watershed yields as observed in eastern Puerto Rico and adjusted to a common intermediate runoff (1,860 mm yr^{-1}), on the basis of the relation between runoff and annual yield.

[DIC, dissolved inorganic carbon; DOC, dissolved organic carbon; POC, particulate organic carbon; DBrx, dissolved bedrock; SBrx, suspended bedrock; mm yr^{-1}, millimeters per year; kmol km^{-2} yr^{-1}, kilomoles per square kilometer per year; *, derived bedrock contribution]

Watershed	Runoff (mm yr^{-1})	Na^+	K^+	Mg^{2+}	Ca^{2+}	$Si(OH)_4$	Cl^-	SO_4^{2-}	NO_3^-	NH_4^+	PO_4^{3-}	DIC	DOC	POC	DBrx	SBrx	Na*	Ca*
		(kmol km^{-2} yr^{-1})													(t km^{-2} yr^{-1})		(kmol km^{-2} yr^{-1})	
Annual net yields																		
Canóvanas	970	426	32	193	280	357	323	44	43	3.6	0.39	927	313	627	47	753	150	267
Cayaguás	1,620	707	88	143	250	662	411	78	82	4.4	0.94	913	389	1,595	73	1,916	357	235
Mameyes	2,750	654	51	183	439	739	542	85	26	2.1	0.41	1,174	573	503	87	604	193	423
Icacos	3,760	745	58	157	264	854	585	54	45	3.7	0.18	868	837	1,788	78	2,148	246	246
Guabá	3,630	735	51	113	170	778	615	43	39	2.6	0.18	587	574	1,954	67	2347	211	152
Annual net yields, adjusted to a common runoff																		
Canóvanas	1,860	713	63	312	448	607	578	80	94	8.5	0.47	1,424	605	1,729	74	2,076	221	429
Cayaguás	1,860	786	106	156	271	748	476	92	97	5.4	1.03	967	475	1,910	82	2,295	380	256
Mameyes	1,860	515	35	148	366	552	393	62	15	1.3	0.35	1,023	380	155	65	186	180	354
Icacos	1,860	486	32	104	183	652	342	25	19	1.9	0.09	666	323	253	55	304	195	172
Guabá	1,860	504	27	95	152	645	411	21	20	1.0	0.10	541	227	196	49	236	153	140
Projected change in net annual yields from current mean-annual runoff to a common mean-annual runoff																		
Canóvanas	888	287	31	119	168	250	254	36	51	4.9	0.08	498	292	1,102	27	1,323	71	162
Cayaguás	271	78	18	13	22	87	65	13	15	1.0	0.09	54	86	315	9	379	23	20
Mameyes	–891	–139	–16	–35	–73	–187	–149	–23	–11	–0.8	–0.06	–151	–194	–348	–22	–418	–12	–69
Icacos	–1,891	–259	–26	–53	–81	–202	–243	–29	–25	–1.8	–0.09	–203	–514	–1,535	–23	–1,844	–51	–75
Guabá	–1,531	–231	–24	–18	–18	–133	–204	–21	–19	–1.6	–0.08	–47	–346	–1,758	–18	–2,112	–58	–12

Watershed	Runoff (mm yr^{-1})	Na^+	K^+	Mg^{2+}	Ca^{2+}	$Si(OH)_4$	Cl^-	SO_4^{2-}	NO_3^-	NH_4^+	$-PO_4^{3-}$	DIC	DOC	POC	DBrx	SBrx	Na*	Ca*
		(percent)																
Percent change in net annual yields from current mean-annual runoff to a common mean-annual runoff																		
Canóvanas	91	67	97	62	60	70	79	82	117	137	21	54	93	176	58	176	47	61
Cayaguás	17	11	21	9	9	13	16	17	19	23	10	6	22	20	13	20	6	9
Mameyes	–32	–21	–31	–19	–17	–25	–27	–27	–44	–38	–16	–13	–34	–69	–25	–69	–6	–16
Icacos	–50	–35	–45	–34	–31	–24	–42	–54	–56	–48	–51	–23	–61	–86	–29	–86	–21	–30
Guabá	–45	–31	–47	–16	–10	–17	–33	–50	–48	–61	–45	–8	–60	–90	–28	–90	–27	–8

Table 11. Interpretation of changes in watershed yields as observed in eastern Puerto Rico and adjusted to a common intermediate mean-annual runoff.

[*, calculated bedrock contribution; DIC, dissolved inorganic carbon; DOC, dissolved organic carbon; POC, particulate organic carbon; DBrx, dissolved bedrock; SBrx, suspended bedrock; <, less than]

	Runoff	Na^+	K^+	Mg^{2+}	Ca^{2+}	$Si(OH)_4$	Cl^-	SO_4^{2-}	NO_3^-	NH_4^+	PO_4^{3-}	DIC	DOC	POC	DBrx	SBrx	Na*	Ca*
Percent change in data ranges normalized to midrange (for all watersheds), before and after projection of data to a common mean-annual runoff																		
Before	118	55	94	52	89	82	62	66	103	73	135	67	91	118	60	118	82	94
After	0	47	118	107	99	30	51	125	147	158	168	90	91	170	51	170	85	102
Change	–100	–14	26	106	11	–63	–17	89	43	117	24	35	–0	44	–14	44	4	8
Degree of overlap of forested and developed watersheds[1]																		
Before	–1	0	0	0	0	–1	–1	0	0	0	0	0	–1	0	0	0	0	0
After	0	1	1	1	0	0	1	1	2	2	1	0	1	2	1	2	1	0
Change	–1	1	1	1	0	–1	2	1	2	2	1	0	2	2	1	2	1	0
Degree of overlap of granitic and volcanic watersheds[2]																		
Before	0	1	1	–1	–1	0	0	0	0	0	0	–1	0	2	0	2	1	–1
After	0	0	0	0	–1	1	0	0	0	0	0	–1	0	0	0	0	0	–1
Change	0	–1	–1	–1	1	1	0	0	0	0	0	1	0	–1	0	–1	–1	1

[1]Before, after: –2, 2•maximum forest<minimum developed; –1, maximum forest<minimum developed; 0, range overlap; 1, maximum developed<minimum forest; 2, 2•maximum developed<minimum forest. Change: –1, from nonoverlap to overlap; 0, overlap before and after; 1, similar lack of overlap before and after; 2, a reversal or loss in lack of overlap.

[2]Before, after: –2, 2•maximum granitic<minimum volcanic; –1=maximum granitic<minimum volcanic; 0, range overlap; 1, maximum granitic<minimum volcanic; 2, 2•maximum granitic< minimum volcanic. Change: –1, from nonoverlap to overlap; 0, overlap before and after; 1, similar lack of overlap before and after; 2, a reversal or loss in lack of overlap.

Canóvanas watershed. The high SO_4^{2-} in the Mameyes, Canóvanas, and Cayaguás rivers is likely influenced by bedrock, because SO_4^{2-} yields of these watersheds exceed atmospheric inputs (table 3). Sulfide ores are found in the region (see Murphy and others, 2012). Additional inputs from human activities cannot be discounted, however, in the developed watersheds.

Landscape Equilibrium

The relation between annual runoff and annual yields of suspended bedrock are modeled in three ways: a standard power-law physical-erosion model (equation 21), a landslide physical-erosion model (equations 22, 24, 25), and as the result of equilibrium erosion (the equilibrium model, equation 16) (fig. 13). The landslide model provides a superior representation of erosion in the Icacos and Canóvanas watersheds, compared with the power-law model, and it is a somewhat more accurate model in the Cayaguás (fig. 13*E,F*). Neither model is superior in describing the Mameyes watershed. The equilibrium model bears little resemblance to observations or other models (fig. 13*B*). Observed annual suspended-bedrock yields were considerably in excess of expected equilibrium yields, except for the Mameyes (table 12, fig. 13*B*).

Contemporary observed suspended-bedrock yields in all study watersheds exceeded equilibrium rates calculated by using Na_2O (table 12). In the Mameyes watershed, physical erosion is modeled to be twice equilibrium when Na_2O is paired with SiO_2, which is the preferred pairing, but it is modeled to be at equilibrium when CaO is paired with SiO_2 (table 12). The two models of physical erosion can be used to estimate the mean-annual runoff for which yields would be in equilibrium (fig. 13, table 13). In all watersheds, current mean-annual runoff is in excess of the equilibrium runoff. Such an excess could imply either that climate has become wetter or stormier, pushing the watersheds out of equilibrium, or that erosion processes have changed owing to land-cover changes.

In the case of the volcanic watersheds, the Canóvanas and the Mameyes, the current mean-annual runoff deviates from equilibrium by less than 600 mm (table 13), and suspended-bedrock yields are considerably smaller than in the granitic watersheds (table 12). This smaller runoff is within the range of annual runoff variation for the Mameyes, and a climatic explanation is possible, although it is contrary to presumed long-term drying trends (Zack and Larsen, 1993). Although substantial parts of the Canóvanas are now in second growth (Murphy and others, 2012), much of the watershed has been deforested, farmed, and grazed, and its somewhat larger deviation from equilibrium could be caused by this history of land-cover change.

The Cayaguás and Icacos watersheds, both on granitic rocks, are much further from equilibrium. We know that deforestation and agriculture have accelerated physical erosion in the Cayaguás; however, the Icacos, which has similar

Table 12. Summary of landscape equilibrium properties, eastern Puerto Rico.

[DBrx, dissolved bedrock; SBrx, suspended bedrock; mm yr^{-1}, millimeters per year; t km^{-2} yr^{-1}, metric tons per square kilometer per year]

River	Observed mean annual runoff (mm yr^{-1})	Observed DBrx yield (t km^{-2} yr^{-1})	Observed SBrx yield (t km^{-2} yr^{-1})	Power-law SBrx yield (t km^{-2} yr^{-1})	Landslide-day SBRx yield (t km^{-2} yr^{-1})	Equilibrium SBrx yield based on Na_2O (t km^{-2} yr^{-1})	Ratio of observed to equilibrium SBrx yields based on Na_2O	Equilibrium SBrx yield based on CaO (t km^{-2} yr^{-1})	Ratio of observed to equilibrium SBrx yields based on CaO
Canóvanas	970	47.0	355	299	184	89	3.99	154	2.30
Cayaguás	1,620	72.7	1,981	1,219	1,031	233	8.48	162	12.22
Mameyes	2,750	87.3	270	230	228	106	2.56	265	1.02
Icacos	3,760	78.1	1,985	1,555	1,481	154	12.91	130	15.22
Guabá	3,630	67.0	1,590	1,648	1,428	137	11.58	60	26.69

Table 13. Observed mean-annual runoff compared with equilibrium runoff for power-law and landslide day erosion models in study watersheds, eastern Puerto Rico.

[mm yr^{-1}, millimeters per year]

River	Observed mean annual runoff (mm yr^{-1})	Equilibrium runoff, power-law model (mm yr^{-1})	Equilibrium runoff, landslide model (mm yr^{-1})	Runoff in excess of equilibrium for power-law model (mm yr^{-1})	Runoff in excess of equilibrium for landslide model (mm yr^{-1})
Canóvanas	970	430	270	540	700
Cayaguás	1,620	670	690	950	930
Mameyes	2,750	2,220	2,240	530	510
Icacos	3,760	1,540	2,370	2,220	1,390
Guabá	3,630	820	200	2,810	3,430

Table 14. Total denudation compared with equilibrium denudation for current mean-annual runoff and projected to a common runoff in study watersheds, eastern Puerto Rico.

[mm yr^{-1}, millimeters per year; m Ma^{-1}, meters per mega-annum (10^6 years)]

River	Observed mean annual runoff (mm yr^{-1})	Observed total denudation (m m.y.$^{-1}$)	Equilibrium denudation, modeled (m m.y.$^{-1}$)	Projected total denudation at 1,860 mm yr^{-1} annual runoff (m m.y.$^{-1}$)	Projected equilibrium denudation at 1,860 mm yr^{-1} annual runoff (m m.y.$^{-1}$)	Equilibrium denudation at equilibrium annual runoff (m m.y.$^{-1}$)
Canóvanas	970	152	51	614	72	36
Cayaguás	1,620	775	116	643	125	84
Mameyes	2,750	135	73	45	65	68
Icacos	3,760	779	87	36	66	72
Guabá	3,630	625	77	157	49	72

Table 15. Excess particulate organic carbon yields from the equilibrium model of study watersheds, eastern Puerto Rico.

[DOC, dissolved organic carbon; POC, particulate organic carbon; mm yr^{-1}, millimeters per year; kmol km^{-2} yr^{-1}, kilomoles per square kilometer per year]

River	Observed mean annual runoff (mm yr^{-1})	Observed DOC yield (kmol km^{-2} yr^{-1})	Observed POC yield (kmol km^{-2} yr^{-1})	Equilibrium POC yield (kmol km^{-2} yr^{-1})	POC yield in excess of equilibrium (kmol km^{-2} yr^{-1})	POC yield in excess of equilibrium (percent)
Canóvanas	970	313	627	157	470	300
Cayaguás	1,620	389	1,595	188	1,407	750
Mameyes	2,750	573	503	197	306	160
Icacos	3,760	837	1,788	139	1,650	1,190
Guabá	3,630	574	1,954	169	1,786	1,060

bedrock and is forested, is even further from equilibrium. For both rivers, the current mean-annual runoff deviates from equilibrium by 900 mm to 2,200 mm. Denudation rates (table 14) that are projected to a common runoff value produce equilibrium rates for the forested watersheds that exceed the predicted denudation rate; these conditions are those needed to develop thicker soils.

Excess POC yields are calculated by assuming that the equilibrium POC yield is in the same proportions compared with equilibrium solid yield as the observed POC yield is to the observed solid yield (table 15). The excess POC yield, which reflects presumed landscape disequilibrium, is the largest part of the organic carbon budget in all study watersheds except the Mameyes.

Summary and Conclusion: General Landscape Disequilibrium and the Carbon Cycle

The biogeochemistry and physical erosion of four research watersheds were examined through the development of simple models that relate observed annual runoff to annual yields for various constituents. Several derived constituents were developed, including the bedrock-derived yields of all measured constituents, dissolved silicate bedrock, suspended silicate bedrock, and the equilibrium production of bedrock-derived solids. Several constituents are largely atmospheric in origin (table 3)—Na^+, Cl^-, SO_4^{2-}, NO_3^- plus NH_4^+, DOC, and POC. Between 10 and 50 percent of K^+ and Mg^{2+} originate in the atmosphere. Less than 10 percent of Ca, $Si(OH)_4$, dissolved bedrock, and suspended bedrock originates in the atmosphere. Conductivity, Cl^-, and $Si(OH)_4$ proved to be an excellent surrogate suite of measurements to use for estimating dissolved bedrock.

At the beginning of the paper, six questions are asked; they can now be answered.

What are the measured rates of chemical and physical denudation and how do these relate to mean-annual runoff in each watershed?

Rates of chemical and physical denudation are summarized in table 14. For dissolved constituents, the relation between annual runoff and annual yields is linear (figs. 10–12). This relation is consistent with results of other studies (White and Blum (1995) and Godsey and others (2009)). Intercepts do not intersect zero, an indication that processes must change as mean-annual runoff approaches zero. Suspended bedrock and particulate organic carbon can be modeled either by a power-law relation or by a model based on accounting for the total runoff of all days having storms large enough to produce landslides (fig. 13*C*, *D*).

How do watersheds compare in weathering, erosion, carbon export, and nutrient export with regard to geology and land cover? Do geology and land cover matter?

Watersheds were compared in two ways, at their current conditions of mean-annual runoff and by using the relation between annual runoff and annual yield to estimate mean-annual yields at a common, intermediate, mean-annual runoff of 1,860 mm yr^{-1}. Current mean-annual runoffs differ widely among the watersheds, because the forested watersheds are relatively wet and the developed watersheds are considerably drier.

Before projection to a common runoff, dissolved bedrock yields, about 47 to 87 t km^{-2} yr^{-1}, differed by a factor of less than 2 among all watersheds but were greater for the wetter watersheds. Silica, Cl^-, and DOC also demonstrated little relation to land cover, mean-annual runoff, or bedrock type. Before projection to a common yield, suspended-bedrock yields, ranging from 600 to 2,350 t km^{-2} yr^{-1}, were threefold to fourfold as great for the watersheds draining granitic rocks.

Upon projection to a common mean-annual runoff, the yield ranges of dissolved bedrock, Na^+, $Si(OH)_4$, and Cl^- became more compact, whereas the yield ranges of DOC and Ca^{2+} changed little. These constituents are primary measures of chemical weathering, seasalt input, and biological activity on the landscape. Narrow ranges indicate that differences in bedrock and land cover did not exert a strong influence on how these constituents were processed in this landscape. DIC, Mg^{2+}, SO_4^{2-}, and Na* showed systematically greater yields in a few watersheds (figs. 10–12), probably for geological reasons. The projected yields of biologically active constituents (K^+, NO_3^-, NH_4^+, PO_4^{3-}), and particulate constituents (suspended bedrock and POC) were considerably greater on developed landscapes (table 10, figs. 11–13), consistent with the effects of land clearing, fertilizer application, and minor domestic or industrial waste inputs. DOC may show a slight human effect in that concentrations in the developed watersheds were greater than in the forested ones; the difference is not as pronounced as with the previous constituents.

Is the landscape in a state of dynamic equilibrium? In essence, are the Luquillo Mountains a model of a quiescent natural landscape or are they changing?

The calculation of equilibrium denudation rates by using measurements of silica, sodium, and total dissolved bedrock appears to be robust (Stallard, 1995a). A notable feature of the approach was the use of conductivity, Cl^-, and $Si(OH)_4$ measurements, when they were appropriately calibrated, to estimate total dissolved bedrock in samples for which it could not be measured because of staff and laboratory limitations. This use of surrogates allowed thousands of additional estimates of total dissolved bedrock. Adding Na^+ to this suite, which now

also includes suspended sediment, K^+, and DOC, would allow especially rigorous characterizations of chemical and physical erosion and carbon export from certain watersheds—those where chemical weathering generates erodible solids, and those solids have low ratios of Na_2O to SiO_2 compared with ratios in bedrock. Such settings would be environments with moderate to intense chemical weathering. Use of total dissolved solids rather than total dissolved bedrock erroneously doubles estimates of solute erosion, and use of suspended sediments (dried at 105°C) rather than suspended bedrock (heated to 550°C) overestimates physical erosion by about 10 percent.

Except possibly for the Mameyes watershed, the current landscape is not in a state of dynamic equilibrium as estimated using the method of Stallard (1995a,b), based on concentrations of silicon and sodium in bedrock, in river-borne solids, and in solution (fig. 12, tables 12–14). The estimates of equilibrium rates are consistent, but slightly greater than, estimates obtained by using cosmogenic ^{10}Be for the Icacos (Brown and others, 1995) and for the Cayaguás (Brown and others, 1998). Observed suspended-bedrock yields are fivefold to tenfold as great as equilibrium yields on the granitic rocks and only slightly elevated on the volcanic rocks. The Mameyes watershed appears to be relatively close to equilibrium.

Brown and others (1995) observed that the Icacos watershed is in a state of dynamic equilibrium, on the basis of a cosmogenic ^{10}Be denudation rate of 43 millimeters per thousand years (mm k.y.$^{-1}$) that matched an estimate of denudation of 75 mm k.y.$^{-1}$, based on limited data. The 75 mm k.y.$^{-1}$ denudation rate is clearly too low, given rates estimated from the Puerto Rico WEBB dataset of 780 mm k.y.$^{-1}$. It is more likely that the Icacos recently departed from equilibrium and that the cosmogenic ^{10}Be in sediments and ridge-crest soils of the Icacos record its former equilibrium denudation rate much as Brown and others (1998) demonstrated for the Cayaguás, where the preagricultural equilibrium rate recorded in sediments is estimated to be 85 mm k.y.$^{-1}$.

The equilibrium denudation rates at the annual runoff rates where the physical-erosion models match the equilibrium rates of sediment production in the Icacos (table 12) are somewhat greater than those based on cosmogenic ^{10}Be, indicating that the denudation rates recorded by ^{10}Be for the Icacos were established under even drier or more quiescent conditions. Clearly, the ridgetops in the Icacos watershed that were sampled for ^{10}Be in soils must still reflect the old equilibrium conditions as evidenced by the clean bioturbation profiles reported in Brown and others (1995). The watershed as a whole, however, is not in this quiescent state.

What does the present dynamic state of the landscape imply regarding past and future response to climate change?

Deforestation and agriculture can easily explain disequilibrium erosion in the two developed watersheds. The disequilibrium is so great for the forested watershed on granitic rock (the Icacos) that other explanations are needed. The equilibrium denudation rates at the annual runoff rates where the models predict equilibrium (table 14) are somewhat greater than those based on cosmogenic ^{10}Be for the Icacos, indicating that the thick soils of this watershed were developed under especially quiescent conditions of physical erosion, compared with today. If the rate change is to be attributed to human activities, trails to mines have crossed the landscape for perhaps 500 years, and paved roads were built into the Icacos watershed in the middle 20th century (Larsen, 2012; Murphy and others, 2012). Alternatively, the forest in the Icacos may be degrading, perhaps from increased nitrogen loading (Stallard, 2012) or invasion by species such as bamboo (Murphy and others, 2012), thereby failing to inhibit erosion, particularly through an increasing rate of landsliding. Climate change, perhaps by increasing the frequency of huge landslide-generating storms, could have caused such a change in erosional style in the forested granitic watersheds; the weather record is not long enough to test this suggestion.

What are the rates of export of carbon in its various forms; how do these rates relate to runoff, and is this carbon being replaced by new photosynthetically fixed carbon?

Rates of carbon export as dissolved-inorganic, dissolved-organic, and particulate-organic carbon are summarized as yields in table 15. The POC yields exceed combined dissolved carbon yields in the granitic watersheds, but they are considerably less than the dissolved yields in the volcanic watersheds. Annual yields of DIC and DOC relate linearly to annual runoff, whereas POC has a steep power-law-style increase with increasing runoff. The POC yields are tied to sediment yields that are, in turn, far in excess of equilibrium yields. This excess implies that much of the present carbon transport in eastern Puerto Rico is the result of erosion in excess of equilibrium rates as hypothesized by Stallard (1998). In essence, soils that have developed for thousands of years are eroding more rapidly than they are now forming. Carbon accumulation is quite rapid, however, and in a landslide scar half of the carbon is regenerated in 80 years and all of it in about 200 years (fig. 2). Thus, eroding carbon is being replaced with new photosynthetic carbon from the atmosphere.

Are rates of carbon processing through the landscape notable on the time scales of human-induced climate change?

Estimates of the combined yields of all forms of carbon from the WEBB watersheds (table 3) range from about 1,800 kmol km^{-2} yr^{-1} (22 t km^{-2} yr^{-1} C) to 3,300 kmol km^{-2} yr^{-1} (40 t km^{-2} yr^{-1} C). The largest observed yield of organic carbon (DOC+POC), 2,600 kmol km^{-2} yr^{-1} (31 t km^{-2} yr^{-1} C), is 2.5 to 4 percent of net primary productivity for tropical

forests, an amount that is relatively small and sustainable. For reference, these POC yields from the granitic watersheds are about half of those estimated by Hilton and others (2008a) for a landslide-prone shalely landscape in New Zealand. For a process to be important to the carbon cycle, it would have to scale to about 6.7 t km^{-2} yr^{-1} C for a global terrestrial phenomenon, or about 250 t km^{-2} yr^{-1} C if confined to humid tropical mountains. The perturbed POC yields (table 15), 300 kmol km^{-2} yr^{-1} (6 t km^{-2} yr^{-1} C) to 1,700 kmol km^{-2} yr^{-1} (22 t km^{-2} yr^{-1} C), are close to and greater than 6.7 t km^{-2} yr^{-1} C but far less than 250 t km^{-2} yr^{-1} C.

Human-accelerated POC burial is a global phenomenon (Stallard, 1998), and these excess POC yields are consistent with it. The lack of evidence in eastern Puerto Rico of human effects for either DOC production or silicate weathering suggests that although the DIC and DOC yields of tropical rivers are large, they are of secondary interest to research of the anthropogenically perturbed carbon cycle at a century time scale.

Eastern Puerto Rico contains a fascinating landscape for examining biogeochemical processes operating at maximal rates. The models presented here, however, represent considerable simplifications of these complex interacting processes. It is hoped that these results inspire others to develop physically based models and geochemical tests that better define the processes and how they respond to environmental and climate change. It is a setting that may have been important to the climate history of our planet, and it probably is representative of the sources of a huge fraction of the clastic sediments that form the geologic record. From the perspective of observation, this landscape, except perhaps for the Mameyes watershed, is far from equilibrium and probably is more representative of conditions during major erosion cycles in the Earth's history than the more quiescent times in between.

Acknowledgments

This work was supported through the United States Geological Survey Water, Energy, and Biogeochemical Budgets program (Larsen and others, 1993; Lins, 1994). This chapter benefited from reviews by Troy Baisden, Alex Blum, and Jamie Shanley. During the last 22 years, management support of this long-term study, from concept to integrated product, has been greatly appreciated.

References

Ashton, P.S., Brokaw, N., Bunyavehchewin, S., Condit, R., Chuyong, G., Co, L., Dattaraja, H.S., Davies, S., Esufali, S., Ewango, C.E.N., Foster, R., Gunatilleke, N., Gunatilleke, S., Hernandez, C., Hubbell, S., Itoh, A., John, R., Kanzaki, M., Kenfack, D., Kiratiprayoon, S., LaFrankie, J., Lee, H.S., Liengola, I., Lao, S., Losos, E.C., Makana, J.R., Manokaran, N., Navarrete, H., Okhubo, T., Pérez, R., Pongpattannanurak, N., Samper, C., Sri-ngernyuang, K., Sukumar, R., Sun, I.F., Suresh, H.S., Tan, S., Thomas, D., Thompson, J., Vallejo, M., Villa Muńoz, G., Valencia, R., Yamakura, T., and Zimmerman, J., 2004, Floristics and vegetation of the forest dynamics plots, *in* Losos, E.C., and Leigh, E.E., Jr., eds., Tropical forest diversity and dynamism—Findings from a large-scale plot network: Chicago, The University of Chicago Press, p. 90–102.

Aufdenkampe, A.K., Hedges, J.I., Richey, J.E., Krusche, A.V., and Llerena, C.A., 2001, Sorptive fractionation of dissolved organic nitrogen and amino acids onto fine sediments within the Amazon Basin: Limnology and Oceanography, v. 46, no. 8, p. 1921–1935.

Aufdenkampe, A.K., Mayorga, E., Hedges, J.I., Llerena, C., Quay, P.D., Gudeman, J., Krusche, A.V., and Richey, J.E., 2007, Organic matter in the Peruvian headwaters of the Amazon—Compositional evolution from the Andes to the lowland Amazon mainstem: Organic Geochemistry, v. 38, p. 337–374.

Beinroth, F.H., Hernández, P.J., Esnard, A.-M., Acevedo, G., and Dubee, B.C., 1992, Organic carbon content of the soils of Puerto Rico, *in* Beinroth, F.H., ed., Organic carbon sequestration in the soils of Puerto Rico—A case study of a tropical environment: Mayagüez, Puerto Rico, University of Puerto Rico Department of Agronomy and Soils, and U.S. Department of Agriculture Soil Conservation Service, p. 57–62, 69 pages.

Berhe, A.A., Harte, J., Harden, J.W., and Torn, M.S., 2007, The significance of the erosion-induced terrestrial carbon sink: BioScience, v. 57, no. 4, p. 337–346.

Bevington, P.R., and Robinson, K.D., 2003, Data reduction and error analysis for the physical sciences—2: New York, McGraw Hill, 320 p.

Bhatt, M.P., and McDowell, W.H., 2007, Controls on major solutes within the drainage network of a rapidly weathering tropical watershed: Water Resources Research, v. 43, p. 1–9.

Blair, N.E., Leithold, E.L., Ford, S.T., Peeler, K.A., Holmes, J.C., and Perkey, D.W., 2003, The persistence of memory—The fate of ancient sedimentary organic carbon in a modern sedimentary system: Geochimica et Cosmochimica Acta, v. 67, no. 1, p. 63–73.

Bot, A.J., Nachtergaele, F.O., and Young, A., 2000, Land resource potential and constraints at regional and country levels: Rome, Land and Water Development Division Food and Agriculture Organization of the United Nations, 214 p.

Brandeis, T.J., Helmer, E.H., and Oswalt, S.N., 2007, The status of Puerto Rico's forests, 2003: U.S. Department of Agriculture Forest Service, Southern Forest Experiment Station Resources Bulletin SRS–119, 75 pages.

Brown, E.T., Stallard, R.F., Larsen, M.C., Bourlès, D.L., Raisbeck, G.M., and Yiou, F., 1995, Pre-anthropogenic denudation rates of a perturbed watershed (Cayaguás River, Puerto Rico) estimated from in-situ-produced ^{10}Be in river-borne quartz: Eos, Transactions, American Geophysical Union, v. 76, no. 46 supplement, p. F685–F686.

Brown, E.T., Stallard, R.F., Larsen, M.C., Bourlès, D.L., Raisbeck, G.M., and Yiou, F., 1998, Determination of predevelopment denudation rates of an agricultural watershed (Cayaguás River, Puerto Rico) using in-situ-produced ^{10}Be in river-borne quartz: Earth and Planetary Science Letters, v. 160, p. 723–728.

Buss, H.L., Brantley, S.L., Sak, P.B., and White, A.F., 2004, Mineral dissolution at the granite-saprolite interface, *in* Wanty, R.B., and Seal, R.R.I., eds., International Symposium on Water-Rock Interaction, 11th, Saratoga Springs, N.Y., July 2004, Proceedings: London, Taylor and Francis, p. 819–823.

Buss, H.L., Bruns, M.A., Schulz, M.S., Moore, J., Mathur, C.F., and Brantley, S.L., 2005, The coupling of biological iron cycling and mineral weathering during saprolite formation, Luquillo Mountains, Puerto Rico: Geobiology, v. 3, p. 247–260.

Buss, H.L., Sak, P.B., Webb, S.M., and Brantley, S.L., 2008, Weathering of the Río Blanco quartz diorite, Luquillo Mountains, Puerto Rico—Coupling oxidation, dissolution, and fracturing: Geochimica et Cosmochimica Acta, v. 72, p. 4488–4507.

Buss, H.L., and White, A.F., 2012, Weathering processes in the Río Icacos and Río Mameyes watersheds in eastern Puerto Rico, ch. I *in* Murphy, S.F., and Stallard, R.F., eds., Water quality and landscape processes of four watersheds in eastern Puerto Rico: U.S. Geological Survey Professional Paper 1789, p. 249–262.

Caine, Nelson, 1980, The rainfall intensity-duration control of shallow landslides and debris flows: Geografiska Annaler, v. 62A, p. 23–27.

Crosta, G.B., 1998, Regionalization of rainfall thresholds—An aid to landslide hazard evaluation: Environmental Geology, v. 35, no. 2–3, p. 131–145.

Dalling, J.W., and Tanner, E.V.J., 1995, An experimental study of regeneration on landslides in montane rain forest in Jamaica: Journal of Ecology, v. 83, no. 1, p. 55–64.

Dean, R.B., and Dixon, W.J., 1951, Simplified statistics for small numbers of observations: Analytical Chemistry, v. 23, no. 4, p. 636–638.

Denman, K.L., Brasseur, G., Chidthaisong, A., Ciais, P., Cox, P.M., Dickinson, R.E., Hauglustaine, D., Heinze, C., Holland, E., Jacob, D., Lohmann, U., Ramachandran, S., da Silva Dias, P.L., Wofsy, S.C., and Zhang, X., 2007, Couplings between changes in the climate system and biogeochemistry, *in* Solomon, Susan, Qin, D., Manning, M., and others, eds., Climate change 2007—The physical science basis. Contribution of Working Group I to the fourth assessment report of the Intergovernmental Panel on Climate Change: Cambridge, United Kingdom, Cambridge University Press, p. 499–587.

Derry, L.A., Pett-Ridge, J.C., Kurtz, A.C., and Troester, J.W., 2006, Ge/Si and ^{87}Sr/^{86}Sr tracers of weathering reactions and hydrologic pathways in a tropical granitoid system: Journal of Geochemical Exploration, v. 88, p. 271–274.

Dong, Hailiang, Peacor, D.R., and Murphy, S.F., 1998, TEM study of progressive alteration of igneous biotite to kaolinite throughout a weathered soil profile: Geochimica et Cosmochimica Acta, v. 62, no. 11, p. 1881–1887.

Fletcher, R.C., Buss, H.L., and Brantley, S.L., 2006, A spheroidal weathering model coupling porewater chemistry to soil thicknesses during steady-state denudation: Earth and Planetary Science Letters, v. 244, p. 444–457.

Foley, J.A., Ramankutty, Navin, Brauman, K.A., Cassidy, E.S., Gerber, J.S., Johnston, Matt, Mueller, N.D., O'Connell, Christine, Ray, D.K., West, P.C., Balzer, Christian, Bennett, E.M., Carpenter, S.R., Hill, Jason, Monfreda, Chad, Polasky, Stephen, Rockström, Johan, Sheehan, John, Siebert, Stefan, Tilman, David, and Zaks, D.P.M., 2011, Solutions for a cultivated planet: Nature, v. 478, p. 337–342.

Galy, Valier, France-Lanord, C., Beyssac, O., Faure, P., Kudrass, H., and Palho, F., 2007, Efficient organic carbon burial in the Bengal fan sustained by the Himalayan erosional system: Nature, v. 450, p. 407–410.

Garrels, R.M., and Lerman, A., 1984, Coupling of the sedimentary sulfur and carbon cycles—An improved model: American Journal of Science, v. 284, p. 989–1007.

Garrels R.M., and Mackenzie, F.T., 1971, Evolution of sedimentary rocks: New York, W.W. Norton and Company, 397 p.

Garwood, N.C., Janos, D.P., and Brokaw, N.V.L., 1979, Earthquake-caused landslides—A major disturbance to tropical forests: Science, v. 205, p. 997–999.

Godsey, S.E., Kirchner, J.W., and Clow, D.W., 2009, Concentration-discharge relationships reflect chemostatic characteristics of U.S. watersheds: Hydrological Processes, v. 23, p. 1844–1864.

Guariguata, M.R., 1990, Landslide disturbance and forest regeneration in the upper Luquillo Mountains of Puerto Rico: Journal of Ecology, v. 78, no. 3, p. 814–832.

Guariguata, M.R., and Larsen, M.C., 1990, Preliminary map showing landslides in El Yunque quadrangle, Puerto Rico: U. S. Geological Survey Open-File Report 89–257, 1 map sheet, scale 1:20,000, text.

Harden, J.W., Berhe, A.A., Torn, M., Harte, J., Liu, S., and Stallard, R.F., 2008, Soil erosion—Data say C sink: Science, v. 320, no. 5873, p. 178–179.

Heartsill-Scalley, Tamara, Scatena, F.N., Estrada, C., McDowell, W.H., and Lugo, A.E., 2007, Disturbance and long-term patterns of rainfall and throughfall nutrient fluxes in a subtropical wet forest in Puerto Rico: Journal of Hydrology, v. 333, p. 472–485.

Hedges, J.I., Mayorga, E., Tsamakis, E., Mcclain, M.E., Aufdenkampe, A.K., Quay, P., Richey, J.E., Benner, R., Opsahl, S., Black, B., Pimentel, T., Quintanilla, J., and Maurice, L., 2000, Organic matter in Bolivian tributaries of the Amazon River—A comparison to the lower mainstream: Limnology and Oceanography, v. 45, no. 7, p. 1449–1466.

Hilton, R.G., Galy, A., and Hovius, N., 2008a, Riverine particulate organic carbon from an active mountain belt: Importance of landslides: Global Biogeochemical Cycles, v. 22, no. GB1012, p. 1–2.

Hilton, R.G., Galy, A., Hovius, N., Chen, M.-C., Horng, M.-J., and Chen, H., 2008b, Tropical-cyclone-driven erosion of the terrestrial biosphere from mountains: Nature Geoscience, v. 1, p. 769–772.

Hooke, R.L., 1994, On the efficacy of humans as geomorphic agents: GSA Today, v. 4, p. 218, 224–225.

Hooke, R.L., 2000, On the history of humans as geomorphic agents: Geology, v. 28, no. 9, p. 843–846.

Jolly, W.T., Lidiak, E.G., Schellekens, J.H., and Santos, J., 1998, Volcanism, tectonic and stratigraphic correlations in Puerto Rico, *in* Lidiak, E.G., and Larue, D.K., eds., Tectonics and geochemistry of the northeastern Caribbean: Geological Society of America Special Paper 322, p. 1–34.

Jupp, D.L., 1976, B-splines for smoothing and differentiating data sequences: Mathematical Geology, v. 8, no. 3, p. 243–266.

Keefer, D.K., 1984, Landslides caused by earthquakes: Geological Society of America Bulletin, v. 95, p. 406–421.

Kennaway, Todd, and Helmer, E.H., 2007, The forest types and ages cleared for land development in Puerto Rico: GIScience and Rempte Sensing, v. 44, no. 4, p. 356–382.

Lal, Rattan, and Pimentel, D., 2008, Soil erosion—A carbon sink or source?: Science, v. 319, p. 1040–1041.

Larsen, M.C., 1997, Tropical geomorphology and geomorphic work—A study of geomorphic processes and sediment and water budgets in montane humid-tropical forested and developed watersheds, Puerto Rico: Boulder, University of Colorado Department of Geography, Ph.D. dissertation, 244 p.

Larsen, M.C., 2012, Landslides and sediment budgets in four watersheds in eastern Puerto Rico, ch. F *in* Murphy, S.F., and Stallard, R.F., eds., Water quality and landscape processes of four watersheds in eastern Puerto Rico: U.S. Geological Survey Professional Paper 1789, p. 153–178.

Larsen, M.C., Collar, P.D., and Stallard, R.F., 1993, Research plan for the investigation of water, energy, and biogeochemical budgets in the Luquillo Mountains, Puerto Rico: U.S. Geological Survey Open-File Report 92–150, 19 p.

Larsen, M.C., and Parks, J.E., 1997, How wide is a road? The association of roads and mass-wasting in a forested montane environment: Earth Surface Processes and Landforms, v. 22, p. 835–848.

Larsen, M.C., and Santiago-Román, A., 2001, Mass wasting and sediment storage in a small montane watershed—An extreme case of anthropogenic disturbance in the humid tropics, *in* Dorava, J.M., Palcsak, B.B., Fitzpatrick, F., and Montgomery, D., eds., Geomorphic processes and riverine habitat: American Geophysical Union Water Science & Application Series, v. 4, p. 119–138.

Larsen, M.C., and Simon, A., 1993, A rainfall intensity-duration threshold for landslides in a humid-tropical environment, Puerto Rico: Geografiska Annaler, v. 75A, p. 13–23.

Larsen, M.C., and Stallard, R.F., 2000, Luquillo Mountains, Puerto Rico—A Water, Energy, and Biogeochemical Budgets program site: U.S. Geological Survey Fact Sheet 163–99, 4 p.

Larsen, M.C., and Torres-Sánchez, A.J., 1992, Landslides triggered by Hurricane Hugo in eastern Puerto Rico, September 1989: Caribbean Journal of Science, v. 28, no. 3–4, p. 113–125.

Larsen, M.C., and Torres-Sánchez, A.J., 1998, The frequency and distribution of recent landslides in three montane tropical regions of Puerto Rico: Geomorphology, v. 24, no. 4, p. 309–331.

Larsen, M.C., Torres-Sánchez, A.J., and Concepcion, I.M., 1999, Slopewash, surface runoff and fine-litter transport in forest and landslide scars in humid-tropical steeplands, Luquillo Experimental Forest, Puerto Rico: Earth Surface Processes and Landforms, v. 24, no. 6, p. 481–502.

Larsen, M.C., Vásquez Conde, M.T., and Clark, R.A., 2001, Landslide hazards associated with flash-floods, with examples from the December 1999 disaster in Venezuela, *in* Gruntfest, Eve, and Handmer, J., eds., Coping with flash floods: Dordrecht, Holland, Kluwer Academic Publishers, NATO ASI Series C: Mathematical and Physical Sciences, p. 259–275.

Leithold, E.L., and Blair N.E., 2001, Watershed control on the carbon loading of marine sedimentary particles: Geochimica et Cosmochimica Acta, v. 54, no. 14, p. 2231–2240.

Lyons, W.B., Nezat, C.A., Carey, A.E., and Hicks, D.M., 2002, Organic carbon fluxes to the ocean from high-standing islands: Geology, v. 30, no. 5, p. 443–446.

Mackenzie, R.C., ed., 1957, Differential thermal analysis of clays: London, Mineralogical Society, 389 p.

Mackenzie, R.C., and Caillère, S., 1979, Thermal analysis, DTA, TG, DTG, *in* Van Olphen, Hendrik, and Fripiat, J.J., eds., Data handbook for clay material and other non-metallic minerals: New York, Pergamon, p. 243–284.

McDowell, W.H., 1998, Internal nutrient fluxes in a Puerto Rican rain forest: Journal of Tropical Ecology, v. 14, p. 521–536.

McDowell, W.H., and Asbury, C.E., 1994, Export of carbon, nitrogen, and major ions from three tropical montane watersheds: Limnology and Oceanography, v. 39, no. 1, p. 111–125.

McDowell, W.H., Bowden, W.B., and Asbury, C.E., 1992, Riparian nitrogen dynamics in two geomorphologically distinct tropical rain-forest watersheds—Subsurface solute patterns: Biogeochemistry, v. 18, no. 2, p. 53–75.

Meybeck, Michel, 1979, Concentration des eaux fluviales en éléments majeurs et apports en solution aux océans: Revue de Geologie Dynamique et de Geographie Physique, v. 21, no. 3, p. 215–246.

Meybeck, Michel, 1993, Riverine transport of atmospheric carbon—Sources, global typology, and budget: Water, Air, and Soil Pollution, v. 70, p.443–463.

Meybeck, Michel, 2003, Global analysis of river systems—From earth system controls to anthropocene syndromes: Philosophical Transactions of the Royal Society [London] Series B—Biological Sciences, v. 358, no. 1440, p. 1935–1955.

Milliman, J.D., and Meade, R.H., 1983, World-wide delivery of river sediment to the oceans: Journal of Geology, v. 91, p. 1–21.

Milliman, J.D., and Syvitski, J.P.M., 1992, Geomorphic/tectonic control of sediment discharge to the ocean—The importance of small mountainous rivers: Journal of Geology, v. 100, p. 525–544.

Molnia, B.F., and Hallam, C.A., 1999, Open skies aerial photography of selected areas in Central America affected by Hurricane Mitch: U.S. Geological Survey Circular 1181, 82 p., 1 CD–ROM.

Montgomery, D.R., and Dietrich, W.E., 1994, A physically based model for the topographic control on shallow landsliding: Water Resources Research, v. 30, no. 4, p. 1153–1171.

Montgomery, D.R., Schmidt, K.M., Greenberg, H.M., and Dietrich, W.E., 2000, Forest clearing and regional landsliding: Geology, v. 28, no. 4, p. 311–314.

Murphy, S.F., Brantley, S.L., Blum, A.E., White, A.F., and Dong, H., 1998, Chemical weathering in a tropical watershed, Luquillo Mountains, Puerto Rico—II. Rate and mechanism of biotite weathering: Geochimica et Cosmochimica Acta v. 62, p. 227–243.

Murphy, S.F., and Stallard, R.F., 2012, Hydrology and climate of four watersheds in eastern Puerto Rico, ch. C *in* Murphy, S.F., and Stallard, R.F., eds., Water quality and landscape processes of four watersheds in eastern Puerto Rico: U.S. Geological Survey Professional Paper 1789, p. 43–84.

Murphy, S.F., Stallard, R.F., Larsen, M.C., and Gould, W.A., 2012, Physiography, geology, and land cover of four watersheds in eastern Puerto Rico, ch. A *in* Murphy, S.F., and Stallard, R.F., eds., Water quality and landscape processes of four watersheds in eastern Puerto Rico: U.S. Geological Survey Professional Paper 1789, p. 1–24.

Pacala, S.W., Hurtt, G.C., Baker, D., Peylin, P., Houghton, R.A., Birdsey, R.A., Heath, L., Sundquist, E.T., Stallard, R.F., Ciais, P., Moorcroft, P., Caspersen, J.P., Shevliakova, E., Moore, B., Kohlmaier, G., Holland, E., Gloor, M., Harmon, M.E., Fan, S.M., Sarmiento, J.L., Goodale, C.L., Schimel, D., and Field, C.B., 2001, Consistent land- and atmosphere-based U.S. carbon sink estimates: Science, v. 292, no. 5525, p. 2316–2320.

Parfitt, R.L., 2009, Allophane and imogolite—Role in soil biogeochemical processes: Clay Minerals, v. 44, p. 135–155.

Peters, N.E., Shanley, J.B., Aulenbach, B.T., Webb, R.M., Campbell, D.H., Hunt, R., Larsen, M.C., Stallard, R.F., Troester, J., and Walker, J.F., 2006, Water and solute mass balance of five small, relatively undisturbed watersheds in the U.S.: Science of the Total Environment, v. 358, p. 221–242.

Petsch, S.T., Berner, R.A., and Eglinton, T.I., 2000, A field study of the chemical weathering of ancient sedimentary organic matter: Organic Geochemistry, v. 31, p. 475–487.

Petsch, S.T., Eglinton, T.I., and Edwards, K.J., 2001, ^{14}C-dead living biomass—Evidence for microbial assimilation of ancient organic carbon during shale weathering: Science, v. 292, p. 1127–1131.

Pett-Ridge, J.C., 2009, Contributions of dust to phosphorus cycling in tropical forests of the Luquillo Mountains, Puerto Rico: Biogeochemistry, v. 96, no. 1, p. 63–80.

Pett-Ridge, J.C., Derry, L.A., and Barrows, J.K., 2009, Ca/Sr and ^{87}Sr/^{86}Sr ratios as tracers of Ca and Sr cycling in the Río Icacos watershed, Luquillo Mountains, Puerto Rico: Chemical Geology, v. 94, no. 1, p. 64–80.

Pett-Ridge, J.C., Derry, L.A., and Kurtz, A.C., 2008, Sr isotopes as a tracer of weathering processes and dust inputs in a tropical granitoid watershed, Luquillo Mountains, Puerto Rico: Geochimica et Cosmochimica Acta, v. 73, p. 25–43.

Prentice, I.C., Farquhar, G.D., Fasham, M.J.R., Goulden, M.L., Heimann, M., Jaramillo, V.J., Kheshgi, H.S., Le Quéré, C., Scholes, R.J., and Wallace, D.W.R., 2001, The carbon cycle and atmospheric carbon dioxide, *in* Houghton, J.T., Ding, Y., Griggs, D.J., Noguer, M., van der Linden, P.J., Dai, X., Maskell, K., and Johnson, C.A., eds., Climate change 2001—The scientific basis. Contribution of Working Group I to the third assessment report of the Intergovernmental Panel on Climate Change: Cambridge, United Kingdom, Cambridge University Press, p. 183–237.

Quinton, J.N., Govers, G., Van Oost, K., and Bardgett, R.D., 2010, The impact of agricultural soil erosion on biogeochemical cycling: Nature Geoscience, v. 3, p. 1–4; doi 10.1038/ngeo838.

Reid, L.M., 1998, Calculation of average landslide frequency using climatic records: Water Resources Research, v. 34, no. 4, p. 869–877.

Runkel, R.L., Crawford, C.G., and Cohn, T.A., 2004, Load Estimator (LOADEST)—A FORTRAN program for estimating constituent loads in streams and rivers: U.S. Geological Survey Techniques and Methods Book 4–A5, 75 p.; program, test files.

Sarmiento, J.L., and Sundquist, E.T., 1992, Revised budget for the oceanic uptake of anthropogenic carbon dioxide: Nature, v. 356, p. 389–393.

Scatena, F.N., and Larsen, M.C., 1991, Physical aspects of Hurricane Hugo in Puerto Rico: Biotropica, v. 23, p. 317–323.

Schellekens, Jaap, Scatena, F.N., Bruijnzeel, L.A., van Dijk, A.I.J.M., Groen, M.M.A., and van Hogezand, R.J.P., 2004, Stormflow generation in a small rainforest catchment in the Luquillo Experimental Forest, Puerto Rico: Hydrological Processes, v. 18, p. 505–530.

Schneider, S.H., 2009, The worst-case scenario: Nature, v. 459, p. 1104–1105.

Schulz, M.S., and White, A.F., 1999, Chemical weathering in a tropical watershed, Luquillo Mountains, Puerto Rico—III. Quartz dissolution rates: Geochimica et Cosmochimica Acta, v. 63, no. 3–4, p. 337–350.

Science Magazine, 2011, News focus—A global perspective on the Anthropocene: Science, v. 334, p. 34–35.

Shanley, J.B., McDowell, W.H., and Stallard, R.F., 2011, Long-term patterns and short-term dynamics of stream solutes and suspended sediment in a rapidly weathering tropical watershed: Water Resources Research, doi no. 10.1029/2010WR009788.

Simon, Andrew, Larsen, M.C., and Hupp, C.R., 1990, The role of soil processes in determining mechanisms of slope failure and hillslope development in a humid-tropical forest, eastern Puerto Rico: Geomorphology, v. 3, p. 263–286.

Simonett, D.S., 1967, Landslide distribution and earthquakes in the Bewani and Torricelli Mountains, New Guinea—A statistical analysis, *in* Jennings, J.N., and Mabbutt, J.A., eds., Landform studies from Australia and New Guinea: Canberra, Australian National University Press, p. 64–84.

Smith, A.L., Schellekens, J.H., and Diaz, A.-L.M., 1998, Batholiths as markers of tectonic change in the northeastern Caribbean, *in* Lidiak, E.G., and Larue, D.K., eds., Tectonics and geochemistry of the northeastern Caribbean: Geological Society of America Special Paper 322, p. 99–122.

Stallard, R.F., 1985, River chemistry, geology, geomorphology, and soils in the Amazon and Orinoco Basins, *in* Drever, J.I., ed., The chemistry of weathering: Dordrecht, Holland, D. Reidel Publishing Co., NATO ASI Series C—Mathematical and Physical Sciences, v. 149, p. 293–316.

Stallard, R.F., 1988, Weathering and erosion in the humid tropics, *in* Lerman, Abraham, and Meybeck, M., eds., Physical and chemical weathering in geochemical cycles: Dordrecht, Holland, Kluwer Academic Publishers, NATO ASI Series C—Mathematical and Physical Sciences, v. 251, p. 225–246.

Stallard, R.F., 1995a, Relating chemical and physical erosion, *in* White, A.F., and Brantley, S.L., eds., Chemical weathering rates of silicate minerals: Washington, D.C., Mineralogical Society of America Reviews in Mineralogy and Geochemistry, v. 31, p. 543–564.

Stallard, R.F., 1995b, Tectonic, environmental, and human aspects of weathering and erosion—A global review using a steady-state perspective: Annual Review of Earth and Planetary Sciences, v. 12, p. 11–39.

Stallard, R.F., 1998, Terrestrial sedimentation and the carbon cycle—Coupling weathering and erosion to carbon burial: Global Biogeochemical Cycles, v. 12, no. 2, p. 231–252.

Stallard, R.F., 1999, Erosion and the effects of deforestation in the Panama Canal Basin, *in* Panama Canal Watershed Monitoring Project, ed., Report of the Panama Canal Watershed Monitoring Project: Panama City, Panama, Smithsonian Tropical Research Institute, ch. II.8, 8 volumes, 21 CD–ROMs.

Stallard, R.F., 2012, Atmospheric inputs to watersheds in the Luquillo Mountains of eastern Puerto Rico, ch. D *in* Murphy, S.F., and Stallard, R.F., eds., Water quality and landscape processes of four watersheds in eastern Puerto Rico: U.S. Geological Survey Professional Paper 1789, p. 85–112.

Stallard, R.F., and Edmond, J.M., 1981, Geochemistry of the Amazon 1. Precipitation chemistry and the marine contribution to the dissolved load at the time of peak discharge: Journal of Geophysical Research—Oceans and Atmospheres, v. 86, p. 9844–9858.

Stallard, R.F., and Edmond, J.M., 1983, Geochemistry of the Amazon 2. The influence of the geology and weathering environment on the dissolved load: Journal of Geophysical Research—Oceans and Atmospheres, v. 88, p. 9671–9688, microfiche supplement.

Stallard, R.F., and Edmond, J.M., 1987, Geochemistry of the Amazon 3—Weathering chemistry and limits to dissolved inputs: Journal of Geophysical Research, v. 92, p. 8293–8302.

Stallard, R.F., and Kinner, D.A., 2005, Estimation of landslide importance in hillslope erosion within the Panama Canal watershed, *in* Harmon, R.S., ed., The Río Chagres, Panama—A multidisciplinary profile of a tropical watershed: Dordtrecht, The Netherlands, Springer Water Science and Technology Library, v. 52, p. 281–295.

Stallard, R.F., Koehnken, L., and Johnsson, M.J., 1991, Weathering processes and the composition of inorganic material transported through the Orinoco River system, Venezuela and Colombia: Geoderma, v. 51, p. 133–165.

Stallard, R.F., and Murphy, S.F., 2012, Water quality and mass transport in four watersheds in eastern Puerto Rico, ch. E *in* Murphy, S.F., and Stallard, R.F., eds., Water quality and landscape processes of four watersheds in eastern Puerto Rico: U.S. Geological Survey Professional Paper 1789, p. 113–152.

Starkel, Leszek, 1972, The role of catastrophic rainfall in the shaping of the relief of the Lower Himalaya (Darjeeling Hills): Geographia Polonica, v. 21, p. 103–147.

Striegl, R.G., Dornblaser, M.M., Aiken, G.R., Wickland, K.P., and Raymond, P.A., 2007, Carbon export and cycling by the Yukon, Tanana, and Porcupine rivers, Alaska, 2001–2005: Water Resources Research, v. 43, p. W02411.

Stumm, Werner, and Morgan, J.J., 1981, Aquatic chemistry: New York, John Wiley, 780 p.

Syvitski, J.P.M., Vörösmarty, C.J., Kettner, A.J., and Green, P., 2005, Impact of humans on the flux of terrestrial sediment to the global coastal ocean: Science, v. 308, p. 376–380.

Tardy, Yves, Bustillo, V., Roquin, C., Mortatti, J., and Reynaldo, R., 2005, The Amazon—Bio-geochemistry applied to river basin management, part I. Hydro-climatology, hydrograph separation, mass transfer balances, stable isotopes, and modelling: Applied Geochemistry, v. 20, p. 1746–1829.

Turner, B.F., Stallard, R.F., and Brantley, S.L., 2003, Investigation of *in situ* weathering of quartz diorite bedrock in the Río Icacos Basin, Luquillo Experimental Forest, Puerto Rico: Chemical Geology, v. 202, no. 3–4, p. 313–341.

U.S. Geological Survey, 2007, Facing tomorrow's challenges—U.S. Geological Survey science in the decade 2007–2017: U.S. Geological Survey Circular 1309, x + 70 p.

United Nations Environment Programme World Conservation Monitoring Centre, 2002, Mountain Watch, 2002—Environmental change and sustainable development in mountains: Cambridge, United Kingdom, United Nations Environment Programme World Conservation Monitoring Centre, 80 p.

Van Oost, Kristof, Quine, T.A., Govers, G., De Gryze, S., Six, J., Harden, J.W., Ritchie, J.C., McCarty, G.W., Heckrath, G., Kosmas, C., Giraldez, J.V., Marques da Silva, J.R., and Merckx, R., 2007, The impact of agricultural soil erosion on the global carbon cycle: Science, v. 318, p. 626–629.

Van Oost, Kristof, Six, J., Govers, G., Quine, T.A., and De Gryze, S., 2008, Soil erosion—A carbon sink or source? Response: Science, v. 319, p. 1040.

Ver, L.M.B., Mackenzie, F.T., and Lerman, A., 1999, Carbon cycle in the coastal zone—Effects of global perturbations and change in the past three centuries: Chemical Geology, v. 159, p. 283–304.

Walker, L.R., Zarin, D.J., Fetcher, N., Myster, R.W., and Johnson, A.H., 1996, Ecosystem development and plant succession on landslides in the Caribbean: Biotropica, v. 28, no. 4a, p. 566–576.

Webb, Richard, 2006, Cartography—A popular perspective: Nature, v. 439, p. 800.

White, A.F., 2002, Determining mineral weathering rates based on solid and solute weathering gradients and velocities—Application to biotite weathering in saprolites: Chemical Geology, v. 190, p. 69–89.

White, A.F., and Blum, A.E., 1995, Effects of climate on chemical weathering in watersheds: Geochimica et Cosmochimica Acta, v. 59, no. 9, p. 1729–1747.

White, A.F., Blum, A.E., Bullen, T.D., Vivit, D.V., Schulz, M.S., and Fitzpatrick, J., 1999a, The effect of temperature on experimental and natural chemical weathering rates of granitoid rocks: Geochimica et Cosmochimica Acta, v. 63, no. 19–20, p. 3277–3291.

White, A.F., Blum, A.E., Schulz, M.S., Vivit, D.V., Stonestrom, D.A., Larsen, M.C., Murphy, S.F., and Eberl, D., 1998, Chemical weathering in a tropical watershed, Luquillo Mountains, Puerto Rico—I. Long-term versus short-term weathering fluxes: Geochimica et Cosmochimica Acta, v. 62, no. 2, p. 209–226.

White, A.F., Bullen, T.D., Vivit, D.V., Schulz, M.S., and Clow, D.W., 1999b, The role of disseminated calcite in the chemical weathering of granitoid rocks: Geochimica et Cosmochimica Acta, v. 63, no. 13–14, p. 1939–1953.

Zack, A.L., and Larsen, M.C., 1993, Island hydrology—Puerto Rico and the U.S. Virgin Islands: National Geographic Research and Exploration—Water Issue, p. 126–134.

Zarin, D.J., 1993, Nutrient accumulation during succession in subtropical lower montane wet forests, Puerto Rico: Philadelphia, University of Pennsylvania, Ph.D. dissertation, 182 p.

Zarin, D.J., and Johnson, A.H., 1995a, Base saturation, nutrient cation, and organic matter increases during early pedogenesis on landslide scars in the Luquillo Experimental Forest, Puerto Rico: Geoderma, v. 65, no. 3–4, p. 317–330.

Zarin, D.J., and Johnson, A.H., 1995b, Nutrient accumulation during primary succession in a montane tropical forest, Puerto Rico: Soil Science Society of America Journal, v. 59, no. 5, p. 1444–1452.

Ziegler, Karen, Chadwick, O.A., White, A.F., and Brzezinski, M.A., 2005, δ^{30}Si systematics in a granitic saprolite, Puerto Rico: Geology, v. 33, no. 10, p. 817–820.